25

MECHANISMS AND CONSEQUENCES OF DRUG–DRUG INTERACTIONS

DORA FARKAS, RICHARD I. SHADER, LISA L. VON MOLTKE, AND DAVID J. GREENBLATT

Tufts University School of Medicine, Boston, Massachusetts

Contents

Preclinical Development Handbook: ADME and Biopharmaceutical Properties, edited by Shayne Cox Gad

25.1 PRINCIPLES OF DRUG–DRUG INTERACTIONS

25.1.1 Introduction

Understanding the mechanisms and consequences of drug–drug interactions is essential for the development of new pharmaceuticals and for the design of multidrug regimens. Drug interactions occur when one drug (the "perpetrator") changes the pharmacokinetic and/or the pharmacodynamic actions of another drug (the "victim"). This interaction can lead to changes in the clearance of the victim drug, which can influence its efficacy and safety. For drugs with narrow therapeutic indices, such as warfarin, digoxin, and theophylline, small changes in plasma concentrations can lead to toxicity.

Even after drugs undergo rigorous safety and efficacy testing during clinical trials, they can be withdrawn from the market due to the unanticipated possibility of toxic interactions with other drugs. For example, in the late 1990s the U.S. FDA recommended the withdrawal of the antihistamine terfenadine after it was discovered that its coadministration with the antifungal ketoconazole was associated with cardiac toxicity, which in a few instances was fatal. Terfenadine has been replaced by its metabolite, fexofenadine, which has similar efficacy but no known cardiac toxicity [1].

Drug–drug interactions are especially a concern for patients taking several drugs concurrently, such as the elderly and patients with serious medical diseases such as cancer or HIV. It is estimated that almost 40% of the elderly take five or more drugs simultaneously [2] and that 90% of them also use over-the-counter (OTC) medications, some of which may also contribute to drug interactions [3]. For example, the H_2 receptor antagonist cimetidine inhibits several cytochrome P450s and interacts with the CYP1A2 substrate theophylline [4]. Elderly patients are also thought to be 3–10 times more likely than younger patients to be susceptible to adverse drug–drug interactions due to changes in hepatic and renal clearance [5, 6]. In addition, with the increasing use of complementary alternative medicines such as herbal supplements, the probability of drug–drug interactions is increased. For example, it is estimated that over 50% of cancer patients take herbal remedies, even though there is evidence for adverse drug interactions with several herbs such as kava-kava, *Ginkgo biloba*, ginseng, and echinacea [6, 7].

Drug–drug interactions are not limited to prescription drugs, OTC drugs, and herbal remedies. Other substances such as foods, beverages, and excipients in drug tablets can enhance or inhibit the disposition of drugs. Grapefruit juice, for example, is an inhibitor of CYP3A, which is responsible for metabolizing an estimated 50% of prescription drugs. Further clinical trials demonstrated that grapefruit juice only inhibits intestinal CYP3A, and therefore, it is only expected to influence the pharmacokinetics of drugs that undergo significant enteric CYP3A metabolism [8], such as short half-life benzodiazepines [9]. More recent evidence suggests that certain other fruit juices also have the potential to inhibit CYP3A. For example, Seville orange juice was shown to inhibit enteric metabolism of felodipine [10] to a similar extent as grapefruit juice. In addition, *in vitro* and animal studies suggest that pomegranate juice is also a significant inhibitor of CYP3A [11, 12].

Interestingly, certain tablet excipients also influence absorption and bioavailability. For example, the cremophores EL and RH 40, which enhance lipid solubility,

have been shown to increase the oral bioavailability of saquinavir and digoxin, respectively [13–15]. However, other excipients such as Tween 80 and HS15 can adversely affect the disposition of drugs by inhibiting the drug transporter P-glycoprotein (also known as ABCB1 and MDR1) and increasing intracellular levels of P-glycoprotein substrates such as the chemotherapy agent daunorubicin [15].

Drug–drug interactions can occur through four mechanisms of drug disposition, collectively known as ADME—*a*bsorption, *d*istribution, *m*etabolism, and *e*limination. Absorption of a drug across a lipid bilayer is influenced by several factors, including physicochemical properties of the drug, such as solubility, lipophilicity, the pH of the environment, gastric emptying rate, gastrointestinal motility, and bile secretion. Antacids such as H_2 receptor antagonists can inhibit the absorption of certain drugs, such as ketoconazole, which need an acidic environment, and the anxiolytic drug clorazepate, which needs an acidic environment to be converted to its metabolite, desmethyldiazepam [16]. Furthermore, multivalent cations, such as calcium, magnesium, zinc, iron, and aluminum, which form chemical complexes, can inhibit the absorption of the antibiotics tetracycline and ciprofloxacin [17, 18]. Thus, the consumption of milk or nutritional supplements containing these minerals is contraindicated with tetracycline. Gastrointestinal motility is also impaired by the anticholinergic effects of marijuana or enhanced by the gastrokinetic agent metoclopramide. A decrease (or increase) in gastrointestinal motility can increase (or decrease) the exposure of the intestine to drugs and may result in toxicity [17].

It was previously believed that when a drug is displaced from its plasma protein binding site by another drug, the victim drug's unbound concentration will increase, leading to increased efficacy or possibly toxicity [19]. There are actually very few cases where displacement from plasma protein causes clinically significant interactions [20, 21]. Exceptions include drugs with high extraction and narrow therapeutic indices. For example, extensively albumin-bound compounds may theoretically displace a drug such as warfarin; however, this effect is only transient and rarely of clinical importance [22, 23]. Some interactions were previously attributed primarily to displacement but were found to be a result of inhibition of clearance. Phenylbutazone, for example, inhibits the metabolism of warfarin [24, 25], while sulfonamides reduce the clearance of tolbutamide [26, 27].

Altered metabolism (including phase I and phase II) is the most common reason for drug interactions since many metabolic enzymes can be inhibited or induced by drugs. Inhibition and induction of transporter proteins, particularly P-glycoprotein, is also a clinically significant pathway for drug–drug interactions and will be discussed in more detail in the following sections.

Clearly, it is impossible for the prescribing physician to remember all potential drug interactions. However, an understanding of the principles of drug–drug interactions can aid in the design of a safe multidrug regimen. New analytical techniques and modeling tools combined with knowledge databases are enabling researchers to make better predictions of possible drug interactions. The goals of this chapter are to discuss (1) the common mechanisms of drug–drug interactions, (2) different experimental systems and modeling tools used to investigate possible drug interactions, and (3) pharmacokinetic principles of drug interactions. In Sections 25.2 and 25.3, we illustrate clinically significant drug–drug and drug–herb interactions in two different case studies.

25.1.2 Mechanisms of Drug–Drug Interactions

Metabolic Interactions While there are several possible mechanisms for drug interactions, most of the interactions occur through alterations of hepatic or enteric drug metabolism. Metabolic interactions occur when a perpetrator drug inhibits or induces the activity of a drug-metabolizing enzyme, resulting in either decreased or increased metabolism of a victim drug. Most of the known drug interactions involve the cytochrome P450s (phase I metabolism); however, interactions may also involve phase II enzymes such as the UDP glucuronidases [28, 29]. Table 25.1 provides selected examples of some common prescription drugs that are inhibitors or inducers of the cytochrome P450s and the transporter P-glycoprotein. According to most studies, CYP2D6 is not an easily inducible enzyme. However, there are some studies that suggest that CYP2D6 might be induced by phenobarbital [30] and carbamazepine [31].

The cytochrome P450s implicated in most drug–drug interactions are CYP1A2, CYP2B6, CYP2C8, CYP2C9, CYP2C19, CYP2D6, and CYP3A4. The CYP3A family, particularly CYP3A4, is considered to be exceptionally important, since it mediates the clearance of many common prescription medications [29, 32]. Many prescription drugs, such as the antifungals ketoconazole and fluconazole, the macrolide antibiotic clarithromycin, and the antidepressant fluoxetine, are potent inhibitors of CYP3A and can lead to significant drug interactions. As mentioned previously, the antihistamine terfenadine was withdrawn from the market after it was discovered that coadministration with ketoconazole could lead to cardiac toxicity. The toxicity resulted from the accumulation of excess terfenadine in the bloodstream, since the CYP3A-mediated metabolism of terfenadine was inhibited by ketoconazole [33]. Antifungal agents also interact with other classes of metabolic enzymes. It is thought that fluconazole and miconazole can interact with the metabolism of warfarin, possibly by inhibiting CYP2C9 [6, 34]. However, not all CYP450 inhibitors lead to clinically significant interactions. For example, the antibiotics azithromycin and dirithromycin are weak CYP3A inhibitors and have not been observed to cause toxic drug–drug interactions [35–37].

Selective serotonin reuptake inhibitors (SSRIs) are also known to interact with most of the major cytochrome P450s. CYP1A2 is inhibited by fluvoxamine and to a lesser extent by citalopram, and CYP2D6 is known to be inhibited significantly by fluoxetine and paroxetine, and to a lesser extent by sertraline and citalopram. Many antineoplastic and antiretroviral drugs also interact with the CYP450s, which can be potentially dangerous when several of these drugs are coadministered. The anticancer drug paclitaxel, frequently used to treat breast and ovarian cancers, has been reported to cause toxicity when coadministered with CYP3A inhibitors such as the antiretrovirals delavirdine and saquinavir. Paclitaxel was also found to interact with the chemotherapeutic agent valspodar, possibly through the inhibition of P-glycoprotein by valspodar [6, 38].

Complicating clinical practice is the interindividual variability due to genetic differences in the drug metabolism enzymes [6]. Genetic differences in drug metabolism were first suggested in the 1950s. Hughes et al. [39] reported significant interindividual variability in the acetylation of isoniazid and observed that "slow acetylators" were more likely to experience toxicity from the drug [40]. In the years following this discovery, many epidemiological studies were carried out to confirm

TABLE 25.1 Prescription Drugs as Inducers and Inhibitors of the Major Cytochrome P450s and P-Glycoprotein

CYP1A2	CYP2B6	CYP2C9	CYP2C19	CYP2D6	CYP2E1	CYP3A4	P-Glycoprotein
			Inducer(s)				
Omeprazole	Rifampin	Rifampin	Rifampin	None known	Isoniazid	Carbamazepine Dexamethasone Rifampin Phenytoin	Rifampin
			Inhibitors				
Fluvoxamine Cimetidine	Ketoconazole Clopidogrel	Sulfaphenzole Fluvoxamine Fluconazole Miconazole	Fluoxetine Fluvoxamine	Fluoxetine Quinidine Methadone Paroxetine	Disulfiram	Clotrimazole Itraconazole Ketoconazole Miconazole Ritonazir Nefazodone	Verapamil Doxorubicin Clarithromycin Ritonavir Omeprazole

Source: Adapted from Refs. 15, 32, 43, 46, and 144.

interindividual differences in drug metabolism. For example, the cytochrome P450s CYP2D6 and CYP2C9 have significant genetic polymorphisms and they also metabolize an estimated 25% [41] and 16% [42] of prescription drugs, respectively. CYP2D6, in particular, has at least 80 allelic variants, resulting in a range from poor to ultrarapid metabolizers, and it is also inhibited by drugs such as fluoxetine and methadone [43]. CYP2C9 has five alleles with varying prevalences among different ethnic groups. Genetic variations in CYP2C9 are also a concern, since CYP2C9 is responsible for metabolizing substrates with narrow therapeutic indices such as warfarin and phenytoin [44].

Some of the most significant drug–drug interactions are due to mechanism-based, or irreversible, inhibition. In this case, the drug binds to the enzyme and can modify the heme, protein, or the complex through covalent binding and inactivate it irreversibly [45]. Mechanism-based inhibitors include paroxetine (CYP2D6) [28], tamoxifen, erythromycin, and fluoxetine (CYP3A4). The CYP3A inhibitor in grapefruit juice, 6′, 7′-dihydroxybergamottin, is also a mechanism-based inhibitor. In clinical trials where midazolam was used as a CYP3A probe, a 10 oz glass of white grapefruit juice led to approximately a 65% increase in midazolam's area under the curve (AUC). Subsequent administration of midazolam demonstrated that complete recovery of CYP3A takes about 3 days [8].

Although less investigated, drug–drug interactions also occur through enzyme induction. Induction is a much slower process than inhibition since it involves transcriptional activation of genes. CYP1A2 clearance is increased by cruciferous vegetables, charcoal-broiled beef, cigarette smoke, and omeprazole. The antibacterial rifampin is an inducer of CYP2C9, CYP2C19 and CYP3A4. CYP3A4 can be induced by a variety of compounds including barbiturates, glucocorticoids, phenytoin, carbamazepine, and St. John's wort [46]. Induction of cytochrome P450s typically occurs through the nuclear receptors primarily AhR, CAR, and PXR. In addition to interindividual differences among the cytochrome P450s, there are also differences in nuclear receptors [47, 48] and in their regulatory proteins [49, 50]. Chang et al. [51] measured the mRNAs of CYP2B6, CAR, and PXR in 12 human liver samples. They found a 240-fold interindividual variability among samples in CAR mRNA levels, and a 278-fold variability in the mRNA levels of CYP2B6. The variability in PXR was about 27-fold and it also correlated well with the variabilities in CYP2B6 and CAR [50]. Individual differences in drug disposition could also be due to genetic variations in drug transporters. In fact, there is recent evidence to suggest that interindividual variability in the metabolism of phenytoin and fexofenadine could be attributed to genetic differences in the transporter P-glycoprotein [52, 53].

Interactions Through Nonneuronal Efflux Transporters Transporters are ubiquitously located throughout the body and play an important role in the disposition of drugs, particularly in the liver, the intestine, and the kidneys. While some transporters can interfere with the delivery of drugs inside the cells, they are essential for maintaining a physiologic barrier at several locations, such as the blood–brain barrier [54], testes, and placenta [15]. Transporters include both uptake and efflux proteins and have been classified into several families, including the ATP-binding cassette transporters (ABCs), the organic anion transporting polypeptides (OATPs), organic anion transporters (OATs), and the organic cation transporters (OCTs). Inhibition or induction of transporters can lead to increased or decreased drug

concentration inside the cells, and therefore a better understanding of these transporters is essential for rational drug design and pharmacokinetic modeling.

The ABC family is further subdivided into several subfamilies such as ABCA, ABCB, and ABCC. The most widely recognized transporter is the multidrug resistance protein, MDR1, also known as ABCB1 or P-glycoprotein [55], and in this chapter we use P-glycoprotein as the model for demonstrating the importance of drug–drug interactions through transporters.

Some drugs such as the immunosuppressant cyclosporin A are interesting in that they are both substrates and inhibitors of P-glycoprotein [15]. For example, it has been shown *in vitro* that cyclosporin A inhibited transport of the cardiac drug digoxin, yet digoxin did not inhibit transport of cyclosporin A [56]. P-glycoprotein is especially critical in maintaining the intactness of the blood–brain barrier and cyclosporin A has led to the accumulation of vinblastine in the brain of mice [57]. In P-glycoprotein knockout mice, a normally harmless dose of the opiate loperamide (used as an antidiarrheal in humans) was lethal as the drug gained entry into the central nervous system [58, 59]. In rats, cyclosporine inhibited P-glycoprotein in other organs such as the testes, where it led to the accumulation of doxorubicin [60]. Cardiac toxicity in rats was also caused by another inhibitor of P-glycoprotein, verapamil, which increased the cardiac levels of the chemotherapeutic agent idarubicin [61].

While the presence of P-glycoprotein is associated with drug efflux from cells, it is important to point out that not all substrates of P-glycoprotein have poor bioavailability. Digoxin, in particular, has an oral bioavailability of 50–85% [62, 63]. Ritonavir, another P-glycoprotein substrate, has a bioavailability of 60% [63, 64]. The reason for the high bioavailability of these drugs is that bioavailability is also influenced by influx processes, which might outweigh the effects of the efflux transporters for some drugs. In addition, similar to enzymes, P-glycoprotein efflux is a saturable process. The K_m for many P-glycoprotein substrates, such as digoxin, verapamil, and indinavir, have been determined and the values are in the micromolar range. Thus, in theory, when the plasma concentration of the drug is significantly higher than its K_m value, the drug might be expected to have high bioavailability [62, 63].

Inhibition of P-glycoprotein can occur through multiple mechanisms and can be classified as competitive inhibition, noncompetitive inhibition, or cooperative stimulation. Inhibition can occur if the inhibitor occupies an active binding site or if it inhibits the ATP hydrolysis process that is necessary for efflux. Verapamil inhibits P-glycoprotein by occupying an active binding site, vanadate interacts with ATP hydrolysis, while cyclosporine inhibits P-glycoprotein through both mechanisms [63, 65]. Cooperative inhibition occurs when two inhibitors act together to inhibit P-glycoprotein. P-glycoprotein is thought to have at least two binding sites, and sometimes inhibitors bind to both sites, leading to synergism between the two binding sites to inhibit P-glycoprotein [66]. Inhibitors that were found to act at both sites included vinblastine, tamoxifen, and quinidine [67]. Modeling inhibition can be quite complex, because in addition to the multiple binding sites on P-glycoprotein, there are also allosteric interactions when multiple binding sites are occupied.

Induction of P-glycoprotein has also been observed in response to common P450 inducers such as 3-methylcholanthrene [68] and dexamethasone [69]. Certain cytotoxic agents such as adriamycin, daunomycin, and mitoxantrone have also been found to induce P-glycoprotein in rodent cells [70]. There is now data to suggest

that induction of P-glycoprotein may occur through multiple mechanisms including PXR. Thus, species differences in P-glycoprotein induction are probably due in part to differences in the activation of species-specific PXR [63]. However, even within the same organism, P-glycoprotein is not necessarily induced to the same extent in every tissue, and the time until maximum induction can also vary significantly. Jette et al. [71] compared induction of P-glycoprotein by 10 mg/kg/day cyclosporine A in various organs in the rat. Whereas P-glycoprotein increased by more than 250% in the stomach, it only increased 69% in the lungs [63]. Furthermore, maximal response was observed after only 5 days in the heart, while it took 15 days for maximal response in the spleen and testes.

Pharmacoenhancement or Augmentatics In the previous sections we have discussed examples of adverse drug–drug interactions. However, the pharmacokinetics of HIV combination protease inhibitors demonstrate the principles of pharmacoenhancement, where the "perpetrator" drug actually improves the effectiveness of the "victim" drug. In this section we illustrate the principles of pharmacoenhancement by discussing the pharmacokinetics of HIV protease inhibitors.

Protease inhibitors (PIs), introduced in the mid-1990s, are now standard therapy for HIV. However, in spite of their effectiveness, there is poor patient compliance, leading to treatment failure within 1 year in 40–60% of cases [72, 73]. Reasons for poor patient compliance include unpleasant side effects, the need for frequent dosing, and food- or fluid-dependent administration regimens. Poor patient compliance allows the viral load to get very high and can lead to resistance to the treatment. Combination PIs, where multiple drugs are combined within one formulation, are more effective in suppressing viral replication by increasing the overall exposure to the boosted drug. In addition, clinical trials have suggested better patient compliance because of fewer food restrictions, simpler dosing regimen, as well as lower interindividual variabilities.

Many PIs are combined with ritonavir as the "perpetrator" drug. Ritonavir, which is usually prescribed as 600 mg twice a day, is generally not well tolerated since it can lead to nausea, diarrhea, and other unpleasant side effects. However, a 100 mg dose of ritonavir has been shown to boost the effectiveness of several other PIs [72]. All approved HIV PIs are predominantly metabolized by CYP3A4, and they are all substrates for P-glycoprotein. Of all PIs, ritonavir is the most potent inhibitor of both CYP3A4 and P-glycoprotein [74]. The combination PI consisting of 400 mg of lopinavir and 100 mg of ritonavir has been shown to be well tolerated and effective [75] and is now a marketed drug as a twice-a-day prescription. The FDA has now approved other once-a-day regimens such as amprenavir and atazanavir for patients who are treatment-experienced. The effectiveness of administering lopinavir/saquinavir once-a-day is being currently evaluated [76]. Other drugs boosted by ritonavir include indinavir, amprenavir, saquinavir, lopinavir, atanazavir, and nelfinavir. Other PIs, such as efivarenz and nevirapine, are inducers of CYP3A4; thus, their inclusion in a treatment regimen might require an increase in the dose of other drugs [74].

The specific type of pharmacoenhancement with ritonavir depends on the individual PIs. The effects will be either (1) to increase C_{max}, C_{min}, and AUC and modestly increase $t_{1/2}$ (primarily C_{max} boosting) or (2) to increase $t_{1/2}$ and C_{min} and modestly increase AUC (primarily $t_{1/2}$ boosting). An increase in C_{min} is associated with higher

efficacy and an increase in C_{max} also leads to higher drug exposure but could also result in toxicity unless the drug is well tolerated. A boosting of C_{max}, C_{min}, and AUC (the first type of effect) is observed with lopinavir and saquinavir, which have high first-pass metabolism. Indinavir and amprenavir have short half-lives and ritonavir primarily increases the $t_{1/2}$ and C_{min} and modestly increases AUC for these drugs (the second effect). It is also fortunate that the AUC and the C_{max} are not significantly boosted since an increase in the C_{max} for these drugs has been associated with adverse side effects [77].

Double-boosted PIs are also gaining popularity, especially in treatment-experienced patients. The advantages of this type of treatment are that (1) the levels of several different PIs are increased simulataneously and they are effective against viruses that might have resistance against one particular drug, and (2) addition of a second booster might further enhance the pharmacokinetic properties of the treatment. For example, addition of saquinavir to an atazanavir/ritonavir combination was reported to increase the C_{max} of atazanavir more than just adding ritonavir. The AUCs of atazanavir and saquinavir also increased compared to single-boosted regimens [78, 79].

While ritonavir seems to be effective in combination PIs, not all patients can tolerate it due to its adverse side effects. Another booster drug is the nonnucleoside reverse transcriptase inhibitor delavirdine, which has been shown to increase the half-life, AUC, and C_{max} of nelfinavir. Nelfinavir is metabolized partially by CYP2D6, which is missing in 7% of Caucasians and 1% of Asians [74]. Other individuals are ultrarapid CYP2D6 metabolizers and need higher doses to reach therapeutic drug concentrations. Thus, interindividual variability in drug-metabolizing phenotype also needs to be taken into consideration when prescribing the specific combination PI therapy.

25.1.3 Methods and Systems for Analyzing Drug–Drug Interactions

In Vitro Systems Several systems are available for studying drug–drug interactions and the choice of system depends on the predicted type of interaction. Clearly, the most relevant system is the human body; however, clinical trials are expensive and only a few compounds can be tested per trial. Furthermore, species differences may limit the usefulness of animal experiments. *In vitro* and *in silico* (computational) studies can be useful in eliminating unlikely drug–drug interactions and determining the probable interactions that could be further investigated in clinical or animal studies. Microsomes are frequently used for inhibition studies because they are inexpensive and allow for simulataneous monitoring of several enzymes including the cytochrome P450s, the flavin monooxygenases, and the UDP-glucuronosyltransferases.

Induction studies are carried out in hepatocytes, since the cellular machinery is necessary for upregulating the transcription of genes. However, primary hepatocytes are known to rapidly lose metabolic functions after isolation; thus, special media and culture conditions are necessary for maintaining them. The main challenge regarding hepatocyte culture is that most factors stimulate either regeneration or differentiation but not both [40]. Long-term cultures of hepatocytes usually require a mitogenic compound, such as epidermal growth factor (EGF), which stimulates DNA synthesis. However, it has been shown that EGF leads to a downregulation

of the metabolic enzymes, specifically CYP1A, CYP2B [80, 81], CYP2C11 [82], and CP3A [83]. Cell density also influences cell proliferation and metabolism. A low cell density increases cell proliferation but reduces the expression and inducibility of metabolic enzymes [84]. Culturing hepatocytes on structural matrix proteins, such as collagen, fibronectin, and laminin, has been found to maintain cell morphology and metabolic functions better than plating them on plastic. Culturing hepatocytes in a sandwich configuration is even more suitable for maintaining metabolically active cells. The most common matrices for sandwich cultures are collagen type I and Matrigel, an extract derived from the basement membrane of the Engelbreth–Holm–Sworm mouse sarcoma [85]. Both collagen–collagen and collagen–Matrigel sandwiches have been shown to maintain morphology and albumin secretion for several weeks [86], and they are also inducible for both CYP1A2 and CYP3A4 in systems with human hepatocytes [87].

In addition to optimizing cell culture parameters, special cell lines have been engineered that constitutively express cytochrome P450s and are also inducible for specific enzymes such as CYP3A4. For example, the DPX-3A4 cell line, which contains a luciferase-linked PXR promoter, has been shown to be inducible by a number of compounds such as rifampin, ginseng, and kava-kava [88]. Other cell lines such as the Fa2N-4 are inducible for multiple enzymes, including CYP1A2, CYP2C9, CYP3A4, and UGT1A and the MDR1 transporter [89]. The WIF-B9 cell line, which is a fusion of rat hepatoma and human fibroblasts, has been shown to constitutively express both human and rat cytochrome P450s [90].

For transporter studies involving P-glycoprotein, the human intestinally derived Caco-2 cell line is the most frequently used. The Madin–Darby canine kidney (MDCK) cells are also frequently tested since they require shorter culture period (3–5 days) and have high levels of P-glycoprotein expression [91, 92]. The two main issues with using cells lines for transporter studies are (1) the influence of passage number on the expression of P-glycoprotein and (2) expression of other transporter proteins. In particular, Caco-2 cells typically express the breast cancer resistance protein (BCRP) and the multidrug resistance-associated protein 2 (MRP2) [93–95].

Pharmacokinetic studies can also be carried out in more physiologic *in vitro* systems such as a bioartificial liver. The main challenge with such systems is designing conditions that can maintain hepatocytes long enough for the studies. Cell lines are easier to maintain than primary hepatocytes, but they usually do not express drug-metabolizing enzymes. Several new cell lines have been developed for this purpose such as a pig hepatocyte cell line and a couple of human-derived lines. The pig hepatocytes have been shown to express most of the cytochrome P450s as well as glutathione *S*-transferase and UDP-glucuronosyltransferase [96]. A HepG2-derived cell line was also found to express CYP3A4 at even higher levels than primary human hepatocytes [97]. Furthermore, a human hepatocellular carcinoma cell line has been engineered to be inducible for CYP3A4. This cell line, FLC-5, was cultured in a radial-flow bioreactor and shown to be inducible for CYP3A4 via PXR activation [98]. Thus, the development of these cell lines is a promising step in designing physiologically based perfused bioreactors for drug metabolism and drug interaction studies.

Computational Modeling and Data Processing Tools Computational (or *in silico*) tools are also used widely in the pharmaceutical industry to evaluate possible

metabolism and toxicity pathways for new drugs. While it is not possible to completely characterize most compounds *in silico*, a lot of the technology is already in place and incorporation of new data could lead to more reliable tools in the near future [99]. Quantitative structure–activity relationship (QSAR) models have been compiled for over 2000 compounds to determine possible substrates for the CYP450s [100]. Although many other pathways and endogenous factors influence the pharmacokinetics of drugs, these models can aid in modeling the binding potential of drugs to enzymes. Structure–activity models have been developed for the major cytochrome P450s, including CYP3A4, CYP2D6, and CYP2C9, and results from these models have shown over 90% correlation with experimental data [101]. More in-depth QSAR models have been built for individual P450s, such as CYP2C9, to examine interactions of the enzyme with a variety of potential inhibitors and also to determine the effect of mutations on enzyme activity [102]. Special computer-based models have also been developed for the prediction of drug–drug interactions, which incorporate all known data on drug metabolism enzymes. One example is Q-DIPS (quantitative drug interactions prediction system), which correctly predicted a potent inhibition of CYP3A4 by ketoconazole, and a weaker inhibition by fluconazole [103]. QSAR models have also been developed for drug transporters, especially P-glycoprotein. These models have identified several potential modulators of transporters in order to overcome drug resistance to many chemotherapeutic compounds [104, 105]. Thus, these models can be useful for discovering new compounds that could enter the drug pipelines; however, the development process of new drugs still relies heavily on *in vitro* and *in vivo* experimentation.

Another challenge of drug development is integration of all known data about a certain enzyme or the affected molecular pathway affected. Integration of data has become especially time consuming with the high throughput methods of genomics, proteomics, and metabonomics, which generate vast amounts of data. The goal of systems biology is to combine experimentally generated data with modeling tools in order to discover potential drug interactions and new therapeutic targets. Although many models have been developed, they are far from being complete, since only 15% of the human genome has known function. Nevertheless, these knowledge databases combined with high throughput screening have become useful for modeling ADME/Tox, discovering potential drug interactions and for visualizing the biological processes influenced by drugs [106].

25.1.4 Pharmacokinetic Principles of Drug–Drug Interactions

Kinetics Pharmacokinetic modeling is an essential tool for understanding drug disposition and for designing safe and effective treatment regimens. The simplest approach assumes linear, first-order Michaelis–Menten kinetics. This type of kinetics is described by

$$v = \frac{V_{\max}[\mathrm{S}]}{K_{\mathrm{M}} + [\mathrm{S}]}$$

where v is the reaction velocity, [S] is the substrate concentration, and K_{M} is the substrate concentration at which the reaction velocity reaches half of the maximal velocity, $V_{\max}$. When $[\mathrm{S}] << K_{\mathrm{M}}$ the reaction displays linear kinetics; thus, the rate is directly proportional to the substrate concentration. When [S] get close to K_{M}

the enzyme starts becoming saturated and eventually the velocity, v, reaches its maximum, V_{max}.

If a drug is metabolized by more than one enzyme, the velocity of the reaction is the sum of the individual rates:

$$v = \frac{V_{max(1)}[S]}{K_{M(1)} + [S]} + \frac{V_{max(2)}[S]}{K_{M(2)} + [S]}$$

In this case each enzyme reaction has its own V_{max} and K_M, denoted by the appropriate subscripts. In order to recognize such a phenomenon, the data needs to be viewed on an Eadie–Hofstee plot (v vs. v/[S]), which will illustrate the biphasic characteristic of the reaction [28].

Inhibition and induction occur through different mechanisms and there are different mathematical models and *in vitro* tools for studying them. Inhibition is primarily a chemical phenomenon involving a reversible or irreversible binding of the inhibitor to the enzyme. For this reason inhibition is usually concentration dependent and is usually quantified by the inhibition constant K_i or the 50% inhibitory concentration, the IC_{50}. Inhibition can be competitive, noncompetitive, or uncompetitive. In competitive inhibition, the inhibitor binds to the active pocket of the enzyme and blocks the binding of the substrate. In noncompetitive inhibition, the inhibitor and the substrate bind independently to different sites, and in uncompetitive inhibition, the inhibitor binds to the substrate–enzyme complex and renders the complex inactive. In all three cases, the inhibitor interferes with the reaction velocity and the Michaelis–Menten kinetics are then modified accordingly [46].

For competitive inhibition,

$$v = \frac{V_{max}[S]}{[S] + K_M(1 + [I]/K_i)}$$

For noncompetitive inhibition,

$$v = \frac{V_{max}[S]}{(1 + [I]/K_i)(K_M + [S])}$$

For uncompetitive inhibition,

$$v = \frac{V_{max}[S]}{[S] + K_M + [I][S]/K_i}$$

The mechanism of inhibition can be determined from plotting experimental data. Figure 25.1 shows the plots of $1/v$, the reciprocal of the velocity, versus [I], the inhibitor concentration, for the three types of inhibition (also known as Dixon plots) [107]. Note that [I] and $1/v$ will be positive for all experimental data and the diagrammed intersection points can only be determined by extrapolating the lines. When the mechanism is competitive, the lines will intersect at the point where $[I] = -K_i$ and $1/v = 1/V_{max}$, and when it is noncompetitive the intersection point is at $[I] = -K_i$ and $1/v = 0$. In uncompetitive inhibition, the slopes are independent of [S] and hence

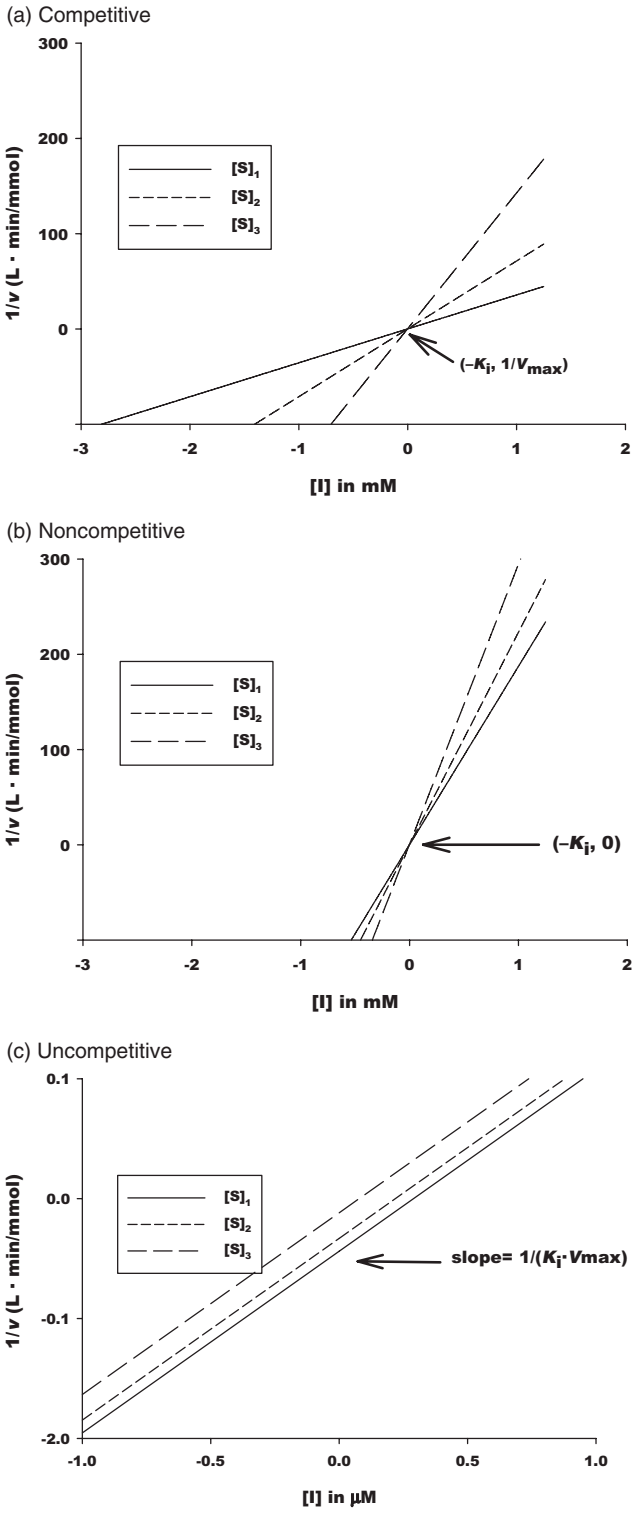

FIGURE 25.1 Relationship between concentration of inhibitor, [I], and the reciprocal of velocity ($1/v$) at different substrate concentrations for (a) competitive, (b) uncompetitive, and (c) noncompetitive inhibition with the following parameters: $K_m = 4.7 \times 10^{-5}$ M; $V_{max} = 22\,\mu$Mol/(L·min); $K_i = 3 \times 10^{-4}$ M. The three substrate concentrations were $[S]_1 = 2 \times 10^{-4}$ M, $[S]_2 = 1 \times 10^{-4}$ M, and $[S]_3 = 5 \times 10^{-5}$ M.

TABLE 25.2 Pharmacokinetic Changes Due to Drug–Drug Interactions

Mechanism of Interaction	Change in Systemic Exposure	Theoretical Change in Exposure[a]
Competitive Inhibition	Increased	$\frac{AUC_i}{AUC} = 1 + \frac{[I]}{K_i}$
Noncompetitive inhibition	Increased	$\frac{AUC_i}{AUC} = 1 + \frac{[I]}{K_i}$
Uncompetitive inhibition	Increased	$\frac{AUC_i}{AUC} = 1 + \left(\frac{[I]}{K_i}\right)\left(\frac{[S]}{[S] + K_M}\right)$
Mechanism-based inhibition (irreversible inactivation)	Increased	$\frac{AUC_i}{AUC} = \frac{V_{max}}{V_{max(inhibited)}}$
Induction	Decreased	$\frac{AUC_i}{AUC} = \frac{V_{max}}{V_{max(inhibited)}}$

[a] AUC_i denotes the area under the curve after administration of the inhibitor. These equations assume that $[S] << K_M$.

Source: Adapted from Ref. 28.

the lines will be parallel [107]. Table 25.2 summarizes the changes in systemic exposure during different drug interaction scenarios [28].

Determining the type of inhibition mechanism and calculation of the inhibition constant, K_i, is very labor intensive, since the reaction velocity needs to be determined at several different inhibitor and substrate concentrations. Before determining the type of inhibition, it is helpful to investigate whether the inhibition is mechanism based, in which the case the inhibitor would irreversibly inactivate the enzyme. In this case, the inhibitor is preincubated with the enzyme for some time period before addition of the substrate. This preincubation allows the inhibitor to bind to the enzyme, and if the mechanism is irreversible, the reaction should proceed significantly slower than without preincubation.

Calculation of the IC_{50} is useful for determining whether the inhibitor is likely to have an *in vivo* significance. The IC_{50} can be determined by plotting the percentage of control (uninhibited) reaction velocity (R) versus the inhibitor concentration [I], at a constant substrate concentration. The resulting sigmoidal curve can be modeled with nonlinear regression and described with the following equation:

$$R = 100\left(1 - \frac{E_{max} C^A}{C^A + IC^A}\right)$$

where E_{max} is the maximum fractional inhibition, C is the concentration of the inhibitor, IC is the concentration that results in a reaction velocity of $50(2 - E_{max})$, which is the velocity at half the maximal inhibition, and A is an exponent relating the sigmoidal shape of the curve. The true IC_{50}, producing a velocity that is 50% of the control value, is calculated as [108]

$$\mathrm{IC}_{50} = \frac{IC}{(2E_{\max} - 1)^{1/A}}$$

Using this approach, the calculation of IC_{50} is model independent, since its value does not depend on the biochemical mechanism of inhibition (competitive vs. noncompetitive vs. uncompetitive). Lower IC_{50} values indicate greater inhibitory potency and IC_{50} will always be greater than or equal to K_i, the inhibition constant. If the mechanism of inhibition is "noncompetitive," they are equal [109]. If the mechanism of inhibition is reversible (competitive or noncompetitive), the preincubation process will not affect inhibitory potency, or may actually decrease inhibitory potency (higher IC_{50}) due to metabolic consumption of inhibitor in the microsomal system. If the inhibition is irreversible, the preincubation will increase inhibitory potency (lower IC_{50}).

Many metabolic enzymes obey atypical or nonlinear enzyme kinetics. CYP3A4 exhibits a sigmoidal saturation curve due to the existence of multiple binding sites on which substrates can bind cooperatively [110]. The v versus [S] plot is described by the following equation:

$$v = \frac{V_{\max}[\mathrm{S}]^n}{S_{50}^n + [\mathrm{S}]^n}$$

in which n refers to a Hill coefficient (which has to be greater than 1.0), and S_{50} is the substrate concentration at which the velocity is half of $V_{\max}$ [28].

Another possible complication in modeling drug–drug interactions is the possibility of concurrent inhibition and induction. Ritonavir is an example, since it is an inhibitor of CYP3A, but long-term administration induces the enzyme through the PXR receptor [111]. St. John's wort was found to produce the same effect; certain components of it are potent inhibitors of CYP3A, yet St. John's wort also activates CYP3A through PXR [112]. Inhibition and induction can be distinguished from each other since they occur on different time scales. Inhibition is an immediate phenomenon and can be studied in microsomes, which do not have the cellular machinery for inducing enzymes. Induction is a time-consuming process, where transcription alone can take 4–6 hours; however, in clinical trials it could take days to see any inductive effects, especially if inhibition is competing with induction. For example, in a trial where ritonavir and alprazolam were coadministered, there was a small decrease in the plasma concentration of alprazolam after 12 days, suggesting that induction was overcoming inhibition [28].

Besides metabolism, efflux transport is also a form of clearance and modeling of transporter systems is useful for determining the most important parameters in this process. Several computational models have been developed to study transporters. Jang et al. [113] modeled the P-glycoprotein-mediated efflux of the anticancer drug paclitaxel. The P-glycoprotein-mediated efflux rate can described as

$$\text{P-gp} - \text{efflux rate} = \frac{J_{\max} \cdot C_{\max}}{K_{\mathrm{M,P\text{-}gp}} + C_{\mathrm{free,c}}}$$

In this equation, which is analogous to the Michaelis–Menten model, $J_{\max}$ is the maximum efflux rate per cell, $K_{\mathrm{M,P\text{-}gp}}$ is the dissociation constant of the efflux process,

and $C_{free,c}$ is the free drug concentration inside the cells [114]. The concentration of the drug is then modeled using mass balance equations, which describe the amount of paclitaxel inside and outside the cells as a function of time. Using this approach, it was determined that the most important factor influencing the transport process is the extracellular drug concentration, followed by intracellular binding capacity and binding affinity, and finally P-glycoprotein expression. Furthermore, it was also shown that, similar to enzyme kinetics, P-glycoprotein efflux is a saturable process [115]. Pharmacokinetic modeling can also be used to determine which transport process is most relevant for a certain drug and what the rate constants are for a particular process [116].

In Vitro/In Vivo Scaling Clearance is an important parameter for *in vitro/in vivo* scaling, particularly in drug–drug interaction studies. *In vitro* studies are usually conducted in liver microsomes and several assumptions need to be made for scaling. First, one must assume that liver metabolism is the major route of clearance and that oxidative metabolism is much more significant than other forms of metabolism such as conjugation, hydrolysis, and reduction. Second, one must also assume that the rates of metabolism *in vivo* will be similar to those *in vitro*. The scaling factor is usually a function of the microsomal protein per gram liver and the weight of the liver in comparison to body weight. Livers are usually assumed to have 45–50 mg microsomes/gram liver. If one is to scale up from hepatocyte experiments, 120,000,000 hepatocytes/gram liver could be used as a scaling factor [28, 117]. If one is scaling up from hepatocyte experiments, it is not necessary to assume that oxidative metabolism is dominant since hepatocytes are capable of carrying out the other forms of biotransformation.

One of the challenges of scaling *in vitro* to *in vivo* is estimating the inhibitor concentration, [I]. In a microsomal incubation, [I] can be calculated directly from the experimental conditions. However, *in vivo* it is not clear what the proper [I] is, since the inhibitor concentration at the site of metabolism cannot be calculated from the administered dose. Some estimates of [I] include total inhibitor concentration in the plasma, unbound concentration in the plasma, or concentration at the target organ such as the intrahepatic concentration. So far, no general estimate has been found to correlate *in vitro* [I] to an *in vivo* [I] in every specific case. Complicating factors include intestinal metabolism, transporters, and flow-dependent clearance. In general, the larger the IC_{50} values, the less potent the inhibitor and the less likely that a clinically significant interaction will occur. Conversely, small IC_{50} values usually indicate a high likelihood of a clinical interaction. Large IC_{50} values are considered to be those higher than 100 μM, while small ones are usually less than 1 μM. The challenge is to interpret "intermediate" values of IC_{50}. Calculating $[I]/K_i$ can also be helpful in determining the likelihood of an *in vivo* interaction. The larger the ratio the more likely the possibility of an interaction. If the ratio is less than 0.5, the interaction is unlikely; but if $[I]/K_i$ is higher than 5, a clinically significant interaction is probable [109, 118].

25.1.5 Conclusions

Drug–drug interactions can occur through multiple pathways, where the perpetrator drug can influence the absorption, distribution, metabolism, and elimination of the

victim drug. Based on empirical data, the most common interactions occur through the inhibition or induction of the cytochrome P450s and the efflux transporter P-glycoprotein. Clinically significant drug interactions can lead to an increase in systemic blood concentrations (possibly causing toxicity), or a decrease in the plasma concentrations (corresponding to lack of efficacy). The success of combination HIV protease inhibitors illustrates the principle of pharmacoenhancement, where the combined formulation of two drugs is designed such that one drug improves the efficacy of the second drug. This improvement usually occurs by increasing the AUC, C_{max}, or the half-life of the boosted drug, thus increasing the overall systemic exposure to the compound. In this section we have also discussed the pharmacokinetic principles of drug–drug interactions as well as the challenges associated with predicting *in vivo* interactions from *in vitro* data. It is clear that it is currently very difficult to make clinically significant predictions based on *in vitro* data, even with the use of mathematical modeling. In Case Study A, we discuss the pharmacokinetics of benzodiazepines, particularly triazolam. We show several aspects of drug interactions with benzodiazepines, including *in vitro* and *in vivo* studies, prediction of clinical interactions, differences between males and females and different age groups, and also pharmacokinetic/pharmacodynamic integration. As is clear from the discussion so far, over-the-counter preparations (including herbal supplements) and foods can significantly contribute to drug–drug interactions. In Case Study B, we review the most commonly used herbs, mechanisms of drug interactions, and reports of clinically significant adverse events.

25.2 CASE STUDY A: DRUG–DRUG INTERACTIONS WITH TRIAZOLAM AND OTHER BENZODIAZEPINES

25.2.1 Introduction

Among the most commonly prescribed benzodiazepines are triazolam, midazolam, lorazepam, diazepam, and alprazolam. Triazolam, a short half-life triazolobenzodiazepine, is now one of the accepted clinical probes for monitoring CYP3A activity in human studies as it is metabolized primarily by CYP3A [119]. Since triazolam is a hypnotic, it has also been useful for pharmacodynamic experiments. The purpose of this case study is to review the series of *in vitro* and *in vivo* experiments that explored the pharmacokinetics and pharmacodynamics of triazolam and related benzodiazepines in the presence of other drugs, particularly CYP3A inhibitors. This case study also discusses (1) contributions from different CYP3A isoforms, (2) hepatic versus intestinal CYP3A, (3) effects of benzodiazepines in young versus elderly individuals, and (4) pharmacokinetic/pharmacodynamic integration.

25.2.2 Metabolic Interactions

Triazolam is metabolized primarily by CYP3A4 and it forms the α-hydroxy and 4-hydroxy metabolites [120]. These compounds have less activity than triazolam and are further conjugated to the glucuronide metabolites [121]. Triazolam metabolism is known to be inhibited by several classes of CYP3A inhibitors such as macrolide antibiotics [122], azole antifungal agents [123], and some SSRI antidepressants [124].

On the other hand, drugs that induce CYP3A would be expected to impair the effectiveness of triazolam. Coadministration of rifampin, an inducer of CYP3A4, greatly reduces the pharmacodynamic effects of triazolam [125]. Coadministration of triazolam with ritonavir poses an interesting clinical dilemma because ritonavir has been shown to concurrently induce and inhibit CYP3A [126]. During short-term administration, ritonavir inhibits the clearance the triazolam, but during long-term dosage the net effect of the coadministration is not easily predicted [111].

25.2.3 *In Vitro* Studies

The metabolism of triazolam was examined *in vitro* in human liver microsomes in the presence of several CYP3A inhibitors including ketoconazole, erythromycin, and several types of SSRIs in order to assess the likelihood of a clinical interaction [33]. Without inhibition, the V_{max} and K_M values for the formation of the 4-OH metabolite were 10.3 nM/min/mg of protein and 304 μM. For the α-OH pathways, these values were 2.4 nM/min/mg and 74 μM, respectively [124]. However, the V_{max}/K_M ratios were the same for both metabolites, suggesting that each pathway contributes equally to clearance.

Ketoconazole was found to be the most potent inhibitor with a K_i of 0.006 μM for the α-OH metabolite and 0.023 for the 4-OH metabolite. The weakest inhibitor was erythromycin with K_i values of 36.6 μM and 111 μM for the α-OH and 4-OH pathways, respectively. Several SSRIs were also inhibitors of CYP3A, including fluoxetine, norfluoxetine, and sertraline.

The metabolism of midazolam was also examined *in vitro* in the presence of SSRIs and azole antifungal agents [127]. Midazolam also forms the α-OH and 4-OH metabolites, and without inhibition the formation of the α-OH metabolite was a higher affinity process (K_M = 3.3 μM) than the formation of the 4-OH metabolite (K_M = 57 μM). Based on the V_{max}/K_M ratios, it was estimated that α-OH accounted for 95% of intrinsic clearance. Competitive inhibition constants (K_i) versus the formation of the α-OH metabolite for the antifungal agents ketoconazole, itraconazole, and fluconazole were 0.0037 μM, 0.27 μM, and 1.27 μM, respectively. The K_i values for the α-OH pathway for fluoxetine and its metabolite norfluoxetine were 11.5 μM and 1.44 μM, respectively, which was consistent with previous clinical findings, which suggested that fluoxetine impairs the clearance of CYP3A substrates. Furthermore, these results suggest that most of the inhibition is due to the metabolite norfluoxetine rather than the parent compound fluoxetine.

The CYP3A family is thought to consist of at least three isoforms—CYP3A4, CYP3A5, and CYP3A7. While CYP3A4 is considered to be the dominant isoform, CYP3A5 has been detected in 10–25% of adult livers [128] and CYP3A7 is thought to be present in up to 50% of adult livers, particularly from African-Americans [129–131]. The metabolism of both triazolam and midazolam, as well as testosterone and nifedipine, was examined in human liver microsomes and recombinant CYP3A4 and CYP3A5 to investigate the contribution of each isoform in the metabolism of these drugs [132]. Overall, CYP3A4 contributed more than CYP3A5 in the metabolism of all the compounds. Ketoconazole significantly inhibited metabolism in microsomes and recombinant CYP3A4. The inhibition for CYP3A5 was 5–19-fold less than for CYP3A4 for all substrates, suggesting that CYP3A5 might not be as significant as CYP3A4 in drug interactions with ketoconazole. Although there seems

to be a significant interindividual variability in CYP3A5 content, with some samples having up to 25% as much CYP3A5 as CYP3A4, the overall net contribution is probably dominated by CYP3A4.

25.2.4 Pharmacokinetic Clinical Studies

It is important to note that clinically significant drug–drug interactions are not very common and, most frequently, coadministration of two drugs results in no change in the pharmacokinetic or pharmacodynamic profile of either drug. Occasionally, there is a change in the kinetic profile but it is only rarely large enough to be clinically significant [133].

Inhibition of triazolam metabolism by ketoconazole was confirmed in clinical trials where a 200 mg dose of ketoconazole reduced the oral clearance of 0.125 mg triazolam ninefold and prolonged half-life fourfold [124]. This degree of inhibition was correctly predicted by an *in vitro–in vivo* scaling model, which assumed competitive inhibition:

$$\text{Fractional decrement} = \frac{I}{I + K_i(1 + S/K_M)}$$

If S is much less than K_M, this equation can be approximated as

$$\text{Fractional decrement} = \frac{I}{I + K_i}$$

This equation holds true in the case of noncompetitive inhibition regardless of the substrate concentration [124].

Triazolam is a relatively high extraction drug, metabolized primarily by CYP3A4, with oral bioavailability around 50%. The plasma levels of high extraction drugs are expected to be influenced significantly when combined with inhibitors of the key metabolic enzymes. Figure 25.2 shows the pharmacokinetic and pharmacodynamic profiles of triazolam when the drug was coadministered with ketoconazole. After coadministration, there was a 10-fold decrease in the clearance of triazolam, which was accompanied by a drop in the pharmacodynamic marker, the digit-symbol-substitution test (DSST). On the other hand, alprazolam is a low extraction drug (also metabolized by CYP3A4) with a bioavailability of 90%. After coadministration with ketoconazole, its clearance was only reduced threefold, in contrast to the 10-fold decrease observed with triazolam [134].

The expression of hepatic and intestinal CYP3A are influenced by different environmental factors and thus their contributions to the metabolism of drugs need to be distinguished. For example, 6,7-dihydroxybergamottin, a component in grapefruit juice, primarily inhibits intestinal CYP3A and is thus only expected to interfere with drugs whose metabolism is primarily carried out by enteric CYP3A. In order to distinguish between the contributions of hepatic and intestinal metabolism, a drug is usually administered in two separate trials: once orally, when the drug undergoes both hepatic and intestinal metabolism, and then intravenously when the contribution from intestinal metabolism is considered negligible. Midazolam is also one

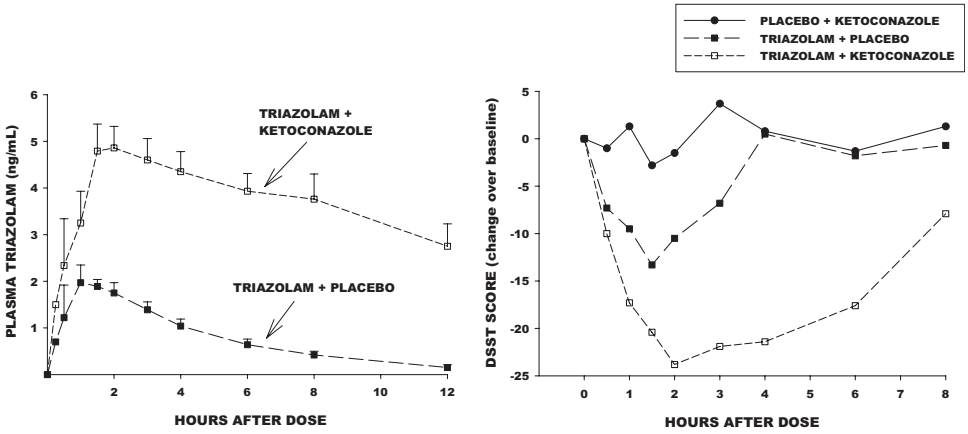

FIGURE 25.2 Pharmacokinetic and pharmacodynamic interactions between triazolam and ketoconazole. Healthy male volunteers received 0.25 mg triazolam and 200 mg ketoconazole or placebos orally. The diagram on the left shows the mean (+SE) plasma concentration of triazolam (ng/mL) with and without ketoconazole. The diagram on the right illustrates the results of the digit-symbol-substitution test (DSST) under the three conditions listed [134].

of the accepted CYP3A clinical probes and its metabolism was studied in the presence of ketoconazole to determine contributions from intestinal and hepatic CYP3A [129]. After ketoconazole administration the AUC of intravenous midazolam increased fivefold, whereas after oral administration it increased 16-fold. The bioavailability of the intestinal component also increased more significantly than the hepatic component after ketoconazole therapy. These results suggest that intestinal CYP3A contributes significantly to midazolam clearance after oral dosage. Interestingly, females had a higher clearance of midazolam than males. Most other studies with benzodiazepines found no statistically significant difference between males and females, although females in general have higher clearances than males, possibly because females have increased enteric CYP3A [135]. However, the sample size in this study was small (three females and six males), thus larger studies would be needed to confirm a difference.

On the other hand, the clearance of CYP3A substrates is found to decrease with age, particularly in men, possibly due to decreases in hepatic and renal clearance [136]. A clinical trial with triazolam showed that elderly women (over 60 years of age) had a small increase in AUC and a decrease in clearance compared with younger women (20–36 years of age) but these differences were not statistically significant. However, in elderly men the AUC values were 75% higher and clearances were 28% lower than in younger men (Fig. 25.3) [137]. These findings concur with previous research, which suggested that age-related decrease in clearance of CYP3A substrates might be more significant in men.

25.2.5 Pharmacokinetic/Pharmacodynamic Integration

The goal of pharmacokinetic/pharmacodynamic (PK/PD) studies is to correlate changes in the plasma levels of drugs with observed pharmacodynamic effects. In

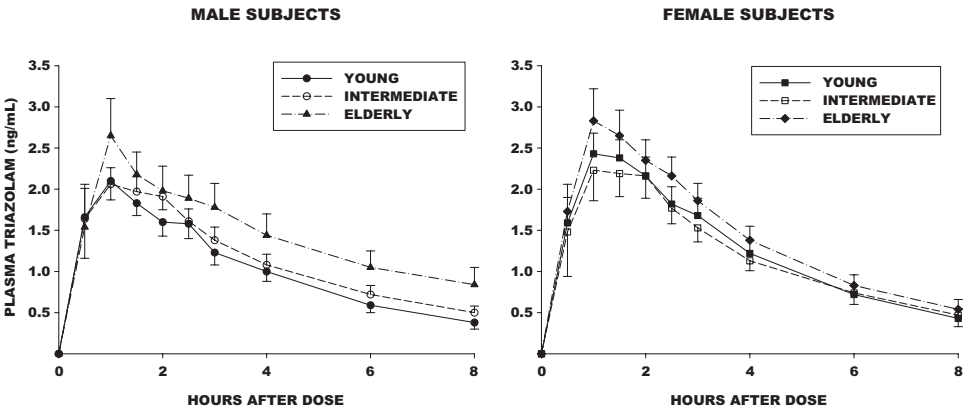

FIGURE 25.3 Mean (±SE) plasma triazolam levels (ng/mL) for male and female volunteers in different age groups after administration of 0.25 mg triazolam. The age groups were young (20–36 years old), intermediate (40–56 years old), and elderly (60–75 years old) [137].

the previous section we discussed that the pharmacokinetics of triazolam were more affected than the pharmacokinetics of alprazolam. Pharmacodynamic studies consisting of electroencephalographic (EEG) beta activity and the digit-symbol-substitution test (DDST) also showed a similar pattern. For alprazolam, ketoconazole increased EEG and DSST by factors of 1.35 and 2.29, respectively, whereas these numbers increased by factors of 2.51 and 4.33, respectively, for triazolam [134]. Thus, the consequences of coadministering a high extraction compound such as triazolam with a CYP3A inhibitor could be clinically more important than administering the CYP3A inhibitor with a low extraction drug such as alprazolam.

The pharmacodynamics of triazolam in elderly volunteers followed a pattern similar to the pharmacokinetics. Probably due to decreased clearance, elderly subjects experienced more pronounced pharmacodynamic effects such as sedation and impairment of motor coordination [137–139]. For example, the values for percent decrement in the DSST after triazolam administration were -5.9 ± 1.9 and -8.6 ± 1.9 in young and elderly women, respectively (Fig. 25.4) [137]. These values in young and elderly men were -5.4 ± 2 and -11.4 ± 2, respectively. It was of note that self-rated sedation actually decreased in elderly subjects after triazolam administration despite an increase in the observer-rated sedation and a decrease in the percent beta amplitude. It is possible that elderly subjects were not aware of their sedation or their reporting did not match with their true sedation levels. Thus, prescribing benzodiazepines for the elderly could be a concern if they are not fully aware of their sedation or cannot report the effects of these drugs.

Another concern with an elderly population is the increase in the likelihood of drug interactions within multidrug regimens. Steroid hormones, such as progesterone, have been known to exert effects on the central nervous system [140]. Thus, the pharmacodynamic interaction between triazolam and progesterone has been investigated in postmenopausal women, since this population previously was likely to be concurrently taking both drugs [141]. In a randomized trial, one group received intravenous triazolam plus oral progesterone (300 mg) or intravenous triazolam plus oral placebo. The pharmacokinetic parameters such as AUC were similar between

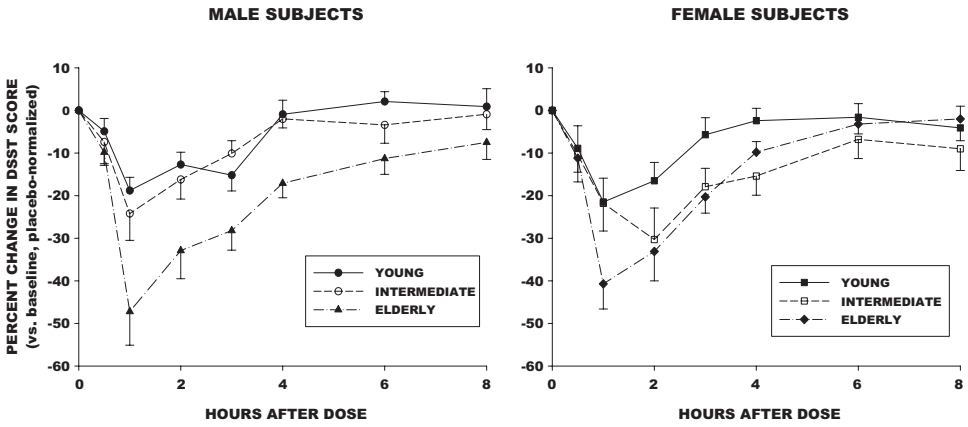

FIGURE 25.4 Percent change (±SE) in digit-symbol-substitution test (DSST) scores for male and female volunteers in different age groups after administration of 0.25 mg triazolam. The age groups were young (20–36 years old), intermediate (40–56 years old), and elderly (60–75 years old) [137].

both groups but pharmacodynamic testing showed that progesterone potentiated the sedative effects of triazolam, suggesting that women taking progesterone might have an increased sensitivity to triazolam or other benzodiazepines. The pharmacodynamic effects of progesterone are attributed to a metabolite 3α-hydroxy-5α-dihydroprogesterone, which modulates the GABA receptor complex and regulates brain excitability [141, 142].

Pharmacodynamic effects are influenced not only by plasma levels but also by the concentration of drug in the brain and the binding of the drug to its receptor. Interestingly, the pharmacodynamic effects of triazolam in the presence of ketoconazole are less potent than expected based on plasma levels. Thus, the effects of ketoconazole on triazolam receptor binding were investigated in mice who received 50 mg/kg ketoconazole and 0.1–0.3 mg/kg of triazolam [143]. Ketoconazole was found in the brains at 31% of the plasma levels and its coadministration also increased triazolam levels in the brain compared to controls. *In vitro* binding studies also demonstrated that ketoconazole inhibits triazolam displacement of [^{3}H]flunitrazepam binding by 36–89% depending on ketoconazole concentration. Thus, these data suggest that, in addition to inhibiting CYP3A metabolism, ketoconazole also interferes with triazolam binding in the brain and could impair its pharmacodynamic effects.

The efflux transporter P-glycoprotein, or MDR1, has been shown to be involved in drug disposition in many organs including the liver, kidney, intestines, and brain. As an efflux transporter, MDR1 can limit the transport of drugs into epithelial cells and enhance the excretion of drugs from hepatocytes and renal tubules [144]. The role of P-glycoprotein is especially critical in the blood–brain barrier, where the endothelial cells lining the blood vessels are joined so closely together that only lipophilic drugs can enter via passive diffusion [63]. Since triazolam needs to cross the blood–brain barrier to reach its receptor, one of the questions is whether efflux transport by P-glycoprotein influences the disposition of triazolam in the brain. The effect of P-glycoprotein on triazolam distribution was investigated by comparing

brain levels of ketoconazole and triazolam in P-glycoprotein-deficient mice and matched controls [145]. Interestingly, triazolam levels were the same in both mouse types, but P-glycoprotein-deficient mice had higher levels of ketoconazole. Coadministration of the two drugs did not alter their levels in the brain. Thus, while triazolam is not a P-glycoprotein substrate in the blood–brain barrier, ketoconazole may be transported by P-glycoprotein.

25.2.6 Conclusions

We have discussed the methods for investigating different aspects of drug–drug interactions. An initial estimate of clinical significance comes from *in vitro* studies with microsomes, which can be later confirmed with clinical trials. In order to differentiate between enteric and hepatic metabolism it is necessary to administer a drug in clinical trials orally and intravenously and compare the clearances from each administration. *In vitro* studies have also shown that, among the CYP3A isoforms, CYP3A4 is probably an important contributor to the metabolism of benzodiazepines. It is also important to specify the study population in clinical trials. As we have shown, there are significant differences between age groups, both in terms of clearance of benzodiazepines and in their pharmacodynamic responses to the drugs. The elderly seem particularly susceptible to the sedative effects of benzodiazepines. This effect may be partially due to lower hepatic clearance. However, the concentration–effect relationship was also more pronounced in the elderly, suggesting that the same concentration produces a more significant effect than in younger volunteers. While a substantial difference between males and females could not be consistently demonstrated in benzodiazepine trials, CYP3A is known to be influenced by the hormonal environment. Thus, sex differences should also be considered as variables in human studies.

25.3 CASE STUDY B: DRUG INTERACTIONS WITH HERBS AND NATURAL FOOD PRODUCTS

25.3.1 Introduction

The consumption of herbal supplements is increasing among both adults and children. Although estimates of the percentage of adults using herbals varies depending on survey methods (ranging from 12% to over 50%), the sales of herbals have been increasing about 25% a year with the approximate yearly sales now being over 4 billion dollars [146]. Herbal usage has become especially common among chronically ill patients, including cancer and HIV patients, who are on multidrug regimens and have an increased risk of drug–herbal interactions. There have also been reports of as many as 45% of adults giving their children herbal supplements as well as 45% of pregnant women consuming herbals [147, 148].

Increased consumption of herbals is a concern for drug manufacturers since the FDA requires proper labeling of pharmaceuticals regarding possible adverse interactions. For example, the consumption of grapefruit juice is contraindicated on the labeling of several drugs, such as lovastatin, atorvastatin, and cyclosporine. Grapefruit juice is also reported to interact with other pharmaceuticals including calcium channel antagonists, sedatives, and HIV protease inhibitors [149]. The FDA is very

aware of clinically significant interactions with herbs and natural food products. In February of 2000 the FDA issued a warning after clinical trials showed a substantial decrease in the plasma levels of indinavir when combined with St. John's wort. The FDA also warned against coadministration of St. John's wort with all other nonnucleoside reverse transcriptase protease, inhibitors, such as nevirapine [147, 150].

While herbs consist of chemical compounds just like pharmaceuticals, it is challenging to conduct a systematic investigation of potential herb–drug interactions because (1) herbs are regulated differently than pharmaceuticals, (2) they consist of several (sometimes over 100) active ingredients, and (3) there are many different preparations and batch-to-batch variations. Many reports of herb–drug interactions originate primarily from case studies rather than controlled trial studies, therefore cause–effect relationships are difficult to prove [151]. In this section we discuss the regulation of herbal products, mechanisms of drug–herb interactions, and clinically significant adverse events.

25.3.2 Regulation of Herbal Supplements

Herbs are considered dietary supplements and are regulated in the United States by the Dietary Supplement Health and Education Act of 1994. This legislation is significantly more lenient than European and Japanese regulations, which treat herbal products the same way as pharmaceuticals [152]. Herbal product manufacturers are allowed to make claims on the function of herbs without proof regarding safety and efficacy; however, they must also state that these statements have not been evaluated by the FDA. Under the Dietary Supplement Health and Education Act, the herb manufacturers are responsible for monitoring the safety of herbal products [153] but the safety guidelines are not well established. Surprisingly, according to surveys almost 60% of adults believe that herbs need approval before being sold [152]. However, manufacturers of herbal and dietary supplements do not need to report adverse events to the FDA, and the FDA needs to prove that supplements are unsafe before they can be removed from the market [154].

Commercially available herbal preparations vary substantially in their compositions and frequently their labeling does not reflect their true compositions. Thin-layer chromatographic analysis of 59 commercial echinacea preparations showed that the labeling was consistent with the content in only 31 samples and 6 samples contained no echinacea at all [155]. Another study with ginseng products showed that there was a 15–200-fold variation in the concentration of ginsenosides and eleutherosides, which are considered the biologically active ingredients [146, 156].

The most commonly used herbs in the United States are echninacea, garlic, *Ginkgo biloba*, saw palmetto, ginseng, grape seed extract, green tea, St. John's wort, bilberry, and aloe [146]. In order to illustrate the major concepts regarding herbal and food–drug interactions, this case study discusses primarily St. John's wort, *Ginkgo biloba*, garlic, and echinacea.

25.3.3 Influence of Herbal Constituents on Drug Metabolism *In Vitro*

Herbs are complex mixtures of chemicals such as flavonoids, polyphenols, alkaloids, triterpenoids, and anthraquinones—all of which have been shown to modulate CYP450 activity *in vitro* [157]. As will be discussed, multiple components may

induce or inhibit an enzyme, but frequently they do not lead to clinically significant interactions.

Hyperforin and hypericin are the two components in St. John's wort believed to be responsible for the antidepressant effects. However, the inhibition and induction capacities of St. John's wort are attributed primarily to hyperforin [158]. *In vitro* studies with cDNA-expressed cytochrome P450 enzyme systems showed that hyperforin is a significant inhibitor of CYP1A2, CYP2C9, CYP2C19, and CYP3A4 with IC_{50} values of 3.87, 0.01, 0.02, and 4.20 μM, respectively. In general, potent inhibitors are considered those with IC_{50} values less than 10 μM [159], although clinically significant interactions are expected when the IC_{50} values are less than 1 μM. Hyperforin also induces intestinal P-glycoprotein in isolated cells [160] and volunteers [161]. This effect is also thought to be mediated by the binding of hyperforin to the pregnane X receptor (PXR) inducing CYP2B6, CYP3A4, and P-glycoprotein [147, 162, 163]. Other herbal inhibitors of P-glycoprotein include ginsenosides, piperine, sylmarin, and catechins from green tea [164].

Consumption of garlic is thought to be beneficial for many health conditions including atherosclerosis and peptic ulcer disease and as a chemopreventative agent for gastric tumors [165]. However, extracts from garlic, in particular, the volatile components, diallyl sulfide, dipropyl sulfide, and dipropyl disulfide, have been shown to interact with a number of CYP450s *in vitro* [166, 167]. CYP2C9, CYP2C19, CYP3A4, CYP3A5, CYP3A7, and CYP2E1 were shown to be inhibited, whereas CYP1A2, CYP2B, and CYP3A were induced [168–170]. Interestingly, garlic seemed to have little effect on CYP2D6 activity (less than 10% inhibition). In the study by Foster et al. [169], modulation of CYP450 was compared across several garlic preparations, specifically garlic oil, odorless garlic preparations, freeze-dried garlic tablets, and three types of garlic bulbs (common, elephant, and Chinese). CYP3A4 was significantly inhibited by all of the products and in the case of the tablets inhibition was over 95%. Inhibition of three CYP3A isoforms (CYP3A4, CYP3A5, CYP3A7) was also compared by the three types of garlic bulbs. All of the isoforms were inhibited, but CYP3A4 was affected the most with inhibition ranging from almost 40% to over 58%. Interestingly, these garlic preparations had little effect on P-glycoprotein compared with verapamil, the positive control [169].

An investigation of 29 constituents of *Ginkgo biloba* revealed inhibitory potential for all of the five major cytochrome P450s (CYP1A2, CYP2C9, CYP2C19, CYP2D6, and CYP3A) in human liver microsomes [171]. Quercetin and amentoflavone inhibited three or more isoforms and nine constituents inhibited CYP3A. The mean IC_{50} values ranged from 0.035 to over 100 μM, although most of the values were between 1 and 30 μM. In cDNA-expressed cytochrome P450 enzyme systems (CYP1A2, CYP2C9, CYP2C19, CYP2D6, and CYP3A4), ginkgolic acids I and II inhibited CYP1A2, CYP2C9, CYP2C19, CYP2D6, and CYP3A4 with the IC_{50} values being 4–5 μM for CYP1A2 and CYP2C19, around 2 μM for CYP2C9, 7–11 μM for CYP2D6, and 6–7 for CYP3A4 [159]. Interestingly, *Ginkgo biloba* increased clearance of the calcium channel blocker nicardipine in rats, suggesting induction of CYP3A2 [172]. Overall, *Ginkgo biloba* increased the expression of CYP2B1/2 and CYP3A1/2 in rats but did not affect CYP1A1/2, CYP2C11, or CYP4A1 [172, 173].

While *Ginkgo biloba* modulated CYP3A *in vitro* and in animal studies, there are few controlled clinical case studies suggesting herb–drug interactions through

enzyme modulation by *Ginkgo biloba* [166, 174]. It must be noted that the absence of evidence for clinically significant CYP3A4 inhibition in humans does not necessarily mean that such an interaction could not occur. *In vitro* studies have demonstrated potent inhibition of this enzyme and conflicting findings on *Ginkgo biloba* in clinical trials could be due to variations in *Ginkgo biloba* preparations [175].

25.3.4 Clinically Significant Drug Interactions

While many of these investigations have been successful at identifying drug-inducing or drug-inhibiting components, many *in vitro* studies did not correctly predict clinically significant interactions [166]. As mentioned in Case Study A, clinically significant drug interactions are relatively rare and occur primarily when the therapeutic index is very narrow or if the perpetrator is a very significant modulator of a metabolic enzyme. Table 25.3 shows representative examples of clinically significant drug–herb interactions.

Warfarin, an example of a drug with a narrow therapeutic index, is metabolized almost exclusively by CYP2C9 [176]. In a small clinical study, American ginseng has been shown to cause a slight but statistically significant decrease in the AUC of warfarin as well as the INR (International Normalized Ratio, a number used to characterize blood clotting) of patients, suggesting that ginseng could decrease the efficacy of warfarin. *Ginkgo biloba* contains several inhibitors of CYP2C9, the most potent being amentoflavone with an IC_{50} around 0.035 μM [171]. Several anectodal case reports suggested potentiation of warfarin coagulation by *Ginkgo biloba*; this phenomenon could not be demonstrated in controlled clinical trials [22, 177].

Herb–drug interactions are a particular concern for the elderly since they (1) are usually on multidrug regimens, increasing the likelihood of interactions, and (2) have decreased hepatic and renal clearance compared to a younger population [178]. Clinical studies with hyperforin in healthy elderly volunteers (60–76 years) showed a 140% induction of CYP3A4 compared to a 98% induction in young volunteers, despite the fact that the young volunteers were administered 2.5 times the dose of the elderly. Interestingly, the serum concentrations were also similar (42.6 ng/mL in

TABLE 25.3 Clinically Significant Interactions Between Herbs and Prescription Drugs

Herb/Food Product	Clinical Interaction	Potential Mechanism
St. John's wort	Digoxin [181]	Induction of P-gp
	Simvastatin [182], alprazolam, midazolam [180, 185]	Induction of CYP3A4
	Amitriptyline [183], indinavir [186], nevirapine [187]	Induction of CYP3A4 and P-gp
	Buspirone [184]	Inhibition of serotonin reuptake
Echinacea	Midazolam [188]	Induction of CYP3A4
	Caffeine [188]	Induction CYP 1A2
Garlic	Ritonavir [191], saquinavir [192]	Induction of transporter, not necessarily P-gp [169]
	Warfarin [195]	Enhancement of anticoagulation
Ginko biloba	Aspirin, warfarin [196], ibupofen [197], rofecoxib [147, 198]	Enhancement of anticoagulation

young vs. 51.2 ng/mL in old) [179]. This data suggests that the elderly are particularly susceptible to the inductive effects of hyperforin on CYP3A4 activity.

The antidepressant effect of St. John's wort has been confirmed in clinical trials [164] and is attributed partially to hyperforin, which inhibits the uptake of neurotransmitters in synapses. However, St. John's wort has been linked to many clinically significant and even potentially fatal drug interactions. Long-term (2 weeks) St. John's wort administration has been shown to induce both intestinal and hepatic CYP3A4 [147, 180]. St. John's wort has been reported to interact with protease inhibitors, oral contraceptives, and anticoagulants, as well as cyclosporine, digoxin, amitryptiline, and theophylline. Effects of these interactions included organ rejection (with cyclosporine), unplanned pregnancies and intermenstrual bleeding (with contraceptives), and decreases in the efficacies of antiretrovirals and anticoagulants [158].

In a clinical study, St. John's wort was also shown to decrease plasma levels of digoxin, probably through the induction of P-glycoprotein [181]. Clinical studies also reported decreased plasma concentration of simvastatin but not pravastatin when combined with St. John's wort [182]. Due to hyperforin's ability to inhibit the reuptake of brain neurotransmitters, such as serotonin, St. John's wort can also interact with antidepressants and anxiolytic drugs. In clinical studies, St. John's wort decreased the plasma and urine concentrations of the tricyclic antidepressant amitriptyline, presumably through the induction of P-glycoprotein and CYP3A4 [183]. In a reported case study, a patient experienced serotonin syndrome after combining St. John's wort with the anxiolytic drug buspirone, which is a 5-HT1 receptor agonist [184]. In multiple clinical studies, the plasma levels of the CYP3A4 probes alprazolam and midazolam were decreased after treatment with St. John's wort [180, 185]. The plasma concentrations of the antiretroviral drugs indinavir [186] and nevirapine [187] were also reduced when the drugs were combined with St. John's wort. Such an interaction could have serious implications, including reduced treatment efficacy and drug resistance [147].

Echinacea represents 10% of the U.S. herb market and is commonly used for immune system stimulation [155]. Echinacea is also known to modulate CYP3A4 and in human studies it was observed to induce hepatic CYP3A4 but inhibit intestinal CYP3A4 [188]. Specifically, echinacea increased the systemic but not the oral clearance of midazolam by 34%. Increase in systemic clearance is probably due to induction of CYP3A4 (since in this case the contribution of intestinal CYP3A4 is considered negligible) whereas with oral clearance, hepatic induction might be counteracted with intestinal inhibition of CYP3A4. Echinacea also reduced the oral clearance of caffeine (CYP1A2 substrate) and tolbutamide (CYP2C9 substrate), although the latter increase was not statistically significant. The clearance of the CYP2D6 substrate dextromethorphan was not affected. Thus, echinacea would be expected to interact with drugs that are substrates for CYP1A2 and CYP3A4 [188].

Garlic has been cultivated for over 5000 years as a culinary and medicinal herb and it was one of the best-selling herbs in 2002 [175, 189]. In clinical studies garlic did not influence the clearance of caffeine, dextromethorphan, and the CYP3A4 substrate alprazolam [190]. While these clinical studies suggest that garlic does not affect CYP3A4, garlic has been shown to decrease the AUC of ritonavir [191] and saquinavir [192]. Thus, the interaction may occur through a transporter, but not necessarily P-glycoprotein [169]. Garlic did not influence the metabolism of

acetaminophen [193], but it did enhance the anticoagulant effects of warfarin, leading to an increase in clotting time [194, 195].

In vitro studies reported that *Ginkgo biloba* is an inhibitor of CYP1A2, CYP2C9, CYP2C19, CYP2D6, and CYP3A4 [171]. Furthermore, several case studies have suggested that this interaction could be of clinical importance; however, this has not been confirmed by clinical studies. In case studies *Ginkgo biloba* has been reported to lead to increased bleeding in patients taking nonsteroidal anti-inflammatory drugs such as aspirin[196], ibuprofen [197], and the cyclo-oxygenase-2 inhibitor rofecoxib [147, 198], and in one case the combination of *Ginkgo biloba* and ibuprofen led to intracerebral bleeding and death [197]. While in a case study *Ginkgo biloba* has been reported to increase the anticoagulant effect of warfarin [196], a randomized clinical trial showed that recommended doses of *Ginkgo biloba* did not affect the pharmacokinetics or pharmacodynamics of warfarin [199].

25.3.5 Conclusions

In vitro and clinical studies have clearly demonstrated the potential for serious and possibly fatal interactions between herbal supplements and prescription medications. In general, the public views these supplements as natural and safe, and more than half of adults believe that herbals need to be approved before reaching the market. With the FDA becoming increasingly aware of herb–drug interactions and requiring proper labeling (as in the case of grapefruit juice), drug developers need to consider the possibility of coadministration with herbal supplements. While it would be impossible to examine all the possible herb–drug interactions, the *in vitro* effects of most commonly used herbs have been examined. Thus, based on metabolic studies, one could predict which herbs a drug might interact with.

St. John's wort is of particular concern, due to its potent induction of both CYP3A4 and P-glycoprotein. Clinical studies have confirmed that this herb can lead to potent interactions with several prescription drugs such as digoxin, antidepressants, benzodiazepines, and antiretrovirals. In the case of cyclosporine, an interaction could lead to organ rejection and be fatal. Other herbs such as echinacea, garlic, and *Ginkgo biloba* have also been reported to interact with prescription drugs. While these are some of the most commonly used herbs, they are not the only ones suspected of drug interactions. Other herbs such as kava-kava, ginger, ginseng, and green tea have also been reported to lead to adverse effects when coadministered with certain prescription drugs, and further clinical studies are necessary to the assess the effects of these herbs on medications [147].

ACKNOWLEDGMENTS

Supported by Grants AT-003540, AG-017880, and AI-058784 from the United States Department of Health and Human Services.

REFERENCES

1. Pratt C, Brown AM, Rampe D, Mason J, Russell T, Reynolds R, Ahlbrandt R. Cardiovascular safety of fexofenadine HCl. *Clin and Exp Allergy* 1999;29(Suppl 3): 212–216.

2. Jorgensen T, Johansson S, Kennerfalk A, Wallander MA, Svardsudd K. Prescription drug use, diagnoses, and healthcare utilization among the elderly. *Ann Pharmacother* 2001;35:1004–1009.
3. Hanlon JT, Fillenbaum GG, Ruby CM, Gray S, Bohannon A. Epidemiology of over-the-counter drug use in community dwelling elderly: United States perspective. *Drugs Aging* 2001;18:123–131.
4. Nix DE, Di Cicco RA, Miller AK, Boyle DA, Boike SC, Zariffa N, Jorkasky DK, Schentag JJ. The effect of low-dose cimetidine (200 mg twice daily) on the pharmacokinetics of theophylline. *J Clin Pharmacol* 1999;39:855–865.
5. Anantharaju A, Feller A, Chedid A. Aging liver. A review. *Gerontology* 2002;48: 343–353.
6. Blower P, de Wit R, Goodin S, Aapro M. Drug–drug interactions in oncology: Why are they important and can they be minimized? *Crit Rev Oncol/Hematol* 2005;55:117–142.
7. Werneke U, Earl J, Seydel C, Horn O, Crichton P, Fannon D. Potential health risks of complementary alternative medicines in cancer patients. *Br J Cancer* 2004;90:408–413.
8. Greenblatt DJ, von Moltke LL, Harmatz JS, Chen G, Weemhoff JL, Jen C, Kelley CJ, LeDuc BW, Zinny MA. Time course of recovery of cytochrome P450 3A function after single doses of grapefruit juice. *Clin Pharmacol Ther* 2003;74:121–129.
9. Greenblatt DJ, Patki KC, von Moltke LL, Shader RI. Drug interactions with grapefruit juice: an update. *J Clin Psychopharmacol* 2001;21:357–359.
10. Malhotra S, Bailey DG, Paine MF, Watkins PB. Seville orange juice–felodipine interaction: comparison with dilute grapefruit juice and involvement of furocoumarins. *Clin Pharmacol Ther* 2001;69:14–23.
11. Hidaka M, Okumura M, Fujita K, Ogikubo T, Yamasaki K, Iwakiri T, Setoguchi N, Arimori K. Effects of pomegranate juice on human cytochrome P450 3A (CYP3A) and carbamazepine pharmacokinetics in rats. *Drug Metab Dispos* 2005;33:644–648.
12. Hidaka M, Fujita K, Ogikubo T, Yamasaki K, Iwakiri T, Okumura M, Kodama H, Arimori K. Potent inhibition by star fruit of human cytochrome P450 3A (CYP3A) activity. *Drug Metab Dispos* 2004;32:581–583.
13. Martin-Facklam M, Burhenne J, Ding R, Fricker R, Mikus G, Walter-Sack I, Haefeli WE. Dose-dependent increase of saquinavir bioavailability by the pharmaceutic aid Cremophor EL. *Br J Clin Pharmacol* 2002;53:576–581.
14. Tayrouz Y, Ding R, Burhenne J, Riedel KD, Weiss J, Hoppe-Tichy T, Haefeli WE, Mikus G. Pharmacokinetic and pharmaceutic interaction between digoxin and Cremophor RH40. *Clin Pharmacol Ther* 2003;73:397–405.
15. Balayssac D, Authier N, Cayre A, Coudore F. Does inhibition of P-glycoprotein lead to drug–drug interactions? *Toxicol Lett* 2005;156:319–329.
16. Ochs HR, Steinhaus E, Locniskar A, Knüchel M, Greenblatt DJ. Desmethyldiazepam kinetics after intravenous, intramuscular, and oral administration of clorazepate dipotassium. *Klin Wochenschrift* 1982;60:411–415.
17. Venkatakrishnan K, Shader RI, Greenblatt DJ. Concepts and mechanisms of drug disposition and drug interactions. In Ciraulo DA, Shader RI, Greenblatt DJ, Creelman W, Eds. *Drug Interactions in Psychiatry*. Philadelphia: Lippincott Williams &Wilkins; 2005, pp 1–46.
18. Kato R, Ueno K, Imano H, Kawai M, Kuwahara S, Tsuchishita Y, Yonezawa E, Tanaka K. Impairment of ciprofloxacin absorption by calcium polycarbophil. *J Clin Pharmacol* 2002;42:806–811.
19. Greenblatt DJ, Sellers EM, Koch-Weser J. Importance of protein binding for the interpretation of serum or plasma drug concentrations. *J Clin Pharmacol* 1982;22:259–263.

20. MacKichan JJ. Protein binding drug displacement interactions fact or fiction? *Clin Pharmacokinet* 1989;16:65–73.
21. Sansom LN, Evans AM. What is the true clinical significance of plasma protein binding displacement interactions? *Drug Safety* 1995;12:227–233.
22. Greenblatt DJ, von Moltke LL. Interaction of warfarin with drugs, natural substances, and foods. *J Clin Pharmacol* 2005;45:127–132.
23. Benet LZ, Hoener BA. Changes in plasma protein binding have little clinical relevance. *Clin Pharmacol Ther* 2002;71:115–121.
24. O'Reilly RA, Trager WF, Motley CH, Howald W. Stereoselective interaction of phenylbutazone with [^{12}C/^{13}C]warfarin pseudoracemates in man. *J Clin Invest* 1980;65: 746–753.
25. Banfield C, O'Reilly R, Chan E, Rowland M. Phenylbutazone–warfarin interaction in man: further stereochemical and metabolic considerations. *Br J Clin Pharmacol* 1983;16:669–675.
26. Rolan PE. Plasma protein binding displacement interactions—why are they still regarded as clinically important? *Br J Clin Pharmacol* 1994;37:125–128.
27. Hansen JM, Christensen LK. Drug interactions with oral sulphonylurea hypoglycaemic drugs. *Drugs* 1977;13:24–34.
28. Venkatakrishnan K, von Moltke LL, Obach RS, Greenblatt DJ. Drug metabolism and drug interactions: application and clinical value of *in vitro* models. *Curr Drug Metab* 2003;4:423–459.
29. Williams JA, Hyland R, Jones BC, Smith DA, Hurst S, Goosen TC, Peterkin V, Koup JR, Ball SE. Drug–drug interactions for UDP-glucuronosyltransferase substrates: a pharmacokinetic explanation for typically observed low exposure (AUC_i/AUC) ratios. *Drug Metab Dispos Biol Fate Chem* 2004;32:1201–1208.
30. Spina E, Avenoso A, Campo GM, Caputi AP, Perucca E. Phenobarbital induces the 2-hydroxylation of desipramine. *Ther Drug Monitor* 1996;18:60–64.
31. Ono S, Mihara K, Suzuki A, Kondo T, Yasui-Furukori N, Furukori H, de Vries R, Kaneko S. Significant pharmacokinetic interaction between risperidone and carbamazepine: its relationship with CYP2D6 genotypes. *Psychopharmacology (Berl)* 2002;162:50–54.
32. Parkinson A. Biotransformation of xenobiotics. In Klaassen C, Ed. *Casarett & Doull's Toxicology*. New York: McGraw-Hill; 1996, pp 113–186.
33. von Moltke LL, Greenblatt DJ, Duan SX, Harmatz JS, Shader RI. *In vitro* prediction of the terfenadine–ketoconazole pharmacokinetic interaction. *J Clin Pharmacol* 1994;34: 1222–1227.
34. Holbrook AM, Pereira JA, Labiris R, McDonald H, Douketis JD, Crowther M, Wells PS. Systematic overview of warfarin and its drug and food interactions. *Arch Intern Med* 2005;165:1095–1106.
35. Thummel KE, Wilkinson GR. *In vitro* and *in vivo* drug interactions involving human CYP3A. *Annu Rev Pharmacol Toxicol* 1998;38:389–430.
36. Baciewicz AM, and Baciewicz FA Jr. Ketoconazole and fluconazole drug interactions. *Arch Intern Med* 1993;153:1970–1976.
37. Gillum JG, Israel DS, Polk RE. Pharmacokinetic drug interactions with antimicrobial agents. *Clin Pharmacokinet* 1993;25:450–482.
38. Advani R, Fisher GA, Lum BL, Hausdorff J, Halsey J, Litchman M, Sikic BI. A phase I trial of doxorubicin, paclitaxel, and valspodar (PSC 833), a modulator of multidrug resistance. *Clin Cancer Res* 2001;7:1221–1229.
39. Hughes H, Biehl J, Jones A, Schmidt L. Metabolism of isoniazid in man as related to the occurence of peripheral neuritis. *Am Rev Tuberculosis* 1954;70:266–273.

40. Farkas D, Tannenbaum SR. *In vitro* methods to study chemically-induced hepatotoxicity: a literature review. *Curr Drug Metab* 2005;6:111–125.
41. Davis MP, Homsi J. The importance of cytochrome P450 monooxygenase CYP2D6 in palliative medicine. *Support Care Cancer* 2001;9:442–451.
42. Schwarz UI. Clinical relevance of genetic polymorphisms in the human CYP2C9 gene. *Eur J Clin Invest* 2003;33 (Suppl 2):23–30.
43. Ingelman-Sundberg M. Genetic polymorphisms of cytochrome P450 2D6 (CYP2D6): clinical consequences, evolutionary aspects and functional diversity. *Pharmacogenomics J* 2005;5:6–13.
44. Rettie AE, Jones JP. Clinical and toxicological relevance of CYP2C9: drug–drug interactions and pharmacogenetics. *Annu Rev Pharmacol Toxicol* 2005;45:477–494.
45. Zhou S, Chan E, Lim LY, Boelsterli UA, Li SC, Wang J, Zhang Q, Huang M, Xu A. Therapeutic drugs that behave as mechanism-based inhibitors of cytochrome P450 3A4. *Curr Drug Metab* 2004;5:415–442.
46. Alfaro CA, Piscitelli SC. Drug interactions. In Atkinson AJ, Daniels CE, Dedrick RL, Grudzinskas CV, Markey SP. eds. *Principles of Clinical Pharmacoglogy*. Boston: Academic Press; 2001, pp 167–180.
47. Ma Q, Lu AY. Origins of individual variability in P4501A induction. *Chem Res Toxicol* 2003;16:249–260.
48. Hustert E, Zibat A, Presecan-Siedel E, Eiselt R, Mueller R, Fuss C, Brehm I, Brinkmann U, Eichelbaum M, Wojnowski L, Burk O. Natural protein variants of pregnane X receptor with altered transactivation activity toward CYP3A4. *Drug Metab Dispos Biol Fate Chem* 2001;29:1454–1459.
49. Cao H, Hegele RA. Human aryl hydrocarbon receptor nuclear translocator gene (ARNT) D/N511 polymorphism. *J Hum Genet* 2000;45:92–93.
50. Tang C, Lin JH, Lu AY. Metabolism-based drug–drug interactions: what determines individual variability in cytochrome P450 induction? *Drug Metab Dispos Biol Fate Chem* 2005;33:603–613.
51. Chang TK, Bandiera SM, Chen J. Constitutive androstane receptor and pregnane X receptor gene expression in human liver: interindividual variability and correlation with CYP2B6 mRNA levels. *Drug Metab Dispos Biol Fate Chem* 2003;31:7–10.
52. Kerb R, Aynacioglu AS, Brockmöller J, Schlagenhaufer R, Bauer S, Szekeres T, Hamwi A, Fritzer-Szekeres M, Baumgartner C, Ongen HZ, Guzelbey P, Roots I, Brinkmann U. The predictive value of MDR1, CYP2C9, and CYP2C19 polymorphisms for phenytoin plasma levels. *Pharmacogenomics J* 2001;1:204–210.
53. Kim RB, Leake BF, Choo EF, Dresser GK, Kubba SV, Schwarz UI, Taylor A, Xie HG, McKinsey J, Zhou S, Lan LB, Schuetz JD, Schuetz EG, Wilkinson GR. Identification of functionally variant MDR1 alleles among European Americans and African Americans. *Clin Pharmacol Ther* 2001;70:189–199.
54. Begley DJ. ABC transporters and the blood–brain barrier. *Curr Pharm Design* 2004;10:1295–1312.
55. Chandra P, Brouwer KL. The complexities of hepatic drug transport: current knowledge and emerging concepts. *Pharm Res* 2004;21:719–735.
56. Okamura N, Hirai M, Tanigawara Y, Tanaka K, Yasuhara M, Ueda K, Komano T, Hori R. Digoxin–cyclosporin A interaction: modulation of the multidrug transporter P-glycoprotein in the kidney. *J Pharmacol Exp Ther* 1993;266:1614–1619.
57. Saito T, Zhang ZJ, Tokuriki M, Ohtsubo T, Shibamori Y, Yamamoto T, Saito H. Cyclosporin A inhibits the extrusion pump function of P-glycoprotein in the inner ear of mice treated with vinblastine and doxorubicin. *Brain Res* 2001;901:265–270.

58. Sadeque AJ, Wandel C, He H, Shah S, Wood AJ. Increased drug delivery to the brain by P-glycoprotein inhibition. *Clin Pharmacol Ther* 2000;68:231–237.
59. Schinkel AH, Wagenaar E, Mol CA, van Deemter L. P-glycoprotein in the blood–brain barrier of mice influences the brain penetration and pharmacological activity of many drugs. *J Clin Invest* 1996;97:2517–2524.
60. Hughes CS, Vaden SL, Manaugh CA, Price GS, Hudson LC. Modulation of doxorubicin concentration by cyclosporin A in brain and testicular barrier tissues expressing P-glycoprotein in rats. *J Neuro-Oncol* 1998;37:45–54.
61. Kang W, Weiss M. Influence of P-glycoprotein modulators on cardiac uptake, metabolism, and effects of idarubicin. *Pharm Res* 2001;18:1535–1541.
62. Kramer WG, Reuning RH. Use of area under the curve to estimate absolute bioavailability of digoxin. *J Pharm Sci* 1978;67:141–142.
63. Lin JH. Drug–drug interaction mediated by inhibition and induction of P-glycoprotein. *Adv Drug Deliv Rev* 2003;55:53–81.
64. Lin JH. Human immunodeficiency virus protease inhibitors. From drug design to clinical studies. *Adv Drug Deliv Rev* 1997;27:215–233.
65. Szabo K, Welker E, Bakos E, Müller M, Roninson I, Varadi A, Sarkadi B. Drug-stimulated nucleotide trapping in the human multidrug transporter MDR1. Cooperation of the nucleotide binding domains. *J Biol Chem* 1998;273:10132–10138.
66. Shapiro AB, Ling V. Positively cooperative sites for drug transport by P-glycoprotein with distinct drug specificities. *Eur J Biochem* 1997;250:130–137.
67. Ayesh S, Shao YM, Stein WD. Co-operative, competitive and non-competitive interactions between modulators of P-glycoprotein. *Biochim Biophys Acta* 1996;1316:8–18.
68. Fardel O, Lecureur V, Corlu A, Guillouzo A. P-glycoprotein induction in rat liver epithelial cells in response to acute 3-methylcholanthrene treatment. *Biochem Pharmacol* 1996;51:1427–1436.
69. Fardel O, Morel F, Guillouzo A. P-glycoprotein expression in human, mouse, hamster and rat hepatocytes in primary culture. *Carcinogenesis* 1993;14:781–783.
70. Chin KV, Chauhan SS, Pastan I, Gottesman MM. Regulation of mdr RNA levels in response to cytotoxic drugs in rodent cells. *Cell Growth Differ* 1990;1:361–365.
71. Jette L, Beaulieu E, Leclerc JM, Beliveau R. Cyclosporin A treatment induces overexpression of P-glycoprotein in the kidney and other tissues. *Am J Physiol* 1996; 270:F756–F765.
72. Boffito M, Maitland D, Samarasinghe Y, Pozniak A. The pharmacokinetics of HIV protease inhibitor combinations. *Curr Opin Infect Dis* 2005;18:1–7.
73. van Heeswijk RP, Veldkamp A, Mulder JW, Meenhorst PL, Lange JM, Beijnen JH, Hoetelmans RM. Combination of protease inhibitors for the treatment of HIV-1-infected patients: a review of pharmacokinetics and clinical experience. *Antiviral Ther* 2001;6:201–229.
74. Moyle G. Use of HIV protease inhibitors as pharmacoenhancers. *AIDS Reader* 2001;11:87–98.
75. Cvetkovic RS, Goa KL. Lopinavir/ritonavir: a review of its use in the management of HIV infection. *Drugs* 2003;63:769–802.
76. Scott JD. Simplifying the treatment of HIV infection with ritonavir-boosted protease inhibitors in antiretroviral-experienced patients. *Am J Health-System Pharm* 2005; 62:809–815.
77. Moyle GJ, Back D. Principles and practice of HIV-protease inhibitor pharmacoenhancement. *HIV Med* 2001;2:105–113.

78. Kashuba AD. Drug-drug interactions and the pharmacotherapy of HIV infection. *Topics HIV Med* 2005;13:64–69.

79. von Hentig NH, Mueller A, Haberl A. The ATSAQ-1 cohort study; pharmakinetic interactions of atazanavir (ATV) and saquinavir (SAQ) in a ritonavir (RTV) boosted protease inhibitor regimen. *XV International AIDS Conference*; 2004.

80. de Smet K, Loyer P, Gilot D, Vercruysse A, Rogiers V, Guguen-Guillouzo C. Effects of epidermal growth factor on CYP inducibility by xenobiotics, DNA replication, and caspase activations in collagen I gel sandwich cultures of rat hepatocytes. *Biochem Pharmacol* 2001;61:1293–1303.

81. de Smet K, Beken S, Depreter M, Roels F, Vercruysse A, Rogiers V. Effect of epidermal growth factor in collagen gel cultures of rat hepatocytes. *Toxicol in Vitro* 1999;13: 579–585.

82. Ching KZ, Tenney KA, Chen J, Morgan ET. Suppression of constitutive cytochrome P450 gene expression by epidermal growth factor receptor ligands in cultured rat hepatocytes. *Drug Metab Dispos Biol Fate Chem* 1996;24:542–546.

83. Greuet J, Pichard L, Ourlin JC, Bonfils C, Domergue J, Le Treut P, Maurel P. Effect of cell density and epidermal growth factor on the inducible expression of CYP3A and CYP1A genes in human hepatocytes in primary culture. *Hepatology* 1997;25:1166–1175.

84. LeCluyse EL. Human hepatocyte culture systems for the *in vitro* evaluation of cytochrome P450 expression and regulation. *Eur J Pharm Sci* 2001;13:343–368.

85. Moghe PV, Coger RN, Toner M, Yarmush ML. Cell–cell interactiOns are essential for MaIntenance of hepatocyte FunctiOn In collagen gel but not On Matrigel. *Biotechnol Bioeng* 1997;56:706–711.

86. Moghe PV, Berthiaume F, Ezzell RM, Toner M, Tompkins RG, Yarmush ML. Culture matrix configuration and composition in the maintenance of hepatocyte polarity and function. *Biomaterials* 1996;17:373–385.

87. LeCluyse E, Madan A, Hamilton G, Carroll K, DeHaan R, Parkinson A. Expression and regulation of cytochrome P450 enzymes in primary cultures of human hepatocytes. *J Biochem Mol Toxicol* 2000;14:177–188.

88. Raucy JL. Regulation of CYP3A4 expression in human hepatocytes by pharmaceuticals and natural products. *Drug Metab Dispos* 2003;31:533–539.

89. Mills JB, Rose KA, Sadagopan N, Sahi J, de Morais SM. Induction of drug metabolism enzymes and MDR1 using a novel human hepatocyte cell line. *J Pharmacol Exp Ther* 2004;309:303–309.

90. Biagini CP, Bender V, Borde F, Boissel E, Bonnet MC, Masson MT, Cassio D, Chevalier S. Cytochrome P450 expression-induction profile and chemically mediated alterations of the WIF-B9 cell line. *Biol Cell* 2005;98:23–32.

91. Polli JW, Wring SA, Humphreys JE, Huang L, Morgan JB, Webster LO, Serabjit-Singh CS. Rational use of *in vitro* P-glycoprotein assays in drug discovery. *J Pharmacol Exp Ther* 2001;299:620–628.

92. Tang F, Horie K, Borchardt RT. Are MDCK cells transfected with the human MRP2 gene a good model of the human intestinal mucosa? *Pharm Res* 2002;19:773–779.

93. Taub ME, Podila L, Ely D, Almeida I. Functional assessment of multiple P-glycoprotein (P-gp) probe substrates: influence of cell line and modulator concentration on P-gp activity. *Drug Metab Dispos Biol Fate Chem* 2005;33:1679–1687.

94. Taipalensuu J, Tornblom H, Lindberg G, Einarsson C, Sjoqvist F, Melhus H, Garberg P, Sjostrom B, Lundgren B, Artursson P. Correlation of gene expression of ten drug efflux proteins of the ATP-binding cassette transporter family in normal human jejunum and

in human intestinal epithelial Caco-2 cell monolayers. *J Pharmacol Exp Ther* 2001;299: 164–170.

95. Prime-Chapman HM, Fearn RA, Cooper AE, Moore V, Hirst BH. Differential multidrug resistance-associated protein 1 through 6 isoform expression and function in human intestinal epithelial Caco-2 cells. *J Pharmacol Exp Ther* 2004;311:476–484.
96. Donato MT, Castell JV, Gomez-Lechon MJ. Characterization of drug metabolizing activities in pig hepatocytes for use in bioartificial liver devices: comparison with other hepatic cellular models. *J Hepatol* 1999;31:542–549.
97. Omasa T, Kim K, Hiramatsu S, Katakura Y, Kishimoto M, Enosawa S, Ohtake H. Construction and evaluation of drug-metabolizing cell line for bioartificial liver support system. *Biotechnol Prog* 2005;21:161–167.
98. Iwahori T, Matsuura T, Maehashi H, Sugo K, Saito M, Hosokawa M, Chiba K, Masaki T, Aizaki H, Ohkawa K, Suzuki T. CYP3A4 inducible model for *in vitro* analysis of human drug metabolism using a bioartificial liver. *Hepatology* 2003;37:665–673.
99. Bugrim A, Nikolskaya T, Nikolsky Y. Early prediction of drug metabolism and toxicity: systems biology approach and modeling. *Drug Discov Today* 2004;9:127–135.
100. Korolev D, Balakin KV, Nikolsky Y, Kirillov E, Ivanenkov YA, Savchuk NP, Ivashchenko AA, Nikolskaya T. Modeling of human cytochrome P450-mediated drug metabolism using unsupervised machine learning approach. *J Med Chem* 2003;46:3631–3643.
101. Manga N, Duffy JC, Rowe PH, Cronin MT. Structure-based methods for the prediction of the dominant P450 enzyme in human drug biotransformation: consideration of CYP3A4, CYP2C9, CYP2D6. *SAR QSAR Environ Res* 2005;16:43–61.
102. Jones JP, He M, Trager WF, Rettie AE. Three-dimensional quantitative structure–activity relationship for inhibitors of cytochrome P4502C9. *Drug Metab Dispos Biol Fate Chem* 1996;24:1–6.
103. Bonnabry P, Sievering J, Leemann T, Dayer P. Quantitative drug interactions prediction system (Q-DIPS): a computer-based prediction and management support system for drug metabolism interactions. *Eur J Clin Pharmacol* 1999;55:341–347.
104. Langer T, Eder M, Hoffmann RD, Chiba P, Ecker GF. Lead identification for modulators of multidrug resistance based on *in silico* screening with a pharmacophoric feature model. *Arch Pharm (Weinheim)* 2004;337:317–327.
105. Rebitzer S, Annibali D, Kopp S, Eder M, Langer T, Chiba P, Ecker GF, Noe CR. *In silico* screening with benzofurane- and benzopyrane-type MDR-modulators. *Farmaco* 2003; 58:185–191.
106. Ekins S, Nikolsky Y, Nikolskaya T. Techniques: application of systems biology to absorption, distribution, metabolism, excretion and toxicity. *Trends Pharmacol Sci* 2005; 26:202–209.
107. Segel I. Enzymes. *Biochemical Calculations*. Hoboken, NJ: John Wiley & Sons, 1976; pp 208–323.
108. von Moltke LL, Greenblatt DJ, Grassi JM, Granda BW, Duan SX, Fogelman SM, Daily JP, Harmatz JS, Shader RI. Protease inhibitors as inhibitors of human cytochromes P450: high risk associated with ritonavir. *J Clin Pharmacol* 1998;38:106–111.
109. von Moltke LL, Greenblatt DJ, Schmider J, Wright CE, Harmatz JS, Shader RI. *In vitro* approaches to predicting drug interactions *in vivo*. *Biochem Pharmacol* 1998; 55:113–122.
110. Shou M, Mei Q, Ettore MW Jr, Dai R, Baillie TA, Rushmore TH. Sigmoidal kinetic model for two co-operative substrate-binding sites in a cytochrome P450 3A4 active site: an example of the metabolism of diazepam and its derivatives. *Biochem J* 1999;340 (Pt 3):845–853.

111. Greenblatt DJ, von Moltke LL, Daily JP, Harmatz JS, Shader RI. Extensive impairment of triazolam and alprazolam clearance by short-term low-dose ritonavir: the clinical dilemma of concurrent inhibition and induction. *J Clin Psychopharmacol* 1999;19: 293–296.

112. Obach RS. Inhibition of human cytochrome P450 enzymes by constituents of St. John's wort, an herbal preparation used in the treatment of depression. *J Pharmacol Exp Ther* 2000;294:88–95.

113. Jang SH, Wientjes MG, Au JL. Kinetics of P-glycoprotein-mediated efflux of paclitaxel. *J Pharmacol Exp Ther* 2001;298:1236–1242.

114. Hunter J, Jepson MA, Tsuruo T, Simmons NL, Hirst BH. Functional expression of P-glycoprotein in apical membranes of human intestinal Caco-2 cells. Kinetics of vinblastine secretion and interaction with modulators. *J Biol Chem* 1993;268:14991–14997.

115. Jang SH, Wientjes MG, Au JL. Interdependent effect of P-glycoprotein-mediated drug efflux and intracellular drug binding on intracellular paclitaxel pharmacokinetics: application of computational modeling. *J Pharmacol Exp Ther* 2003;304:773–780.

116. Hoffmaster KA, Zamek-Gliszczynski MJ, Pollack GM, Brouwer KL. Multiple transport systems mediate the hepatic uptake and biliary excretion of the metabolically stable opioid peptide [D-penicillamine2,5]enkephalin. *Drug Metab and Dispos Biol Fate Chem* 2005;33:287–293.

117. Zahlten RN, Stratman FW. The isolation of hormone-sensitive rat hepatocytes by a modified enzymatic technique. *Arch Biochem Biophys* 1974;163:600–608.

118. Bertz RJ, Granneman GR. Use of *in vitro* and *in vivo* data to estimate the likelihood of metabolic pharmacokinetic interactions. *Clin Pharmacokinet* 1997;32:210–258.

119. Greenblatt DJ, von Moltke LL, Harmatz JS, Durol AL, Daily JP, Graf JA, Mertzanis P, Hoffman JL, Shader RI. Differential impairment of triazolam and zolpidem clearance by ritonavir. *J Acquir Immune Defic Syndr* 2000;24:129–136.

120. Kronbach T, Mathys D, Umeno M, Gonzalez FJ, Meyer UA. Oxidation of midazolam and triazolam by human liver cytochrome P450IIIA4. *Mol Pharmacol* 1989;36:89–96.

121. Eberts FS Jr, Philopoulos Y, Reineke LM, Vliek RW. Triazolam disposition. *Clin Pharmacol Ther* 1981;29:81–93.

122. Phillips JP, Antal EJ, Smith RB. A pharmacokinetic drug interaction between erythromycin and triazolam. *J Clin Psychopharmacol* 1986;6:297–299.

123. Varhe A, Olkkola KT, Neuvonen PJ. Oral triazolam is potentially hazardous to patients receiving systemic antimycotics ketoconazole or itraconazole. *Clin Pharmacol Ther* 1994;56:601–607.

124. von Moltke LL, Greenblatt DJ, Harmatz JS, Duan SX, Harrel LM, Cotreau-Bibbo MM, Pritchard GA, Wright CE, Shader RI. Triazolam biotransformation by human liver microsomes *in vitro*: effects of metabolic inhibitors and clinical confirmation of a predicted interaction with ketoconazole. *J Pharmacol Exp Ther* 1996;276:370–379.

125. Villikka K, Kivistö KT, Backman JT, Olkkola KT, Neuvonen PJ. Triazolam is ineffective in patients taking rifampin. *Clin Pharmacol Ther* 1997;61:8–14.

126. Hsu A, Granneman GR, Bertz RJ. Ritonavir. Clinical pharmacokinetics and interactions with other anti-HIV agents. *Clin Pharmacokinet* 1998;35:275–291.

127. von Moltke LL, Greenblatt DJ, Schmider J, Duan SX, Wright CE, Harmatz JS, Shader RI. Midazolam hydroxylation by human liver microsomes *in vitro*: inhibition by fluoxetine, norfluoxetine, and by azole antifungal agents. *J Clin Pharmacol* 1996;36:783–791.

128. Wrighton SA, Ring BJ, Watkins PB, Vandenbranden M. Identification of a polymorphically expressed member of the human cytochrome P-450III family. *Mol Pharmacol* 1989;36:97–105.

129. Tsunoda SM, Velez RL, von Moltke LL, Greenblatt DJ. Differentiation of intestinal and hepatic cytochrome P450 3A activity with use of midazolam as an *in vivo* probe: effect of ketoconazole. *Clin Pharmacol Ther* 1999;66:461–471.
130. Schuetz JD, Beach DL, Guzelian PS. Selective expression of cytochrome P450 CYP3A mRNAs in embryonic and adult human liver. *Pharmacogenetics* 1994;4:11–20.
131. Kuehl P, Zhang J, Lin Y, Lamba J, Assem M, Schuetz J, Watkins PB, Daly A, Wrighton SA, Hall SD, Maurel P, Relling M, Brimer C, Yasuda K, Venkataramanan R, Strom S, Thummel K, Boguski MS, Schuetz E. Sequence diversity in CYP3A promoters and characterization of the genetic basis of polymorphic CYP3A5 expression. *Nat Genet* 2001;27:383–391.
132. Patki KC, von Moltke LL, Greenblatt DJ. *In vitro* metabolism of midazolam, triazolam, nifedipine, and testosterone by human liver microsomes and recombinant cytochromes p450: role of CYP3A4 and CYP3A5. *Drug Metab Dispos Biol Fate Chem* 2003; 31:938–944.
133. Greenblatt DJ, von Moltke LL. Drug–drug interactions: clinical perspective. In Rodrigues AD, ed. *Drug–Drug Interactions*. New York: Marcel Dekker; 2002, pp 565–584.
134. Greenblatt DJ, Wright CE, Von Moltke LL, Harmatz JS, Ehrenberg BL, Harrel LM, Corbett K, Counihan M, Tobias S, Shader RI. Ketoconazole inhibition of triazolam and alprazolam clearance: differential kinetic and dynamic consequences. *Clin Pharmacol Ther* 1998;64:237–247.
135. Gorski JC, Jones DR, Haehner-Daniels BD, Hamman MA, O'Mara EM Jr, Hall SD. The contribution of intestinal and hepatic CYP3A to the interaction between midazolam and clarithromycin. *Clin Pharmacol Ther* 1998;64:133–143.
136. Cotreau MM, von Moltke LL, Greenblatt DJ. The influence of age and sex on the clearance of cytochrome P450 3A substrates. *Clin Pharmacokinet* 2005;44:33–60.
137. Greenblatt DJ, Harmatz JS, von Moltke LL, Wright CE, Shader RI. Age and gender effects on the pharmacokinetics and pharmacodynamics of triazolam, a cytochrome P450 3A substrate. *Clin Pharmacol Ther* 2004;76:467–479.
138. Greenblatt DJ, Divoll M, Abernethy DR, Moschitto LJ, Smith RB, Shader RI. Reduced clearance of triazolam in old age: relation to antipyrine oxidizing capacity. *Br J Clin Pharmacol* 1983;15:303–309.
139. Greenblatt DJ, Harmatz JS, Shapiro L, Engelhardt N, Gouthro TA, Shader RI. Sensitivity to triazolam in the elderly. *N Engl J Med* 1991;324:1691–1698.
140. Callachan H, Cottrell GA, Hather NY, Lambert JJ, Nooney JM, Peters JA. Modulation of the GABAA receptor by progesterone metabolites. *Proc R Soc London Ser B Biol Sci* 1987;231:359–369.
141. McAuley JW, Reynolds IJ, Kroboth FJ, Smith RB, Kroboth PD. Orally administered progesterone enhances sensitivity to triazolam in postmenopausal women. *J Clin Psychopharmacol* 1995;15:3–11.
142. McAuley JW, Kroboth PD, Stiff DD, Reynolds IJ. Modulation of [^{3}H]flunitrazepam binding by natural and synthetic progestational agents. *Pharmacol Biochem Behav* 1993;45:77–83.
143. Fahey JM, Pritchard GA, von Moltke LL, Pratt JS, Grassi JM, Shader RI, Greenblatt DJ. Effects of ketoconazole on triazolam pharmacokinetics, pharmacodynamics and benzodiazepine receptor binding in mice. *J Pharmacol Exp Ther* 1998;285:271–276.
144. Lin JH, Yamazaki M. Role of P-glycoprotein in pharmacokinetics: clinical implications. *Clin Pharmacokinet* 2003;42:59–98.
145. von Moltke LL, Granda BW, Grassi JM, Perloff MD, Vishnuvardhan D, Greenblatt DJ. Interaction of triazolam and ketoconazole in P-glycoprotein-deficient mice. *Drug Metab Dispos Biol Fate Chem* 2004;32:800–804.

146. Bent S, Ko R. Commonly used herbal medicines in the United States: a review. *Am J Med* 2004;116:478–485.

147. Izzo AA. Herb–drug interactions: an overview of the clinical evidence. *Fundam Clin Pharmacol* 2005;19:1–16.

148. Ernst E. Are herbal medicines effective? *Int J Clin Pharmacol Ther* 2004;42:157–159.

149. Greenblatt DJ, Patki KC, von Moltke LL, Shader RI. Drug interactions with grapefruit juice: an update. *J Clin Psychopharmacol* 2001;21:357–359.

150. James, JS. St. John's Warning: Do Not Combine with Protease Inhibitors, NNRTI's. http://www.aids.org/atn/a-337-02.html. 2005.

151. Fugh-Berman A, Ernst E. Herb–drug interactions: review and assessment of report reliability. *Br J Clin Pharmacol* 2001;52:587–595.

152. Lewis JD, Strom BL. Balancing safety of dietary supplements with the free market. *Ann Intern Med* 2002;136:616–618.

153. Dietary Supplement Health Education Act of 1994. http://www.fda.gov/opacom/laws/dshea.html.

154. Dietary Supplements: Questions Answers. US Food Drug Aministration; Center for Food Safety Applied Nutrition; 2001. http://www.cfsan.fda.gov/~dms/ds-faq.html.

155. Gilroy CM, Steiner JF, Byers T, Shapiro H, Georgian W. Echinacea and truth in labeling. *Arch Intern Med* 2003;163:699–704.

156. Harkey MR, Henderson GL, Gershwin ME, Stern JS, Hackman RM. Variability in commercial ginseng products: an analysis of 25 preparations. *Am J Clin Nutr* 2001;73:1101–1106.

157. Zhou S, Gao Y, Jiang W, Huang M, Xu A, Paxton JW. Interactions of herbs with cytochrome P450. *Drug Metab Rev* 2003;35:35–98.

158. Ioannides C. Pharmacokinetic interactions between herbal remedies and medicinal drugs. *Xenobiotica* 2002;32:451–478.

159. Zou L, Harkey MR, Henderson GL. Effects of herbal components on cDNA-expressed cytochrome P450 enzyme catalytic activity. *Life Sci* 2002;71:1579–1589.

160. Perloff MD, von Moltke LL, Stormer E, Shader RI, Greenblatt DJ. Saint John's wort: an *in vitro* analysis of P-glycoprotein induction due to extended exposure. *Br J Pharmacol* 2001;134:1601–1608.

161. Dresser GK, Schwarz UI, Wilkinson GR, Kim RB. Coordinate induction of both cytochrome P4503A and MDR1 by St John's wort in healthy subjects. *Clin Pharmacol Ther* 2003;73:41–50.

162. Moore LB, Goodwin B, Jones SA, Wisely GB, Serabjit-Singh CJ, Willson TM, Collins JL, Kliewer SA. St. John's wort induces hepatic drug metabolism through activation of the pregnane X receptor. *Proc Nat Acad Sci USA* 2000;97:7500–7502.

163. Wentworth JM, Agostini M, Love J, Schwabe JW, Chatterjee VK. St John's wort, a herbal antidepressant, activates the steroid X receptor. *J Endocrinol* 2000;166:R11–R16.

164. Zhou S, Lim LY, Chowbay B. Herbal modulation of P-glycoprotein. *Drug Metab Rev* 2004;36:57–104.

165. Levi F, Pasche C, La Vecchia C, Lucchini F, Franceschi S. Food groups and colorectal cancer risk. *Br J Cancer* 1999;79:1283–1287.

166. Delgoda R, Westlake AC. Herbal interactions involving cytochrome P450 enzymes: a mini review. *Toxicol Rev* 2004;23:239–249.

167. Guyonnet D, Belloir C, Suschetet M, Siess MH, Le Bon AM. Liver subcellular fractions from rats treated by organosulfur compounds from Allium modulate mutagen activation. *Mutat Res* 2000;466:17–26.

168. Wu CC, Sheen LY, Chen HW, Kuo WW, Tsai SJ, Lii CK. Differential effects of garlic oil and its three major organosulfur components on the hepatic detoxification system in rats. *J Agric Food Chem* 2002;50:378–383.

169. Foster BC, Foster MS, Vandenhoek S, Krantis A, Budzinski JW, Arnason JT, Gallicano KD, Choudri S. An *in vitro* evaluation of human cytochrome P450 3A4 and P-glycoprotein inhibition by garlic. *J Pharm Pharm Sci* 2001;4:176–184.

170. Chen HW, Tsai CW, Yang JJ, Liu CT, Kuo WW, Lii CK. The combined effects of garlic oil and fish oil on the hepatic antioxidant and drug-metabolizing enzymes of rats. *Br J Nutr* 2003;89:189–200.

171. von Moltke LL, Weemhoff JL, Bedir E, Khan IA, Harmatz JS, Goldman P, Greenblatt DJ. Inhibition of human cytochromes P450 by components of *Ginkgo biloba*. *J Pharm Pharmacol* 2004;56:1039–1044.

172. Shinozuka K, Umegaki K, Kubota Y, Tanaka N, Mizuno H, Yamauchi J, Nakamura K, Kunitomo M. Feeding of *Ginkgo biloba* extract (GBE) enhances gene expression of hepatic cytochrome P-450 and attenuates the hypotensive effect of nicardipine in rats. *Life Sci* 2002;70:2783–2792.

173. Ginkgo. In LaGow B, Ed. *PDR for Herbal Medicine*. Montvale, NJ: Thomson PDR; 2004, pp. 368–378.

174. Gurley BJ, Gardner SF, Hubbard MA, Williams DK, Gentry WB, Cui Y, Ang CY. Cytochrome P450 phenotypic ratios for predicting herb-drug interactions in humans. *Clin Pharmacol Ther* 2002;72:276–287.

175. Sparreboom A, Cox MC, Acharya MR, Figg WD. Herbal remedies in the United States: potential adverse interactions with anticancer agents. *J Clin Oncol* 2004;22:2489–2503.

176. Yamazaki H, Shimada T. Human liver cytochrome P450 enzymes involved in the 7-hydroxylation of *R*- and *S*-warfarin enantiomers. *Biochem Pharmacol* 1997;54:1195–1203.

177. Engelsen J, Nielsen JD, Winther K. Effect of coenzyme Q10 and *Ginkgo biloba* on warfarin dosage in stable, long-term warfarin treated outpatients. A randomised, double blind, placebo-crossover trial. *Thromb Haemost* 2002;87:1075–1076.

178. Cotreau MM, von Moltke LL, Greenblatt DJ. The influence of age and sex on the clearance of cytochrome P450 3A substrates. *Clin Pharmacokinet* 2005;44:33–60.

179. Gurley BJ, Gardner SF, Hubbard MA, Williams DK, Gentry WB, Cui Y, Ang CY. Clinical assessment of effects of botanical supplementation on cytochrome P450 phenotypes in the elderly: St John's wort, garlic oil, Panax ginseng and *Ginkgo biloba*. *Drugs Agin* 2005;22:525–539.

180. Markowitz JS, Donovan JL, DeVane CL, Taylor RM, Ruan Y, Wang JS, Chavin KD. Effect of St John's wort on drug metabolism by induction of cytochrome P450 3A4 enzyme. *JAMA* 2003;290:1500–1504.

181. Jöhne A, Brockmöller J, Bauer S, Maurer A, Langheinrich M, Roots I. Pharmacokinetic interaction of digoxin with an herbal extract from St. John's wort (*Hypericum perforatum*). *Clin Pharmacol Ther* 1999;66:338–345.

182. Sugimoto K, Ohmori M, Tsuruoka S, Nishiki K, Kawaguchi A, Harada K, Arakawa M, Sakamoto K, Masada M, Miyamori I, Fujimura A. Different effects of St. John's wort on the pharmacokinetics of simvastatin and pravastatin. *Clin Pharmacol Ther* 2001;70:518–524.

183. Jöhne A, Schmider J, Brockmöller J, Stadelmann AM, Störmer E, Bauer S, Scholler G, Langheinrich M, Roots I. Decreased plasma levels of amitriptyline and its metabolites on comedication with an extract from St. John's wort (*Hypericum perforatum*). *J Clin Psychopharmacol* 2002;22:46–54.

184. Dannawi M. Possible serotonin syndrome after combination of buspirone and St John's wort. *J Psychopharmacol* 2002;16:401.
185. Wang Z, Gorski JC, Hamman MA, Huang SM, Lesko LJ, Hall SD. The effects of St John's wort (*Hypericum perforatum*) on human cytochrome P450 activity. *Clin Pharmacol Ther* 2001;70:317–326.
186. Piscitelli SC, Burstein AH, Chaitt D, Alfaro RM, Falloon J. Indinavir concentrations and St John's wort. *Lancet* 2000;355:547–548.
187. de Maat MM, Hoetelmans RM, Matht RA, van Gorp EC, Meenhorst PL, Mulder JW, Beijnen JH. Drug interaction between St John's wort and nevirapine. *AIDS* 2001;15:420–421.
188. Gorski JC, Huang SM, Pinto A, Hamman MA, Hilligoss JK, Zaheer NA, Desai M, Miller M, Hall SD. The effect of Echinacea (*Echinacea purpurea* root) on cytochrome P450 activity *in vivo*. *Clin Pharmacol Ther* 2004;75:89–100.
189. Blumenthal M. Herbs continue slide in mainstream market: sales down 14 percent. *HerbalGram* 2003;58:71.
190. Markowitz JS, DeVane CL, Chavin KD, Taylor RM, Ruan Y, Donovan JL. Effects of garlic (*Allium sativum* L.) supplementation on cytochrome P450 2D6 and 3A4 activity in healthy volunteers. *Clin Pharmacol Ther* 2003;74:170–177.
191. Gallicano K, Foster B, Choudhri S. Effect of short-term administration of garlic supplements on single-dose ritonavir pharmacokinetics in healthy volunteers. *Br J Clin Pharmacol* 2003;55:199–202.
192. Piscitelli SC, Burstein AH, Welden N, Gallicano KD, Falloon J. The effect of garlic supplements on the pharmacokinetics of saquinavir. *Clin Infect Dis* 2002;34:234–238.
193. Gwilt PR, Lear CL, Tempero MA, Birt DD, Grandjean AC, Ruddon RW, Nagel DL. The effect of garlic extract on human metabolism of acetaminophen. *Cancer Epidemiol Biomarkers Prev* 1994;3:155–160.
194. Hu Z, Yang X, Ho PC, Chan SY, Heng PW, Chan E, Duan W, Koh HL, Zhou S. Herb–drug interactions: a literature review. *Drug* 2005;65:1239–1282.
195. Evans V. Herbs and the brain: friend or foe? The effects of ginkgo and garlic on warfarin use. *J Neurosci Nurs* 2000;32:229–232.
196. Matthews MK Jr. Association of *Ginkgo biloba* with intracerebral hemorrhage. *Neurology* 1998;50:1933–1934.
197. Meisel C, Jöhne A, Roots I. Fatal intracerebral mass bleeding associated with *Ginkgo biloba* and ibuprofen. *Atherosclerosis* 2003;167:367.
198. Hoffman T. Ginkgo, Vioxx and excessive bleeding—possible drug–herb interactions: case report. *Hawaii Med J* 2001;60:290.
199. Jiang X, Williams KM, Liauw WS, Ammit AJ, Roufogalis BD, Duke CC, Day RO, McLachlan AJ. Effect of ginkgo and ginger on the pharmacokinetics and pharmacodynamics of warfarin in healthy subjects. *Br J Clin Pharmacol* 2005;59:425–432.

26

SPECIES COMPARISON OF METABOLISM IN MICROSOMES AND HEPATOCYTES

NIELS KREBSFAENGER
Schwarz Biosciences, Monheim, Germany

Contents

26.1 INTRODUCTION AND GENERAL ASPECTS

Species differences in metabolism may have significant impact on pharmacokinetics and toxicity of drugs. Therefore detailed knowledge of comparative metabolism across species is key for species selection in preclinical safety testing and interpretation of any animal data in respect to relevance for humans.

From the safety perspective, the primary concern is to identify any unique or major human metabolites. Early identification will allow for timely assessment of

Preclinical Development Handbook: ADME and Biopharmaceutical Properties,
edited by Shayne Cox Gad

potential safety issues in the development process and thereby reduce the risk for subjects included in clinical trials as well as for possible delays in the development process.

Since in early drug development animal and human *in vivo* metabolism data are usually lacking, *in vitro* species comparisons provide useful information to support a preliminary species selection for preclinical safety testing and interpretation of animal data.

26.1.1 Relevance of Liver Preparations for Metabolism Studies *In Vitro*

The liver is the major organ for biotransformation of xenobiotics including drugs. The majority of xenobiotic metabolizing enzymes (XMEs) are expressed in the liver and usually their abundance is higher than in other organs or tissues. Several standard methods have been established to investigate hepatic metabolism *in vitro* and there is comprehensive knowledge of their potential and limitations. Therefore, liver preparations such as tissue slices, hepatocytes, or microsomes are valuable and accepted tools for comparative studies on drug metabolism across species *in vitro* (see Section 26.1.5). As orally administered drugs enter first the liver via the portal vein before being distributed in the systemic circulation, and metabolism may have substantial impact on the toxicity of xenobiotics (see Chapter 28 in this volume), hepatotoxicity is a general concern in drug development (see Section 26.1.3). Therefore, toxicity testing in hepatocytes along with metabolism studies may provide additional useful information in early drug development.

However, it should be kept in mind that the liver is not the only metabolically competent organ. For example, cytochrome P450 (CYP) 3A4 is also expressed at high levels in the gut and may substantially contribute to metabolism of drugs even before they enter the liver. CYP1A1 expression is significantly induced in the lung by smoking but there is no such enzymatic activity in the liver, and several prodrugs are cleaved by plasma esterases. Accordingly, *in vitro* metabolism data based on liver preparations alone are not always fully predictive for the situation *in vivo*. Therefore, additional testing using, for example, pulmonary, intestinal, or kidney (microsomal) preparations may be appropriate in specific cases.

26.1.2 Liver Microsomes Versus Hepatocytes

Liver microsomes and primary hepatocytes are the most common *in vitro* systems to assess species differences in metabolism *in vitro*. However, they differ in many respects (Table 26.1).

Microsomes are subcellular membrane fractions obtained by differential centrifugation (see Section 26.2.1), which contain primarily the membrane-bound (smooth endoplasmic reticulum) phase I XMEs (CYPs). Liver microsomes of various species are commercially available (see Section 26.2.3) and are standard for screening of metabolic stability, CYP profiling, and inhibition (see Chapter 21 in this volume). Besides CYP-dependent metabolism, flavin-containing monooxygenase (FMO) and uridine diphosphoglucuronosyltransferase (UGT) metabolism can also be investigated in microsomes if the appropriate cofactors are added to the incubation (i.e., $FADH_2$ or UDP-glucuronic acid, respectively). Epoxide hydrolase

TABLE 26.1 Comparative Characteristics and Properties of Liver Microsomes and Primary Hepatocytes

Characteristic	Liver Microsomes	Primary Hepatocytes	
		Cryopreserved	Freshly Isolated
Metabolic competence	Phase I (CYPs, EH) No transporters High enzyme activities FMOs and UGTs (if supplemented with specific cofactors) Carboxylesterases (depending on preparation method)	Phases I and II Transporters Low enzyme activities	Phases I and II Transporters Low to intermediate enzyme activities
Cofactors	To be supplemented	Intrinsic	Intrinsic
Batch characterization	Usually precharacterized (enzyme activities, protein content, genotyping)	Usually precharacterized (enzyme activities, inducibility, viability, genotyping)	Limited precharacterization (characterization usually in parallel to experiment)
Incubation time (type)	Up to 1 hour (subcellular suspension)	Up to 2–4 hours (suspension) Days—weeks (plated[a])	Up to 2–4 hours (suspension) Days—weeks (plated)
Toxicity testing	Not possible	Limited	Various parameters possible
Species available[b]	Many	Many	Some
Availability	Excellent	Good	Unpredictable
Costs	Less expensive	Expensive	Most expensive

[a]Plating of cryopreserved hepatocytes is not possible with all species.
[b]See Table 26.6.

(EH) and—depending on the preparation method—carboxylesterase activity may also be maintained. Enzyme activities are comparably high and compensate for the limited incubation time due to enzyme degradation over time.

The major limitation of liver microsomes is the lack of phase II metabolic competence. Predictions for compounds that are readily conjugated may therefore be misleading. For example, compounds with free amino, carboxy, or hydroxy functions may be acetylated, glucuronidated, or sulfated without prior functionalization. Microsomal incubations may therefore overestimate the metabolic stability of such compounds. Similarly, the comparison of metabolic profiles over species is evidently limited if phase II metabolism is involved in biotransformation.

Primary hepatocytes overcome the obstacle of lacking phase II metabolism and provide the advantages of a "living" cellular test system such as intrinsic formation of cofactors, regeneration of XMEs (though not constant over time), and the

possibility to implement the assessment of liver function and toxicological parameters (see Section 26.1.3). Hepatocytes allow also for investigation of XME induction. In addition, test substance concentrations at the enzyme are expected to be closer to the physiological situation compared to noncellular microsomal incubations due to the preserved natural orientation for linked enzymes and intact cellular and subcellular compartmentation as well as presence of transporters (see Chapter 12 in this volume). Overall, primary hepatocytes provide a much more physiological test situation. Freshly isolated primary hepatocytes and some batches of plateable cryopreserved hepatocytes can be cultured for up to weeks ahead, maintaining hepatocyte properties and forming organ-like structures (e.g., polarity, junctional complexes, bile canaliculi, and glycogen particles) [1, 2], although nonparenchymal cells are usually underrepresented.

The major limitations of primary hepatocytes are the high interbatch variability and lower enzyme activities, which may further decrease significantly during prolonged incubation. Also, primary hepatocytes are considerably more expensive than liver microsomes. Another drawback with freshly isolated primary hepatocytes as compared to cryopreserved hepatocytes and microsomes is the limited availability and lack of precharacterization; that is, the batch characteristics usually are only determined in parallel with the actual experiment.

26.1.3 Toxicity Testing in Primary Hepatocyte Metabolism Studies

During the last decade liver toxicity has been one of the most frequent reasons for pharmacovigilance safety reports and the withdrawal from the market of an approved medicinal product [3].

Accumulation of the parent drug itself or its metabolites in the liver (see Chapter 13 in this volume) and formation of reactive metabolites[1] are potential cause for concern. Even at therapeutic dose levels, drugs may affect expression of XMEs (induction or inhibition) and increase production of reactive metabolites. Therefore, the use of metabolically competent and potentially inducible hepatocytes is recommended as an *in vitro* tool for the early detection and mechanistic investigation of potential hepatotoxicity [3]. The concomitant assessment of liver function and toxicological parameters within comparative metabolism studies in hepatocytes offers the chance to link potential hepatotoxicity with critical metabolite(s) and identify possible species differences early on. This may help to interpret *in vivo* findings and their relevance for humans (Fig. 26.1). However, it should be stressed that cultured hepatocytes clearly do not represent the complex *in vivo* situation and important mechanisms of liver toxicity such as those mediated via an immunological cascade or idiosyncratic reactions are not represented.

Many of the standard clinical chemistry parameters for liver injury measured in plasma samples in *in vivo* studies can also be assessed in the supernatant of hepatocyte cultures *in vitro* (Table 26.2). *In vivo*, increases in the levels of alanine aminotransferase (ALT) and aspartate aminotransferase (AST) in serum, in combination with increased bilirubin levels, are actually considered to be the most

[1]Potential structural alerts for hepatotoxicity are furans, quinones, epoxides, thiophenes, carboxylic acids, phenoxyl radicals, phenols, acyl halides, acyl glucuronides, aniline radicals, and aromatic and hydroxy amines.

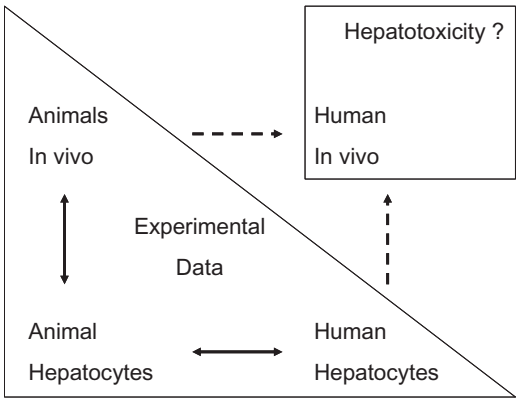

FIGURE 26.1 Prediction of human hepatotoxicity. Combining human *in vitro*, animal *in vitro*, and animal *in vivo* data improves the prediction of human hepatotoxicity *in vivo*. Human hepatocytes can provide the "missing link" for species extrapolation while animal *in vivo* data "test" the relevance of the respective *in vitro* data.

TABLE 26.2 Examples for Liver Function and Toxicological Parameters in Hepatocytes

Parameter	Correlation/Function	Assessment
Cell morphology and general appearance	General cell viability, necrotic or apoptotic cells, extra- or intracellular precipitates, etc.	Microscopical "in-life" examination of cells in culture well
Albumin secretion	Synthesis competence	Clinical chemistry of supernatant
ALT	Hepatocellular damage	Clinical chemistry of supernatant
AST	Hepatocellular damage	Clinical chemistry of supernatant
LDH	Hepatocellular damage	Clinical chemistry of supernatant
γ-GT	Hepatobiliary damage	Clinical chemistry of supernatant
aP	Hepatobiliary damage	Clinical chemistry of supernatant
GLDH	Mitochondrial damage	Clinical chemistry of supernatant
Lactate	Mitochondrial damage	Clinical chemistry of supernatant
ATP	Mitochondrial damage	Terminal intracellular detection
GSH	Redox status	Terminal intracellular detection
Trypan blue exclusion	Membrane integrity	Terminal staining of cells in well
Neutral red uptake	Membrane integrity	Terminal staining of cells in well
MTT reduction	Mitochondrial activity	Terminal staining of cells in well
XTT reduction	Mitochondrial activity	Terminal staining of cells in well
Sulforhodamine B staining	Protein content	Terminal staining of cells in well
Hoechst 33258 staining	DNA content	Terminal sampling of cells/DNA
Expression profiling	mRNA (or protein) levels	Terminal sampling of cells/mRNA

relevant signal of liver toxicity, and an increase of ALT activity in the range of two- to fourfold and higher compared to concurrent control average or individual pretreatment values should raise concern as an indication of potential hepatic injury [3]. ALT is considered a more specific and sensitive indicator of hepatocellular injury than AST.

TABLE 26.3 General Rules on Interspecies Differences in DMPK

Species	DMPK Characteristics
Human	Polymorphisms (e.g., CYP2C9, CYP2C19, CYP2D6, NAT1, NAT2)
Dog	Low acetylation, high capacity for deacetylation; different absorption due to higher pH in gastrointestinal tract than in humans (consider use of synthetic gastric fluid to mimic human situation)
Rat	Often gender differences that are not observed in other species; abundant tetrahydrofolate (protects, e.g., against methanol ocular damage)
Rabbit	Low sulfation
(Mini)Pig	Low sulfation; gastrointestinal conditions similar to humans
Cat	Low glucuronidation; high sulfation

In addition, in cultured hepatocytes conventional cytotoxicity staining or expression profiling can be terminally performed (Table 26.2). Toxicogenomic data may support the elucidation of hepatotoxic mechanisms or interspecies differences and the development of appropriate biomarkers for liver toxicity.

26.1.4 Species Characteristics and Differences in Metabolism

As pointed out earlier, the knowledge of qualitative and quantitative interspecies differences in metabolism is key in species selection for preclinical safety studies and interpretation of any animal data.

Although there are some "general rules" on species differences in drug metabolism and pharmacokinetics (DMPK) (Table 26.3) like a decreasing rate of metabolism with an increasing size of organism, that is, mouse > rat > dog > human (see Chapter 29 in this volume for allometric scaling), which is also reflected *in vitro*, experimental testing of individual compounds is *conditio sine qua non* as there are also numerous more subtle but often decisive distinctions and the metabolic fate of a new chemical entity (NCE) cannot be reliably predicted today. The complexity of interspecies differences in the XME pattern is probably best exemplified by the many species differences in CYP isoforms [4]. Similarly, several species differences in isoforms have been identified for the major phase II XMEs: UGTs [5], sulfotransferases (SULTs) [6], *N*-acetyltransferases (NATs) [7], and glutathione *S*-transferases (GSTs) [8]. Information on typical phase I and II XME activities in liver preparations of different species is available on the websites of commercial vendors (Table 26.4) or, for example, in Refs. 9 and 10 (see Section 26.2.1).

For example, species comparison of 7-ethoxycoumarin (7-EC) phase I and II metabolism *in vitro*, which is typically used for (pre)characterization of human and animal hepatocytes (Table 26.5), suggests that human metabolism is best represented in cynomolgus monkeys with respect to the metabolite profile (glucuronidated metabolite (7-HCG) > sulfated metabolite (7-HCS) > O-deethylated metabolite (7-HC)); however, rats would be the more appropriate model with respect to the rate of metabolism (monkey ≈ rabbit ≈ dog > rat > human) [10].

26.1.5 Regulatory and Strategic Aspects

The importance of species comparisons in metabolism for safety assessment of NCEs and their metabolite(s) during drug development is reflected in several

TABLE 26.4 Examples of Commercial Sources for Liver Preparations and/or Specialized CROs for *In Vitro* Metabolism Studies (Status August 2006)

CRO/Vendor	Website @ www.	Comment[a]
BD Biosciences	bdbiosciences.com (gentest.com)	M, cH, fH, Services
GenPharmTox BioTech AG	genpharmtox.com	Services
In Vitro Technologies, Inc.	invitrotech.com	M, cH, fH, Services
tebu-bio	tebu-bio.com	M, cH, Services
XenoTech, LLC	xenotechllc.com	M, cH, fH, Services

[a]M, microsomes; cH, cryopreserved hepatocytes; fH, freshly isolated hepatocytes.

TABLE 26.5 Typical Marker Reactions for (Pre)Characterization of Human and Animal Liver Microsomes and Hepatocytes

XME	Marker Reaction
	Phase I
CYP(s)	7-Ethoxycoumarin O-deethylation (formation of 7-hydroxycoumarin)
Human isoenzyme	
CYP1A2	Phenacetin O-deethylation
CYP2A6	Coumarin 7-hydroxylation
CYP2B6	*S*-mephenytoin N-demethylation
CYP2C8	Taxol 6-hydroxylation
CYP2C9	Diclofenac 4′-hydroxylation
CYP2C19	*S*-mephenytoin 4′-hydroxylation
CYP2D6	Bufuralol 1′-hydroxylation
CYP2E1	Chlorzoxazone 6-hydroxylation
CYP3A4/5	Testosterone 6β-hydroxylation
	Phase II
UGT(s)	7-Hydroxycoumarin glucuronidation
SULT(s)	7-Hydroxycoumarin sulfation
GST(s)	1-Chloro-2,4-dinitro-benzene glutathione conjugation
NAT1 (human)	*p*-Aminobenzoic acid N-acetylation
NAT2 (human)	Sulfamethazine N-acetylation

regulatory guidance documents (status August 2006; see Chapter 37 in this volume):

- ICH M3, 1997: *Guidance for Industry on Nonclinical Safety Studies for the Conduct of Human Clinical Trials for Pharmaceuticals* [11].
- EMEA, 2000: *Note for Guidance on Repeated Dose Toxicity* [12].
- FDA/CDER, 2005: *Draft Guidance for Industry on Safety Testing of Drug Metabolites* [13].
- FDA/CDER, 1997: *Guidance for Industry: Drug Metabolism/Drug Interaction Studies in the Drug Development Process: Studies In Vitro* [14].

According to ICH M3, "exposure data in animals should be evaluated prior to human clinical trials. Further information on ADME[2] in animals should be made available to compare human and animal metabolic pathways. Appropriate information should usually be available by the time the Phase I (Human Pharmacology) studies have been completed."

The EMEA *Note for Guidance on Repeated Dose Toxicity* emphasizes the importance of comparative metabolism data for species selection in preclinical safety studies: "Within the usual spectrum of laboratory animals used for toxicity testing, the species should be chosen based on their similarity to humans with regard to pharmacokinetic profile including biotransformation. Exposure to the main human metabolite(s)[3] should be ensured. If this can not be achieved in toxicity studies with the parent compound, specific studies with the metabolite(s) should be considered."

And the FDA/CDER *Draft Guidance for Industry on Safety Testing of Drug Metabolites* encourages that "attempts be made to identify as early as possible during the drug development process differences in drug metabolism in animals used in nonclinical safety assessments compared to humans. It is especially important to identify metabolites that may be unique to humans."

Although the ultimate confirmation and justification on species selection can only be made after animal and human *in vivo* metabolite profiles are available (see Chapters 23 and 27 in this volume), this is, not before Clinical Phase I, *in vitro* species comparisons including human material provide an important—and the only—possibility to rationalize the species selection for pre-IND safety studies; usually on genotoxicity and repeated dose toxicity in one rodent and one nonrodent animal species [11] (see Chapter 37 in this volume). They further offer the possibility to compare human and several standard laboratory and potentially also nonstandard animal species in a relatively efficient approach. In addition, though obviously preferable, in contrast to *in vivo* studies, radiolabeled test substance is often not necessarily required to obtain at least qualitatively comparable metabolite profiles and "identify" the major metabolite(s) if state-of-the-art analytical equipment, usually HPLC/MS,[4] is available (see Chapter 27 in this volume).

While the early identification of unique or major metabolites will allow for timely assessment of potential safety issues, the discovery of unique or major human metabolites late in drug development can cause development delays and could have possible implications for marketing approval.

Accordingly, sponsors are encouraged by regulators "to conduct *in vitro* studies to identify and characterize unique human or major metabolites early in drug development" [13]. Liver preparations such as microsomes, hepatocytes, or tissue slices are considered appropriate for this purpose. This approach is also regarded as the "best practice" in the U.S. pharmaceutical industry [15, 16].

In vitro metabolism studies are not classical safety studies and regulatory agencies in the Unites States, Europe, and Japan therefore do not require compliance

[2]ADME: absorption, distribution, metabolism, excretion.

[3]The FDA/CDER *Draft Guidance for Industry on Safety Testing of Drug Metabolites* defines major metabolites primarily as those identified in human plasma that account for greater than 10% of drug-related material (administered dose or systemic exposure, whichever is less).

[4]HPLC, high performance liquid chromatography; MS, mass spectrometry.

with "Good Laboratory Practice" (GLP) regulations. However, testing under GLP may be considered since this may add to quality and improved processing and documentation, especially if studies are outsourced to contract research organizations (CROs), and there appears to be increasing interest in GLP compliance by regulators also for safety-related studies.

26.2 MATERIALS, METHODS, AND TECHNICAL ASPECTS

26.2.1 Preparation and Characterization of Liver Microsomes and Hepatocytes

Preparation of Liver Microsomes The generalized procedure for preparation of (liver) microsomes by differential centrifugation is shown in Fig. 26.2. Tissue samples are homogenized and centrifuged at a lower force (e.g., 9000 *g*) to form a premicrosomal pellet containing cell debris, nuclei, peroxisomes, lysosomes, and mitochondria. The resulting postmitochondrial supernatant is subsequently centrifuged at a higher force (e.g., 138,000 *g*) to precipitate the microsomes. The cytosolic supernatant may directly be used in metabolism studies; the microsomal pellet is resuspended in buffer and is ready for direct use or storage below –70 °C until use.

A more detailed description of the procedure is given in Ref. 17. The assessment of different protocols [18–24] shows that there are a number of methodological variables such as the number of strokes used to homogenize the liver samples (four to eight), the centrifugation parameters (9000 *g* for 20 min to 18,000 *g* for 10 min in the first step and 100,000–143,000 *g* for 60–90 min in the second step), compositions of the homogenization and final suspension buffers (EDTA, potassium chloride,

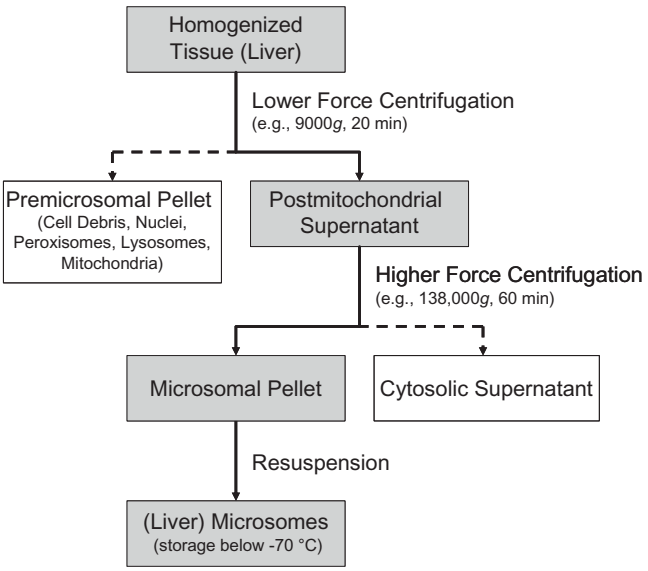

FIGURE 26.2 Preparation of (liver) microsomes. The generalized differential centrifugation procedure for preparation of microsomes is shown. For more detailed information (e.g., on tissue homogenization, buffer composition, repetition of steps), please refer to the references as given in the text.

glycerol, sucrose), and repetition of steps for more thorough extraction. Relative volumes, concentrations, and dilutions of the samples also differ. These variables may significantly affect the recovery and specific activities of microsomal components but do not appear to affect enzyme kinetics [17].

Preparation of Freshly Isolated Hepatocytes There are two principal methods for isolation of primary hepatocytes: (1) *in situ* liver perfusion in anesthetized animals and (2) perfusion of human or animal liver samples after liver resection.

For the first method, the animal is anesthetized and the liver is perfused *in situ* via the vena portae with EGTA[5]/washing buffer to remove blood and prevent clotting of the capillaries. Subsequently, perfusion is continued with collagenase buffer to dissociate the cells from their matrix. After perfusion the liver is removed from the animal, the liver capsula is removed, and the cells are dissociated carefully in suspension buffer. The liver cell suspension is filtered and the filtrate is gently centrifuged for sedimentation of the hepatocytes. The cell pellet is washed in suspension buffer, centrifuged again, and resuspended in suspension buffer.

For the second method, the resected liver tissue is immediately transferred into ice-cold suspension buffer for storage and transport up to some hours until further processing. Liver samples are perfused with EGTA/washing buffer to remove blood and prevent clotting of the capillaries. Perfusion is performed by (several) blunt-end cannulae inserted into vessels of the cut surface. Thereafter, perfusion is continued with collagenase buffer to dissociate the cells from their matrix. The tissue is transferred into a large Petri dish with suspension buffer and the liver cells are gently scraped out with a spatula. The liver cell suspension is filtered and the filtrate is gently centrifuged for sedimentation of the hepatocytes. The cell pellet is washed in suspension buffer, centrifuged again, and resuspended in suspension buffer.

Detailed procedures for the isolation of primary rat and human hepatocytes by these methods are described in Ref. 9. Like with the preparation of microsomes, multiple variations of the general procedures have been described [25–31]. In principle, both methods are suitable for different species such as mouse, rat, rabbit, dog, minipig, or monkey. However, applicability may be limited by size of the organ or tissue sample or due to practical limitations; for example, human and sometimes animal livers may not be available for perfusion *in situ* but only after resection.

The freshly isolated primary hepatocytes may be used directly in suspension [9, 32], culture plated on collagen-coated wells (Fig. 26.3) [1, 26, 27, 29, 33], or cryopreserved and precharacterized for later use [9, 32, 34, 35].

(Pre)characterization of Liver Preparations Microsomes and cryopreserved hepatocytes are usually precharacterized for XME activities and total protein and CYP content or cell viability and inducibility, respectively. Liver preparations of individual human donors are usually supplemented with information on the respective donor, such as age, gender, race, smoking habits, and premedication, and sometimes are also genotyped for polymorphic XMEs such as CYP2C9, CYP2C19, CYP2D6, NAT1, or NAT2. This enables one to select batches of preferred characteristics for the intended type of study and compound under investigation (Section 26.2.3).

[5]EGTA, ethylene glycol bis(β-aminoethyl-ether)-*N*,*N*,*N*′,*N*′-tetraacetic acid.

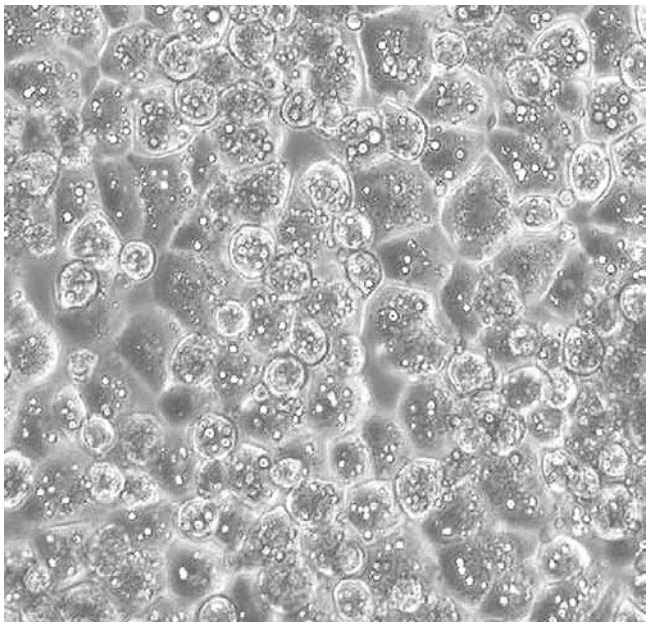

FIGURE 26.3 Light microscopical picture of plated primary human hepatocytes in culture. (Courtesy of GenPharmTox BioTech AG, Martinsried, Germany.)

If freshly isolated primary hepatocytes are directly employed after isolation, precharacterization is usually limited to cell viability and donor information but further indepth characterization (e.g., for enzyme activities) may only be performed concomitant to the actual experiment.

Typical marker reactions for (pre)characterization of human and animal liver microsomes and hepatocytes are listed in Table 26.5. A more comprehensive list of preferred and acceptable substrates, inhibitors, and inducers for *in vitro* experiments and the respective concentration ranges is given on the FDA website *Drug Development and Drug Interactions: Table of Substrates, Inhibitors and Inducers* at http://www.fda.gov/cder/drug/drugInteractions/tableSubstrates.htm#major. Information on typical marker substrate activities for phase I and II XMEs in liver preparations of different species are available on the websites of commercial vendors (Table 26.4) or, for example, in Refs. 9 and 10.

26.2.2 Experimental Study Design

In the following, the principal experimental study designs for investigating metabolic stabilities and metabolite profiles of NCEs in liver microsomes, hepatocyte suspensions, and cultured hepatocytes are described. Depending on the test item properties and intended purpose of the study (e.g., for screening or a development project), manifold variations may be advisable, which cannot be discussed in detail here. However, some general points to consider will be highlighted later in the subsection "Points to Consider."

Metabolic Stability and Metabolite Profile in Liver Microsomes An aliquot of test item stock solution(s) is added to the prewarmed reaction mix(es) including liver microsomes of the desired species, incubation buffer, and NADPH or a NADPH regenerating system and is incubated at 37 °C for different time intervals (usually 10–60 min). The reaction is terminated by addition of organic solvent (e.g., ice-chilled acetonitrile or methanol) and kept cool during sample preparation. In many cases, after centrifugation of the precipitated microsomal components, the supernatant can be directly submitted to HPLC-UV/VIS,[6] -FLD, -RD, and/or -MS analysis.

The loss of parent compound and/or formation of metabolite(s) is calculated compared to a zero time point control, a control without test item, and/or a control without NADPH to correct for chemical degradation, non-CYP-dependent metabolism, and artifact peaks. From this the rate of metabolism (i.e., metabolic half-life, intrinsic clearance, or simply percentage of test compound metabolized/remaining after a certain time) and/or qualitative information on the metabolite profile (i.e., minor, intermediate, major abundance of phase I metabolites) is derived.

Metabolic Stability and Metabolite Profile in Hepatocyte Suspensions An aliquot of test item stock solution(s) is added to the prewarmed reaction mix(es) including hepatocytes of the desired species and incubation buffer and is incubated at 37 °C under slight agitation (e.g., at 40 rpm in a shaking water bath) for different time intervals (usually 15–120 min, maximum 4 hours). The reaction is terminated by addition of organic solvent (e.g., ice-chilled acetonitrile or methanol) and kept cool during sample preparation. In many cases, after centrifugation of the precipitated hepatocytes and other components, the supernatant can be directly submitted to analysis. The loss of parent compound and/or formation of metabolite(s) is calculated compared to a zero time point control and/or a control with heat-inactivated hepatocytes to correct for chemical degradation and artifact peaks. From this the rate of metabolism and/or qualitative information on the phase I and II metabolite profile is derived.

Metabolic Stability and Metabolite Profile in Cultured Hepatocytes An aliquot of test item stock solution(s) is added to the preincubated hepatocyte culture (attachment phase of at least 4 hours, for long-term cultures often overnight) including hepatocytes of the desired species and incubation buffer and is incubated at 37 °C and 5% CO_2 for different time intervals (usually 2–24 hours, maximum several days). The reaction is terminated by addition of organic solvent (e.g., ice-chilled acetonitrile or methanol) and/or removal of the supernatant and kept cool during sample preparation. In many cases, after centrifugation of the precipitated hepatocytes and other components, the supernatant can be directly submitted to analysis.

The loss of parent compound and/or formation of metabolite(s) is calculated compared to a zero time point control and/or a control with heat-inactivated hepatocytes to correct for chemical degradation and artifact peaks. From this the rate of metabolism and/or qualitative information on the metabolite profile is derived.

As discussed in Section 26.1.3, it should be noted that cultured hepatocytes in addition allow for the concomitant assessment of several liver function and

[6]HPLC, high performance liquid chromatography; UV/VIS, ultraviolet/visible light detector; FLD, fluorescence detector; RD, radiometric detection; MS, mass spectrometry.

toxicological parameters, thereby offering the chance to link potential hepatotoxicity with critical metabolite(s) and identify possible species differences early in drug development.

Points to Consider Low solubility of the test item in aqueous buffer at physiological pH is often a challenge in *in vitro* drug metabolism studies. Precipitation in the incubation mix is difficult to note due to the turbidity of the suspension; light microscopy with cultured hepatocytes may sometimes reveal precipitates, but in general solubility may already be limited before any precipitate is visible. The situation is even complicated by potentially solubilizing effects of lipids and proteins within the incubation.

Usually, stock solutions of the test item in organic solvent such as dimethyl sulfoxide, acetonitrile, ethanol, or methanol are prepared to enhance solubility for the serial dilution as well as within the actual incubation. If the high concentration stock solution was prepared in solvent, serial dilutions should also be prepared with solvent—not medium—to assure correct concentrations of the lower concentration stock solutions (i.e., to prevent precipitation during the serial dilution). Usually, final concentrations of up to 1% organic solvent are employed and tolerated by (sub)cellular test systems. However, it should be noted that different solvents interact with different XMEs even at considerably lower concentrations [36]. Another aspect linked with test item solubility is the recovery rate, which, if possible, may be worthwhile examining for proper interpretation of *in vitro* metabolism data.

Test item concentrations generally vary between 0.1 and 100 μM. In most cases, in early development the actual concentration in plasma or liver *in vivo* is not known but will usually be within this range. For determination of the rate of metabolism, lower concentrations of 0.1 or 1 μM are recommended in order not to overload the test system, while higher test item concentrations of 10 or 100 μM will facilitate detection of (minor) metabolites due to a higher absolute amount of metabolism. It should, however, be noted that metabolite profiles (*in vitro* and *in vivo*!) may differ for very high versus very low test item concentrations due to other sets of XMEs being preferred; for example, UGTs are low affinity but high capacity enzymes while SULTs show high affinity but low capacity. Appropriate test system concentrations, buffer composition, and detailed incubation/cultivation procedures may be derived from the commercial vendor's information (Section 26.2.3) or the referenced literature.

Incubation times are generally limited by loss of enzyme activity to about 1 or 2 hours for microsomes and hepatocyte suspensions, respectively. If minor metabolism is observed, incubation times may be extended (for up to 4 hours in suspension cultures) or cultured hepatocytes should be used, enabling incubation for up to several days. Chemical stability of the test item under the incubation conditions should also be considered.

For examination of metabolite profiles (see Chapter 27 in this volume), the use of a radiolabeled test item is obviously preferable as drug-related peaks are easier to differentiate from background and artifacts; metabolites can—at least approximately—easily be quantified and recovery can be assessed. However, metabolite profiles can also be derived from cold test substance if appropriate detection is possible, for example, by UV/VIS or FLD for absorbing compounds or by full-scan or targeted mass detection. In each case, it should be carefully considered which kind

of metabolites would be detected—or missed—with the respective analytical method given its limitations and the structure and properties of the test compound (see Chapter 27 in this volume).

26.2.3 Commercial Suppliers and CROs

There are a number of commercial sources for liver preparations and/or CROs for outsourcing *in vitro* metabolism studies (Table 26.4). Standard species for which microsomes and hepatocytes are available are listed in Table 26.6. Preparations from other species are sometimes also available as "custom preparations," however, usually at substantially higher costs and sometimes unacceptable timelines.

When purchasing liver preparations, besides precharacterization data, quality, price, and a well established shipment procedure should be considered. Especially when liver preparations of "critical" species such as minipig (agricultural species) or monkey (strict animal welfare legislation) are purchased from vendors abroad, customs may delay delivery and biomaterials may degrade if not maintained appropriately. Therefore, especially in the case of freshly isolated hepatocytes, although there are elaborate shipment procedures established nowadays, it may be preferable to choose a local supplier in order to ensure the best possible quality and prompt delivery.

While some milligrams of test substance per species should usually be sufficient, it is difficult to give even a general rule on costs and timelines for outsourcing studies on species comparisons/metabolite profiles due to the many different possible study designs (number of replicates, time points, controls, etc.) and analytical methods (cold versus radiolabeled test substance, metabolite profile "scan" versus metabolite identification, etc.).

TABLE 26.6 Standard Species[a] for Which Microsomes and Hepatocytes Are Commercially Available at the Vendors Listed in Table 26.4 (Status August 2006)

Species	Strain	Liver Microsomes	Cryopreserved Hepatocytes	Freshly Isolated Hepatocytes
Human	Individual donor	+	+	+
	Pooled	+	+	
Monkey	Cynomolgus	+	+	+
	Rhesus	+	+	
	Marmoset	+	+	
Minipig	Goettingen	+	+	
	Yucatan	+		
	Sinclair	+		
Dog	Beagle	+	+	+
Rabbit	New Zealand White	+	+	
Guinea pig	Dunkin–Hartley	+	+	
Hamster	Golden Syrian	+		
Rat	Sprague–Dawley	+	+	+
	Wistar Han	+	+	
	Fischer 344	+		
Mouse	CD-1	+	+	+
	B6C3F1	+		

[a]Additional species may be available as "custom preparations."

26.3 CONCLUSION

Species differences in metabolism may have significant impact on pharmacokinetics and toxicity of drugs. Therefore detailed knowledge of comparative metabolism across species is key for species selection in preclinical safety testing and interpretation of any animal data in respect to relevance for humans. Although there are some "general rules" on species differences in drug metabolism and pharmacokinetics, experimental testing of individual compounds is *conditio sine qua non*, as there are also numerous more subtle but often decisive distinctions and the metabolic fate of an NCE cannot be reliably predicted today.

Liver preparations such as tissue slices, hepatocytes, or microsomes are valuable and accepted tools for comparative studies on drug metabolism across species *in vitro*. While liver microsomes of various species are easily commercially available and are standard for screening of metabolic stability, CYP profiling, and inhibition, freshly isolated or cryopreserved hepatocytes in suspension represent a well established, commercially readily available, and easy-to-handle *in vitro* system that generally correctly predicts interspecies differences in phase I and II metabolism of NCEs. If longer incubation periods are required (i.e., if the rate of metabolism is low or minor metabolites are to be assessed), hepatocyte culture systems may be used. Such systems allow in addition for the concomitant assessment of liver function and toxicological parameters within comparative metabolism studies and thereby offer the chance to link potential hepatotoxicity with critical metabolite(s) and identify possible species differences early on. This may help to interpret *in vivo* findings and their relevance for humans.

Although all *in vitro* systems have their inherent limitations and the ultimate confirmation and justification on species selection can only be made after animal and human *in vivo* metabolite profiles are available, *in vitro* species comparisons including human material provide an important—and the only—possibility to rationalize the species selection for early *in vivo* safety studies, and they further offer the possibility to compare human and several standard laboratory and potentially also nonstandard animal species in a relatively efficient approach.

REFERENCES

1. Koebe HG, Pahernik S, Eyer P, Schildberg FW. Collagen gel immobilization: a useful cell culture technique for long-term metabolic studies on human hepatocytes. *Xenobiotica* 1994;24(2):95–107.
2. Yamamoto N, Wu J, Zhang Y, Catana AM, Cai H, Strom S, Novikoff PM, Zern MA. An optimal culture condition maintains human hepatocyte phenotype after long-term culture. *Hepatol Res* 2006;35:169–177.
3. EMEA. *Guideline on Detection of Early Signal of Drug-Induced Hepatotoxicity in Non-Clinical Studies*. EMEA/CHMP/SWP/150115/2006.
4. Nelson DR, Koymans L, Kamataki T, Stegeman JJ, Feyereisen R, Waxman DJ, Waterman MR, Gotoh O, Coon MJ, Estabrook RW, Gunsalus IC, Nebert DW. P450 superfamily: update on new sequences, gene mapping, accession numbers and nomenclature. *Pharmacogenetics* 1996;6(1):1–42.

5. Mackenzie PI, Bock WK, Burchell B, Guillemette C, Ikushiro S, Iyanagi T, Miners JO, Owens IS, Nebert DW. Nomenclature update for the mammalian UDP glycosyltransferase (UGT) gene superfamily. *Pharmacogenetic Genomics* 2005;15(10):677–685.
6. Blanchard RL, Freimuth RR, Buck J, Weinshilboum RM, Coughtrie MW. A proposed nomenclature system for the cytosolic sulfotransferase (SULT) superfamily. *Pharmacogenetics* 2004;14(3):199–211.
7. Vatsis KP, Weber WW, Bell DA, Dupret J-M, Evans DA, Grant DM, Hein DW, Lin HJ, Meyer UA, Relling MV, Sim E, Suzuki T, Yamazoe Y. Nomenclature for *N*-acetyltransferases. *Pharmacogenetics* 1995;5(1):1–17.
8. Mannervik B, Board PG, Hayes JD, Listowsky I, Pearson WR. Nomenclature for mammalian soluble glutathione transferases. *Methods Enzymol* 2005;401:1–8.
9. Gebhardt R, Hengstler JG, Müller D, Glöckner R, Buenning P, Laube B, Schmelzer E, Ullrich M, Utesch D, Hewitt N, Ringel M, Reder-Hilz B, Bader A, Langsch A, Koose T, Burger H-J, Maas J, Oesch F. New hepatocyte *in vitro* systems for drug metabolism: metabolic capacity and recommendations for application in basic research and drug development, standard operation procedures. *Drug Metab Rev* 2003;35(2&3):145–213.
10. Li AP, Lu C, Brent JA, Pham C, Fackett A, Ruegg CE, Silber PM. Cryopreserved human hepatocytes: characterization of drug-metabolizing enzyme activities and applications in higher throughput screening assays for hepatotoxicity, metabolic stability, and drug-drug interaction potential. *Chem Biol Interact* 1999;121(1):17–35.
11. ICH M3. *Guidance for Industry on Nonclinical Safety Studies for the Conduct of Human Clinical Trials for Pharmaceuticals*; 1997.
12. EMEA. *Note for Guidance on Repeated Dose Toxicity*; 2000. EMEA/CPMP/SWP/1042/99 corr.
13. FDA/CDER. *Draft Guidance for Industry on Safety Testing of Drug Metabolites*; 2005.
14. FDA/CDER. *Guidance for Industry: Drug Metabolism/Drug Interaction Studies in the Drug Development Process: Studies In Vitro*; 1997.
15. Baillie TA, Cayen MN, Fouda H, Gerson RJ, Green JD, Grossman SJ, Klunk LJ, LeBlanc B, Perkins DG, Shipley LA. Drug metabolites in safety testing. *Toxicol Appl Pharmacol* 2002;182:188–196.
16. Hastings KL, El-Hage J, Jacobs A, Leighton J, Morse D, Osterberg R. Drug metabolites in safety testing. *Toxicol Appl Pharmacol* 2003;190(1):91–92.
17. Nelson AC, Huang W, Moody DE. Variables in human liver microsome preparation: impact on the kinetics of L-α-acetylmethadol (LAAM) N-demethylation and dextromethorphan O-demethylation. *Drug Metab Dispos* 2001;29(3):319–325.
18. Boobis AR, Brodie MJ, Kahn GC, Fletcher DR, Saunders JH, Davies DS. Monooxygenase activity of human liver in microsomal fractions of needle biopsy specimens. *Br J Clin Pharmacol* 1980;9:11–19.
19. Raucy J, Lasker JM. Isolation of P450 enzymes from human livers. *Methods Enzymol* 1991;206:577–594.
20. Kharasch ED, Thummel KE. Identification of cytochrome P450 2E1 as the predominant enzyme catalyzing human liver microsomal defluorination of sevoflurane, isoflurane, and methoxyflurane. *Anesthesiology* 1993;79:795–807.
21. Guengerich FP. In Hayes A, Ed. *Analysis and Characterization of Enzymes in Principles and Methods of Toxicology*. New York: Raven Press; 1994, pp 1259–1313.
22. Rodrigues AD, Kukulka MJ, Surber BW, Thomas SB, Uchic JT, Rotert GA, Michel G, Thome-Kromer B, Machinist JM. Measurement of liver microsomal cytochrome P450 (CYP2D6) activity using [*O*-methyl-^{14}C]dextromethorphan. *Anal Biochem* 1994;219:309–320.

23. de Duve C. Tissue fractionation past and present. *J Cell Biol* 1971;50:20d–55d.
24. Papac DI, Franklin MR. N-benzylimidazole, a high magnitude inducer of rat hepatic cytochrome P-450 exhibiting both polycyclic aromatic hydrocarbon- and phenobarbital-type induction of phase I and phase II drug-metabolizing enzymes. *Drug Metab Dispos* 1988;16:259–264.
25. DeLeve LD. Cellular target of cyclophosphamide toxicity in the murine liver: role of glutathione and site of metabolic activation. *Hepatology* 1996;24(4):830–837.
26. Hengstler JG, Utesch D, Steinberg P, Ringel M, Swales N, Biefang K, Platt KL, Diener B, Boettger T, Fischer T, Oesch F. Cryopreserved primary hepatocytes as an *in vitro* model for the evaluation of drug metabolism and enzyme induction. *Drug Metab Rev* 2000;32:81–118.
27. Li AP, Roque AP, Beck DJ, Kaminski DL. Isolation and culturing of hepatocytes from human livers. *Methods Cell Sci* 1992;14(3):139–145.
28. Moldeus P, Hogberg J, Orrenius S. Isolation and use of liver cells. *Methods Enzymol* 1978;51:60–70.
29. Ryan CM, Carter EA, Jenkins RL, Sterling LM, Yarmush ML, Malt RA, Tompkins RG. Isolation and long-term culture of human hepatocytes. *Surgery* 1993;113:48–54.
30. Seglen PO. Preparation of isolated rat liver cells. *Methods Cell Biol* 1976;13:29–83.
31. Steffan AM, Gendrault JL, McCuskey RS, McCuskey PA, Kirn A. Phagocytosis, an unrecognized property of murine endothelial liver cells. *Hepatology* 1986;6(5):830–836.
32. Elaut G, Papeleu P, Vinken M, Henkens T, Snykers S, Vanhaecke T, Rogiers V. Hepatocytes in suspension. *Methods Mol Biol* 2006;320:255–263.
33. Dunn JC, Yarmush ML, Koebe HG, Tompkins RG. Hepatocyte function and extracellular matrix geometry: long-term culture in a sandwich configuration. *FASEB J* 1989;3(2):174–177. Erratum in: *FASEB J* 1989;3(7):1873.
34. Loretz LJ, Li AP, Flye MW, Wilson AG. Optimization of cryopreservation procedures for rat and human hepatocytes. *Xenobiotica* 1989;19(5):489–498.
35. Gomez-Lechon MJ, Lahoz A, Jimenez N, Castell VJ, Donato MT. Cryopreservation of rat, dog and human hepatocytes: influence of preculture and cryoprotectants on recovery, cytochrome P450 activities and induction upon thawing. *Xenobiotica* 2006;36(6):457–472.
36. Busby WF Jr, Ackermann JM, Crespi CL. Effect of methanol, ethanol, dimethyl sulfoxide, and acetonitrile on *in vitro* activities of cDNA-expressed human cytochromes P-450. *Drug Metab Dispos* 1999;27(2):246–249.

27

METABOLITE PROFILING AND STRUCTURAL IDENTIFICATION

MEHRAN F. MOGHADDAM
Celgene, San Diego, California

Contents

27.1 INTRODUCTION

In the pharmaceutical and agrichemical arena, transformation of a compound into its metabolite(s) via *in vivo* or *in vitro* biochemical reactions is referred to as biotransformation reactions. Metabolite profiling refers to the process of identifying

Preclinical Development Handbook: ADME and Biopharmaceutical Properties,
edited by Shayne Cox Gad

all drug related metabolites generated through biotransformation reactions in animals or in *in vitro* systems. In animals, this process may result in the presence of metabolites in the circulation and in any and all tissues as well as the excreta, collectively referred to as animal matrices. In general, biotransformation reactions deactivate/detoxify xenobiotics and render them more water soluble and hence more amendable to excretion (Fig. 27.1a). This leads to clearance of drugs from the body. However, there are clear examples of bioactivation of compounds after biotransformation, which may lead to generation of pharmacologically or toxicologically active metabolites. As depicted in Fig. 27.1b, biotransformation can be beneficial in timely degradation of drugs so they do not accumulate in the body and exert their effects continuously. Also, generation of pharmacologically active metabolites can be viewed as a beneficial aspect of biotransformation. At the same time, the process of biotransformation can have deleterious effects on drug action when it results in rapid clearance of a drug or transforms it into toxic metabolites.

The goal of the ensuing discussion is to provide readers unfamiliar with the field of drug metabolite identification and profiling with an overall knowledge of the concepts involved and to enable them to understand the literature in this area of science.

27.2 WHY IS METABOLITE PROFILING IMPORTANT?

Metabolite profiling should be conducted as early in the process of drug discovery and development as possible for several reasons.

27.2.1 Biotransformation-Assisted Drug Design and Discovery

By identifying metabolite(s) of a compound in *in vitro* systems early in the discovery process, one may uncover the metabolic "weak spots" on a molecule. Medicinal chemists should be informed as soon as metabolites have been identified in order to stabilize "weak spots" on the experimental molecules via chemical modifications. This allows medicinal chemists to engender metabolic stability into and lower metabolic clearance of the chemical series of interest in a timely fashion [1]. Additionally, metabolites with chemical features capable of generating adverse effects should be pointed out to guide chemists to eliminate progenitors to such moieties.

27.2.2 Discovery of Pharmacologically Active Metabolites

In some instances, biotransformation of a drug can lead to a pharmacologically active metabolite (Fig. 27.1a). Although one may envision a more extensive definition, the literature defines a pharmacologically active metabolite as a metabolite with activity against the same pharmacological target as the parent drug [2, 3]. An example of a published pharmacologically active metabolite is Clarinex™ (desloratadine), which is a metabolite of Claritin™ (loratadine) with a 10-fold

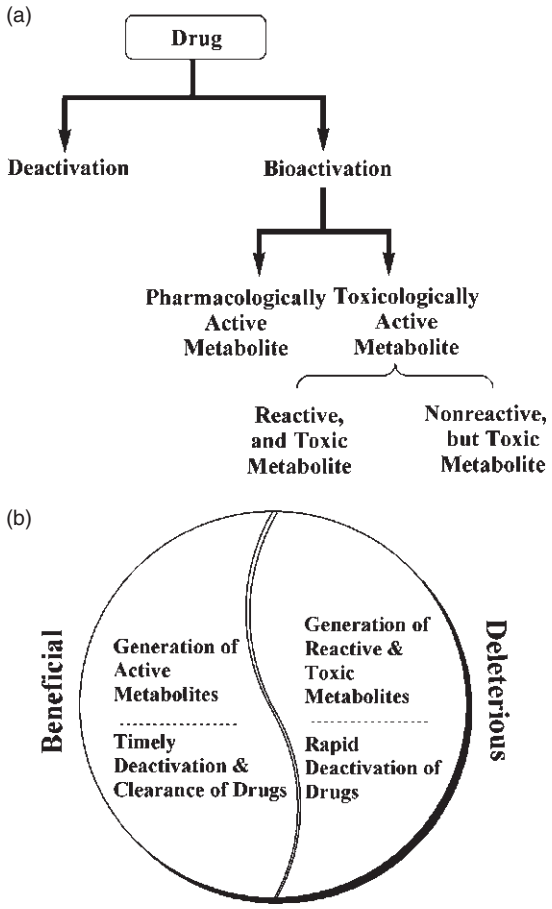

FIGURE 27.1 (a) Drug metabolism results in deactivation or bioactivation of a drug. Bioactivation of a drug leads to formation of either pharmacologically or toxicologically active metabolites. Toxic metabolites may or may not be chemically reactive in nature. (b) Drug metabolism is a process that can be viewed as beneficial or deleterious depending on the outcome. It may be beneficial if it generates pharmacologically active metabolites and degrades the drug slowly. However, it will be viewed as a deleterious process if it generates reactive metabolites and/or results in rapid clearance of drugs.

increase in its potency, longer half-life, and greater exposure [2]. Other examples include 6-*O*-glucuronide of morphine with higher levels of exposure and lower incidences of side effects, Allegra™ (fexofenadine) with no cardiac side effects as opposed to terfenadine, its parent drug, and Zyrtec™ (cetirizine) with a higher affinity for H1 receptor and a lack of distribution to brain (therefore nonsedative) as opposed to its parent drug, Atarax™ (hydroxyzine).

Early knowledge of the metabolic profile of a compound allows one to monitor it in plasma during pharmacokinetic (PK) and efficacy studies. In the discovery setting, this establishes the relevance of metabolites generated *in vitro* to *in vivo*

findings and potentially uncovers pharmacologically active metabolites. Knowledge of active metabolites can assist in establishment of better PK/PD (pharmacokinetic/pharmacodynamic) correlations. Determination of the extent of contribution of an active metabolite to the efficacy of a drug is needed for more accurate dose selection in the clinic. Furthermore, pharmacologically active metabolites can be synthesized and tested as potential drugs themselves [3].

27.2.3 Detection of Toxicologically Active Metabolites

Early identification of metabolites may assist in safety assessment of molecules in the discovery process. From a regulatory and safety perspective, it is critical to demonstrate that all human metabolites are present in animal species tested in toxicology studies. This could be partially assessed by conducting *in vitro* studies with hepatocytes, S9 fractions, or microsomes from human and preclinical species, as discussed later.

In 2002, a group of scientists from the pharmaceutical industry proposed a guideline, "metabolites in safety testing" or "MIST," for assessing the safety of metabolites [4]. It was primarily proposed that human metabolites present in circulation at 25% or more of the total drug related material should be considered for testing. In 2005, in order to address this issue, the U.S. Food and Drug Administration (FDA) put forth a draft guidance (http://www.fda.gov/cder/guidance/6366dft.pdf). This document makes recommendations on when and how to identify, characterize, and evaluate major metabolites or metabolites unique to humans for safety. Unique metabolites are defined as metabolites that occur in humans only, and therefore have not been adequately tested for safety in preclinical species in toxicology testing. Major metabolites are defined as those identified in human plasma that account for greater than 10% of the drug related material (administered dose or systemic exposure, whichever is less), which again were not present in the preclinical species at significant amounts. The FDA recommends that attempts be made to identify any major metabolites or metabolites unique to humans, as early as possible so these molecules can be synthesized and properly tested for safety in a timely manner. It is warned that discovery of major metabolites or metabolites unique to humans late in the development process can cause delays and have possible implications for marketing approval of new drugs.

Although a cutoff point of 10% of circulating drug related material is used by the FDA, the Environmental Protection Agency (EPA) regards the threshold for metabolite identification and toxicological testing at 5% [5]. There are clear examples of metabolites circulating at levels below 10%, which have been reported to cause toxicity. Therefore it has been stated by the FDA that the issue of safety concerns should be handled on a case-by-case basis regardless of how a "major metabolite" is defined [5].

Some examples cited by the FDA include felbamate, cyclophosphamide, and acetaminophen. Felbamate, used for the treatment of epilepsy, has been associated with aplastic anemia and hepatotoxicity, both attributed to a reactive metabolite, atropaldehyde [6]. Atropaldehyde is found as a mercapturic acid urinary metabolite (~2% of felbamate concentration in urine) and mercapturic alcohol (~13% of felbamate concentration in urine). Cyclophosphamide is not directly cytotoxic. However, it is metabolized to several toxic metabolites, one of which, 4-

hydroxycyclophosphamide, represented about 8% of total plasma exposure [7]. Acetaminophen liver toxicity is attributed to *N*-acetyl-*p*-benzoquinonimine (NAPQI), detected in urine as thioether metabolites. The thioethers constitute approximately 9% of a therapeutic dose of acetaminophen [8]. Figure 27.2 shows the decision tree presented by the FDA regarding metabolite testing for safety. It is important to note that reactive metabolites often are too reactive to remain in the matrix. This makes their detection in circulation difficult and they may only be observed as conjugates in excreta or not detected at all (bound residues in tissues). Reactive metabolites have been implicated in idiosyncratic reactions as well. This is a subject worthy of a lengthy discussion; however, it is not the focus of this chapter so the reader is referred to a recent review article on this subject [9]. In brief, more than 10% of acute liver failures from consumption of drugs are due to idiosyncratic reactions. Liver failure is now a leading cause of drug failure in the clinic. Remarkably, most routine animal toxicology testing fails to predict this problem in humans. In fact, idiosyncratic reactions do not occur in most patients at any dose, but, when they take place they can be fatal. These reactions are characterized by immune reactions and are generally referred to as hypersensitivity, allergic, type B, or type II reactions.

Smith and Obach [10] have proposed that decisions regarding safety testing of metabolites should be based on absolute abundance of the molecules rather than their relative abundance (compared to the parent) as was proposed by MIST or FDA guidelines. This suggestion was based on the consideration that the presence of a metabolite as some percentage of the parent drug does not convey the concentrations to which an animal or target cells are exposed. For example, given equal potencies, exposing an animal to a metabolite present at 1% of the dose of drug A dosed at 100 mg/kg would constitute a greater risk than exposing the same animal to a metabolite present at 50% of drug B dosed at 1 mg/kg. These authors have

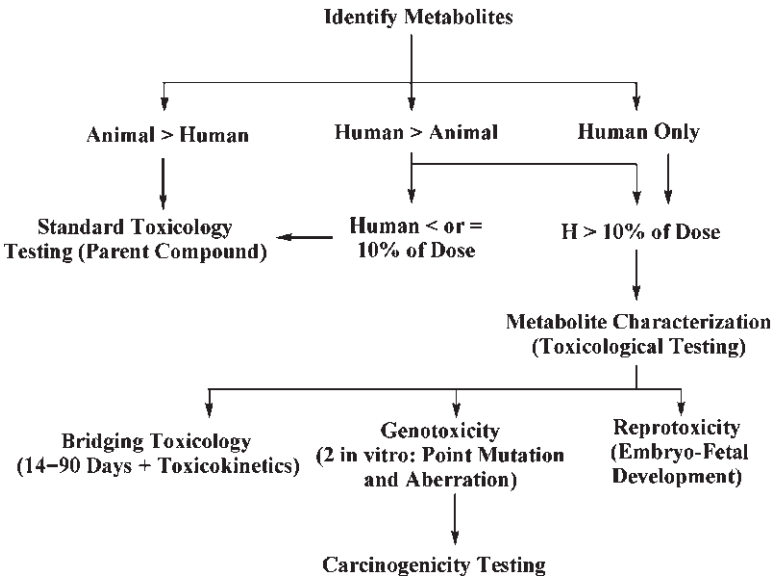

FIGURE 27.2 FDA decision tree for safety testing of metabolites.

proposed a new flowchart for metabolite testing. The reader is encouraged to follow the development of this matter carefully by looking for future FDA guidelines.

It is noteworthy that all of the guidelines or recommendations just discussed require a human study using radiolabeled drugs to conduct thorough metabolite identification and profiling studies before accurate measurements of each circulating metabolite can be assessed.

27.3 HOW ARE METABOLITES GENERATED?

Although many organs are capable of metabolizing xenobiotics in animals, the liver is universally recognized as the major site of drug metabolism. Therefore, it is common to use hepatic subcellular fractions such as microsomes and S9 fractions for the generation of metabolites. Some of the advantages offered by the use of subcellular fractions include relative ease of preparation (Fig. 27.3), ease of storage, commercial availability, relative low cost, flexibility in the manner of use, amenability to high throughput screening, and utility in mechanistic studies with inhibitors. The disadvantages of the use of microsomes and S9 fractions include potential

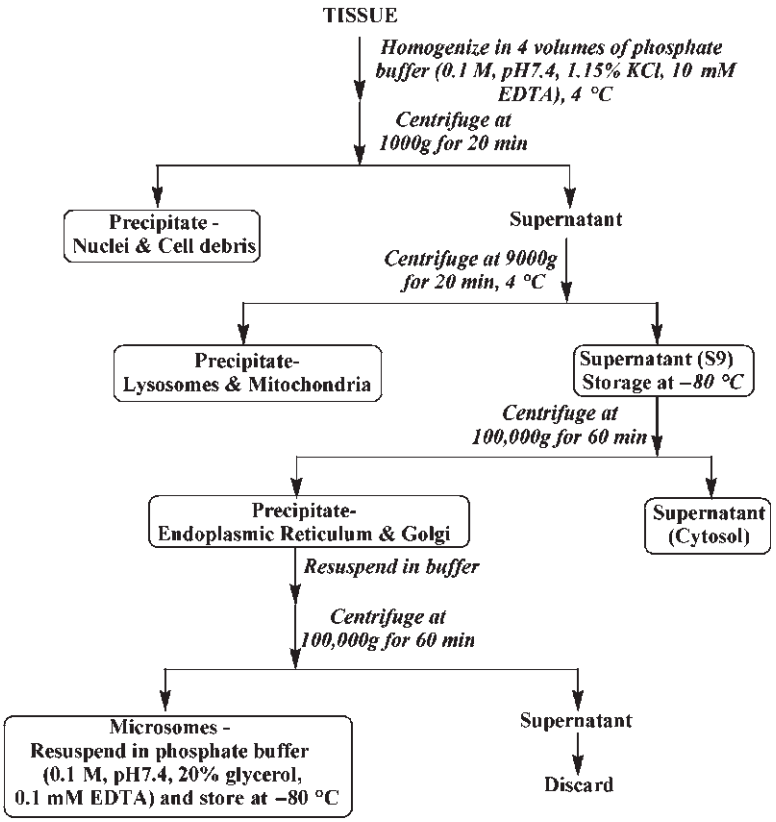

FIGURE 27.3 A scheme for preparation of subcellular fractions. Buffers other than phosphate buffer may be used provided the pH values indicated are observed.

inactivation of some enzymes during preparations (FMOs), loss of cellular compartmentalization, lack of all cellular enzymes resulting in limited metabolism, and absence of cofactors, which will need to be added or regenerated during the course of an incubation. Consequently, the utility of intact hepatocytes offers a viable and advantagous alternative for generation of hepatic metabolites. When prepared correctly [11], these cells have all their subcellular fractions and compartments intact and functioning, do not require cofactors, will provide sequential metabolism of compounds, and are therefore more representative of *in vivo* metabolism. Additionally, hepatocytes are correctly predictive of interspecies differences in drug metabolism [12]. The most important factors prohibiting the use of hepatocytes are that it is more complicated to isolate intact fresh hepatocytes than subcellular fractions, it is more costly to procure commercial cryopreserved hepatocytes, and there are limitations associated with cell viability during incubation and freezer storage. It has been recommended that the incubation of hepatocyte suspensions should not exceed 4 hours [12]. It was demonstrated that while this period is sufficiently long to determine metabolic stability and to allow generation of the main metabolites of a test compound, it may be too short to allow generation of some minor, particularly phase II, metabolites [12].

Regardless of which *in vitro* system is used, it is recommended that human biological reagents be utilized in parallel to those from animal species used for pharmacokinetic and efficacy studies. This allows the investigator to quickly determine species differences in metabolite generation and have a chance for an early look into the possibility of formation of metabolites unique to humans. Furthermore, such studies may unravel species differences in rates of clearance and assist in selection of animal species most relevant to the human. Additionally, they assist in determination of whether the metabolic clearance is the cause of rapid clearance in animal species used in PK studies.

In addition to the *in vitro* mixtures, animal matrices are valuable sources of metabolites. These matrices include plasma, urine, bile, feces, and specific tissues. In order to better understand when and how to best utilize these matrices, one must understand the anatomy and physiology of the test subject. Figure 27.4 is a diagram of the anatomical features of an animal as it relates to drug metabolism. As can be observed, after oral administration (left side of the diagram) a drug enters the stomach and is exposed to gastric hydrochloric acid. In humans, the pH of the stomach can be as low as 1 during the fasted state and as high as 5 in the fed state [13]. In animals, varying levels of acidity are observed in different species [14]. The low pH may result in chemical degradation of drugs in the stomach. The basicity of the gastrointestinal tract is elevated going from the stomach to the colon and rectum, where the pH is around 8 [15]. In the small intestine, hydrolytic enzymes secreted by the pancreas may metabolize a drug. The large intestine has a large reservoir of microbial populations, which can perform hydrolytic and reductive biotransformations of the drugs and/or their metabolites. These metabolites, along with any unchanged drug molecules, are excreted in the feces.

The major site of absorption is the small intestine. A drug molecule and/or its metabolites or degradation products can be absorbed through the wall of the small intestine and enter the portal vein. The intestinal epithelial cells, also known as enterocytes, are enzymatically active and can metabolize xenobiotics. Once these molecules enter the portal vein, they are carried to the liver, where further

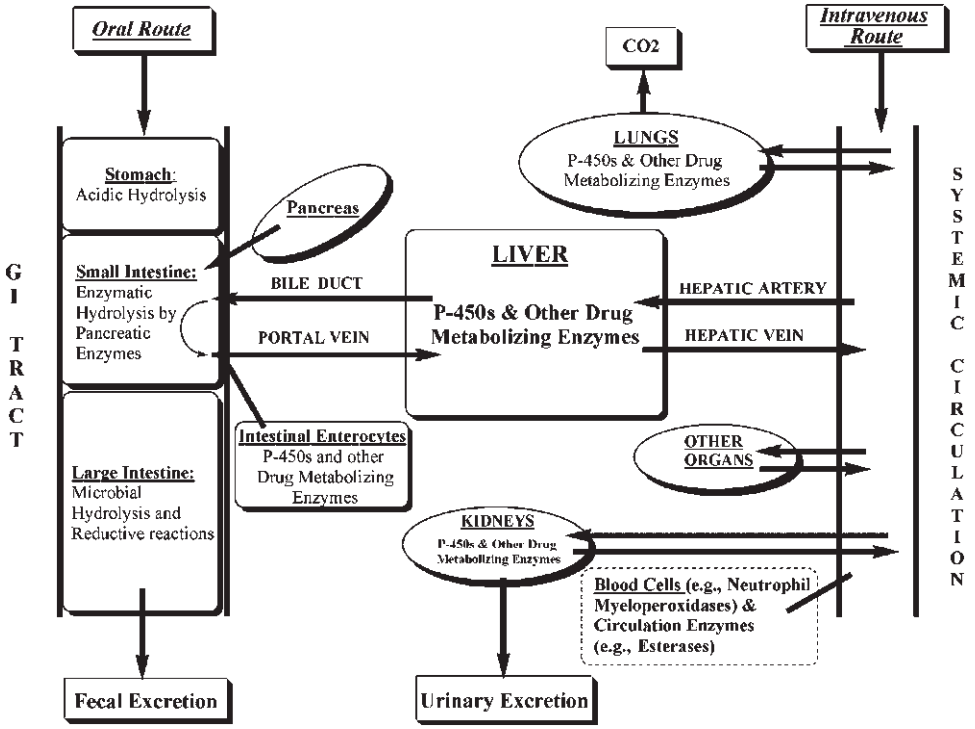

FIGURE 27.4 A schematic of mammalian anatomy as it relates to drug metabolism.

metabolism may take place; a process referred to as "first-pass effect." Some of the unmetabolized drug and/or its metabolites may be secreted into the bile and return to the small intestine via the bile duct. A fraction of these molecules can be reabsorbed through the small intestine wall and enter the portal circulation again, a process referred to as "enterohepatic recirculation." When molecules leave the liver they enter the hepatic vein and move toward the systemic circulation, which in turn carries them to the peripheral tissues and organs. These molecules can go back into the systemic circulation and travel back to the liver and bile duct. Other molecules present in circulation can enter the lung and kidney, both of which are metabolically active organs. In the lung, drug molecules can be converted into metabolites or be extensively metabolized to CO_2 and exhaled. In the kidney, both parent drugs and their metabolites can be filtered out of circulation at the glomerulus or be secreted out by the epithelial cells of the loop of Henle into the urine [13]. These molecules are then excreted in urine (or may be reabsorbed within the loop of Henle). Blood itself is a metabolizing tissue, which has circulating enzymes such as esterases. Additionally, cells such as neutrophils in the blood contain myeloperoxidases capable of metabolizing drugs [16].

In the following sections, examples describe how some of the matrices described earlier may be used in metabolite profiling. In PK and efficacy studies, plasma samples are prepared routinely from serially collected systemic blood. Identification of circulating metabolites in PK studies can prove very valuable in validating the importance of the metabolites identified in *in vitro* studies. Also, by simultaneous

monitoring of a parent compound and its circulating metabolites, one may be able to identify pharmacologically active metabolites. This is helpful when there are inconsistencies between maximum plasma concentration and the time to reach that concentration and the maximum efficacy and the time to reach that effect for a drug candidate. Of course, it is important to note that delayed effects are not always due to late forming metabolites and can simply be due to delayed pharmacological effects of a parent molecule. When animals are dually cannulated in the bile duct and portal vein (Fig. 27.4), metabolite profiling of the blood from the portal vein offers a way to differentiate between hepatic and prehepatic (intestinal) metabolism. In these studies, it is imperative to have animals dually cannulated to prevent hepatic metabolites from enterohepatic recirculation via the bile duct (Fig. 27.4).

27.4 WHAT ARE BIOTRANSFORMATION REACTIONS AND HOW DO THEY GENERATE REACTIVE METABOLITES?

Enzymatic reactions responsible for the transformation of xenobiotics to their metabolites are referred to as biotransformation reactions. As mentioned previously, these reactions are generally designed to render xenobiotics more water soluble and therefore more amenable to excretion. The liver is the main site of biotransformation. However, other organs, although usually not to the same extent, are capable of participating in this process. These reactions reduce the half-life of a compound and diminish its oral bioavailability due to the first-pass effect in the liver. Traditionally, biotransformation reactions are grouped into phase I and phase II reactions (Table 27.1).

TABLE 27.1 List of Phase I and II Drug Metabolizing Enzymes

Enzyme	Reaction
Phase I	
Cytochrome P450s (CYP450)	Oxidation and reduction
Monoamine oxidases (MAOs)	Oxidation
Flavin-containing monooxygenases (FMOs)	Oxidation
Alcohol dehydrogenases (ADHs)	Oxidation and reduction
Aldehyde dehydrogenases (ALDHs)	Oxidation and reduction
Xanthine oxidases (XOs)	Oxidation
Epoxide hydrolases (EHs)	Hydrolysis
Carboxylesterases and peptidases	Hydrolysis
Carbonyl (keto) reductases	Reduction
Phase II	
UDP-glucuronosyltransferase	Glucuronidation
UDP-glycosyltransferase	Glycosidation
Sulfotransferase	Sulfation
Methyltransferase	Methylation
Acetyltransferase	Acetylation
Amino acid transferases	Amino acid conjugation
Glutathione-*S*-transferase	Glutathione conjugation
Fatty acid transferases	Fatty acid conjugation

Phase I reactions include hydrolytic, reductive, and oxidative reactions. Esterases, amidases, and epoxide hydrolases are among the hydrolytic enzymes. There are many reductive enzymes such as keto-reductases that catalyze phase I reactions. Finally, oxidative reactions of phase I enzymes are catalyzed by cytochrome P450s, dehydrogenases (i.e., alcohol or aldehyde dehydrogenases), and flavin-containing monooxygenases (FMOs). These highly prevalent oxidative reactions serve to introduce hydroxyl groups on xenobiotics as well as to modify molecules by oxidative N-, S-, and O-dealkylations, which in turn serve to generate free amines, sulfhydryls, and alcohols. A survey of 300 commonly prescribed drugs from multiple therapeutic areas has revealed that cytochrome P450s are responsible for the biotransformation of about half of the marketed drugs [17]. Cytochrome P450s are a superfamily of heme-containing isozymes. They are embedded primarily in the lipid bilayer of the endoplasmic reticulum of liver cells, which are converted into microsomes during homogenization of liver samples. These enzymes have broad substrate specificities and require reduced nicotinamide adenine dinucleotide phosphate (NADPH) as a cofactor. The dominant cytochrome (CYP) isozymes involved in human metabolism of drugs are CYP3A4, CYP2D6, CYP2C9, CYP2C19, CYP1A2, and CYP2E1; ranked according to their order of importance [18]. CYP3A4 were found to be responsible for ~40% of CYP-catalyzed drug metabolism.

Phase II reactions catalyzed by transferases are characterized as conjugation reactions (Table 27.1). These include glucuronidation, sulfation, glutathione and amino acid conjugation, acetylation, and methylation reactions of drugs. Glucuronidation reactions, catalyzed by uridine-diphosphoglucuronosyltransferase or UDPGT (microsomal) using UDP-glucuronic acid (UDPGA) as the endogenous reagent, are the most common phase II reactions. UDPGTs are ubiquitous to most tissues [18]. The net result of this reaction is addition of β-glucuronic acids to alcohols, carboxylic acids, amines, and sulfhydryls. These glucuronides can be deconjugated by β-glucuronidases, which are often used as biochemical tools to free the parent compound during the metabolite identification process. Drug glucuronide conjugates formed in the liver or intestinal enterocytes are excreted into the small intestine after secretion into the bile. Once in the small intestine, these conjugates can be hydrolyzed back to the parent drug by β-glucuronidases secreted into the lumen of the small intestine by the pancreas. The drug molecule can then be reabsorbed (enterohepatic recirculation). The kidney is also a significant site of glucuronidation and is capable of excretion of glucuronides into the urine.

It is not the objective of this chapter to discuss all the biotransformation reactions extensively, as this subject has been reviewed at length in comprehensive review articles [19, 20]. However, a brief overview of this subject is presented to provide the reader with the basic understanding of the subject. Selected examples of phase I biotransformation reaction mechanisms are presented in Fig. 27.5. These general reactions show oxidation of double bonds, heteroatoms, and carbons. Mechanisms of oxidation alpha to heteroatoms like nitrogen, oxygen, and sulfur, which ultimately can lead to cleavage of the carbon–heteroatom bonds, are also depicted. It is worth discussing the reaction mechanism for glucuronidation (Fig. 27.6) because of its prevalence and implication in the development of adverse effects, which will be discussed later. As can be observed, the lone pairs of electrons from an alcohol conduct an SN2 attack on the anomeric carbon of glucuronic acid, which has a phosphoester linkage to the uridinyldiphosphate molecule in UDPGA. This results

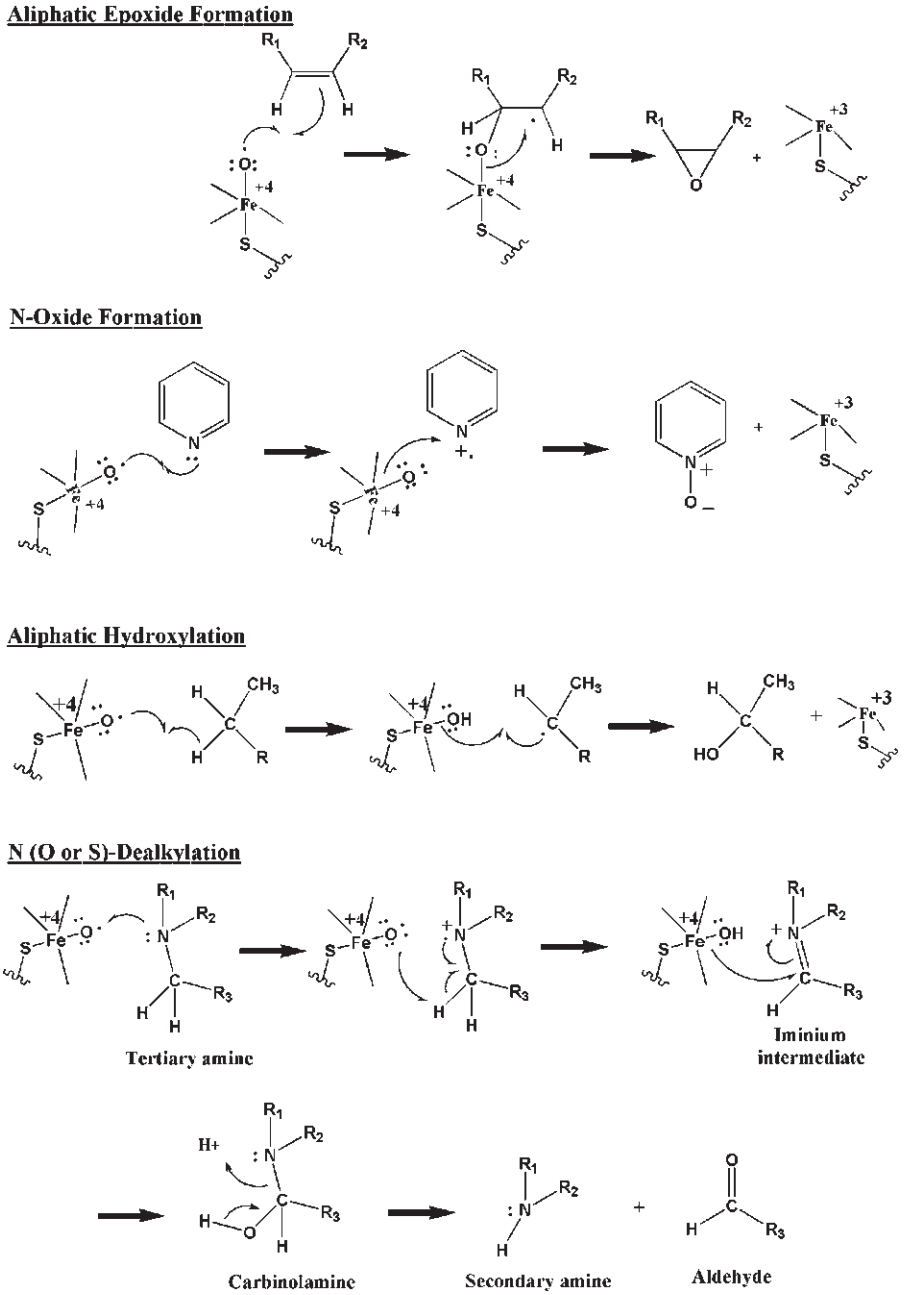

FIGURE 27.5 Selected examples of P450 oxidative reaction mechanisms.

in a substitution of the UDP, an inversion of the bond into a β-bond and hence, formation of a β-glucuronide conjugate.

Reactive metabolites have become an increasingly important topic of discussion in recent years due to the adverse effects associated with them. They are the unintended products of what was traditionally referred to as "detoxification pathways"

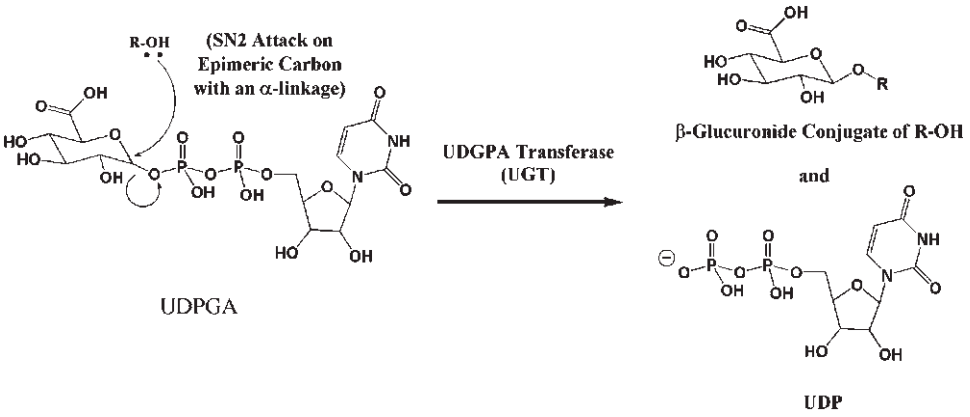

FIGURE 27.6 UDPGA transferase mechanism of glucuronidation. A conjugating nucleophile displaces the uridinyldiphospho moiety of UDPGA by an SN2 attack on the anomeric carbon of glucuronic acid.

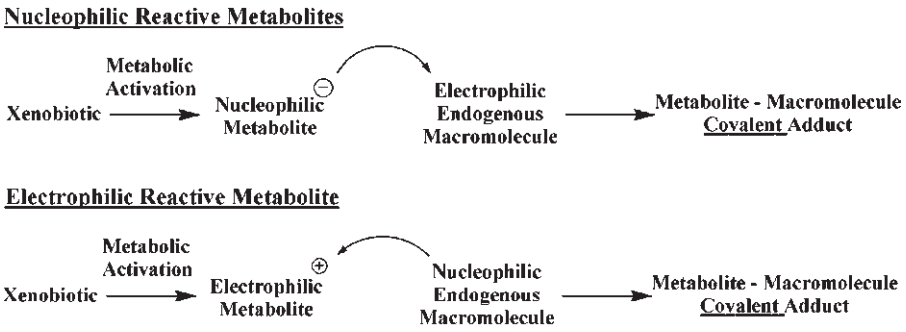

FIGURE 27.7 Covalent binding to cellular constituents can be conducted by nucleophilic or electrophilic reactions.

[21]. In general, reactive metabolites can be categorized as electrophilic or nucleophilic compounds (Fig. 27.7). After metabolic activation into a nucleophilic compound, a xenobiotic can react with an electrophilic endogenous molecule and form a stable covalent bond. Xenobiotics with a potential to form electrophilic metabolites draw reactions from nucleophilic endogenous molecules and form adducts. In such a way, reactive metabolites can cause enzyme deactivation, lead to off target toxicity, and cause idiosyncratic reactions. As shown in Fig. 27.8, the methylenedioxyphenyl moiety present in many xenobiotics such as Ecstasy (methylenedioxyamphetamine, MDA) can be metabolized to a nucleophilic carbene metabolite, which can covalently bind the heme group within the active site of P450s like CYP2D6, hence resulting in severe toxicity [22]. Demethylenation of the methylenedioxy moiety may play a role in the toxicity of such groups due to formation of quinone type intermediates [20, 23]. Aniline is an example of a compound that can be metabolized to form an electrophilic reactive metabolite, namely, a reactive nitrene (Fig. 27.8).

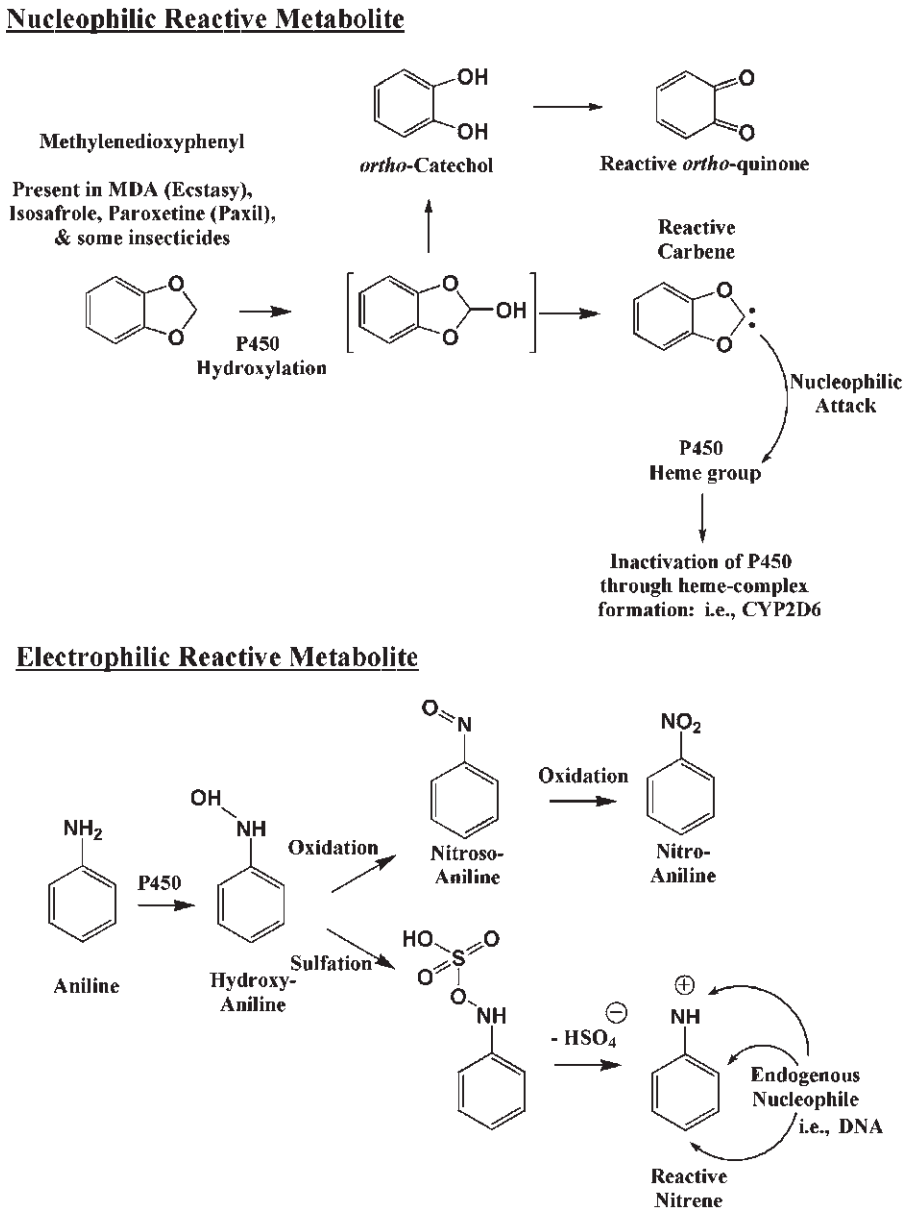

FIGURE 27.8 Selected examples of nucleophilic and electrophilic reactions of reactive metabolites.

Diclofenac, a widely used nonsteroidal anti-inflammatory drug (NSAID), can cause a rare but serious hepatotoxicity [24]. Around four in 100,000 users (180 confirmed cases in the first three years of marketing in the U.S.) of diclofenac users developed severe liver damage with an 8% rate of fatality [24]. Diclofenac contains two masked anilines and a carboxylic acid moiety, all of which provide opportunities for reactive metabolite formation. Figure 27.9 describes biotransformation of the

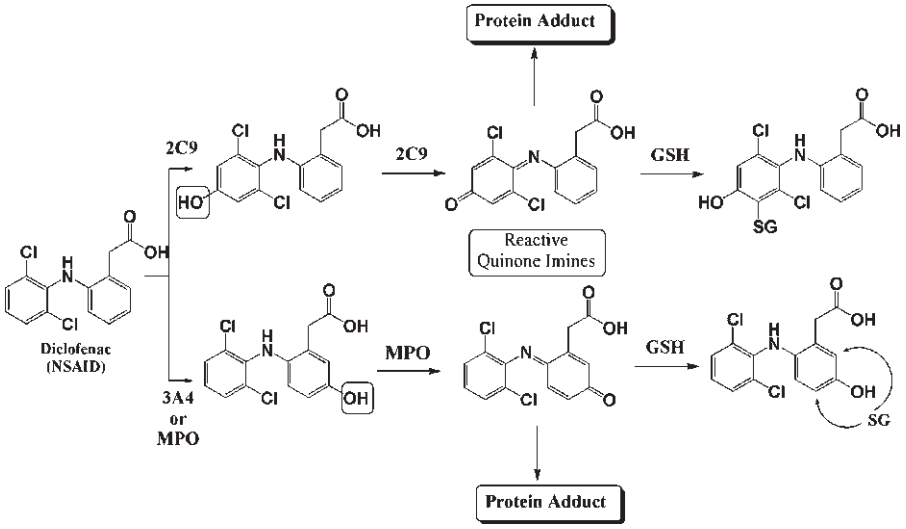

FIGURE 27.9 Potential bioactivation of diclofenac to reactive species.

anilinic groups of diclofenac into electrophilic reactive metabolites capable of binding nucleophilic molecules. As shown, the two aromatic rings can be hydroxylated *para* to the nitrogen by CYP2C9 and CYP3A4 or myeloperoxidases (MPOs). Further metabolism results in the two respective *para*-aminoquinones, which can undergo nucleophilic attacks at *meta* positions to the nitrogen by nucleophiles like glutathione or macromolecules to form covalent adducts. The carboxylic acid moiety on this, as well as many other drugs, is a suitable site for acyl glucuronidation.

A glucuronide conjugate of a carboxylic acid is referred to as an acyl glucuronide. Acyl glucuronides, but not ether glucuronides (of alcohols), have been implicated in irreversible binding of proteins resulting in haptenization and immune reactions. The first documentation of such adduct formation was by Smith et al. [25] using zomepirac, an NSAID with adverse effects, in human plasma and *in vitro* using albumin. The mechanism of toxin formation was described as shown in Fig. 27.10, based on mechanisms previously described for reaction of bilirubin glucuronides [26], glycosylation of hemoglobin [27–29], and albumin [30, 31]. As illustrated in Fig. 27.10, a 1-*O*-acyl glucuronide, which is formed via the mechanism described in Fig. 27.6, can undergo several routes of metabolism. The arrow labeled as 1 shows intramolecular migration of the constituent. During this process the hydroxyl group on C2 of the glucuronic acid substitutes the hydroxyl group of the anomeric carbon (C1) via an SN2 reaction. This process is referred to as "acyl migration" and the acyl group can continue to migrate to the other hydroxyl groups on C3 and C4. The transacylated metabolite, 2-*O*-acyl glucuronide, can exist in two isomeric forms, one of which can undergo a ring opening to yield a reactive aldehyde. Reaction of this aldehyde with an amino group on a protein, referred to as "glycation" of the protein, results in a Schiff base formation. This constitutes a stable covalent linkage of the acyl group to the protein mediated by the glucuronic acid. At this point, the acyl group–protein complex is haptenized and recognizable by the immune system as an antigen. Formation of antibodies against this hapten will be problematic and a

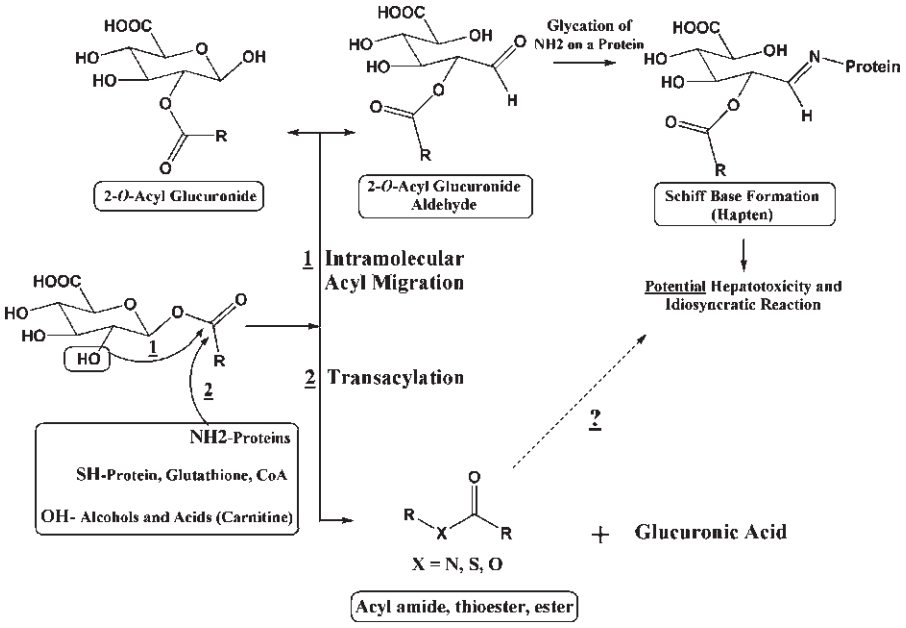

FIGURE 27.10 Formation of an acyl glucuronide and its reactivity.

potential reason for idiosyncratic reactions. Indeed, circulating antibodies against diclofenac–liver protein adducts have been detected in the sera of seven out of seven patients with diclofenac-induced hepatotoxicity [24].

Additionally, the same observation was made in 12 of 20 subjects on diclofenac without hepatotoxicity, and none of the control subjects had this circulating antibody [24]. The other path for an acyl glucuronide metabolism is path 2 in Fig. 27.10. In this case, a nucleophilic moiety such as an amine, sulfhydryl, or hydroxyl group of another molecule will displace the glucuronide moiety to form an acyl amide, thioester, or ester. If these transacylating groups are positioned on macromolecules, haptenization may take place depending on the stability of the covalent bond, this time through a direct linkage of the xenobiotic to a macromolecule.

In order to understand whether reactive metabolites are formed by a drug or drug candidate and to estimate the extent of their formation, elaborate methods have been developed using trapping agents [32]. From a practical standpoint, during the course of drug discovery and development, most compounds with reactive metabolites, if capable of generating significant adducts and adverse effects, will be excluded due to their poor pharmacokinetics (i.e., exposure) or *in vitro* and *in vivo* toxicity. Furthermore, it is difficult to justify eliminating a compound from the discovery process simply based on its ability to form reactive metabolites, unless these data are coupled with toxicity data. This is because there are *in vivo* mechanisms to degrade most covalently bound adducts and prevent adverse effects. Until there are elaborate correlations established to link particular types and levels of adduct formation to incidences of adverse effects and idiosyncratic reactions, the utility of reactive metabolite trapping experiments in the discovery setting is unclear. This is particularly true in most discovery groups because to quantitate the extent of adduct

formation, radiolabeled drugs are needed and these generally are not available in the early discovery process. However, trapping experiments may be useful in confirming or removing doubts about specific chemical moieties' ability to generate reactive metabolites if such moieties are associated with toxicity.

27.5 HOW ARE METABOLITES ISOLATED AND IDENTIFIED?

Many techniques are employed for isolation and identification of metabolites. Due to the complexity of matrices that contain metabolites, often one has to use a chromatographic method to separate metabolites from each other and from unrelated chemical entities such as endogenous compounds. In the past, gas or liquid chromatography (GC or LC) was used to accomplish such a task. Analytes were first extracted from the matrices using volatile organic solvents and injected onto a GC column. The compounds of interest eluting off the GC column could be condensed and isolated into cooled vessels and reconstituted in appropriate solvents for the purpose of structural analysis. In the case of liquid chromatography, analytes eluting from the LC column were collected manually or using an automated fraction collector. After evaporation of the LC solvent, analytes of interest were reconstituted into solvents appropriate for structural analysis.

With development of tandem gas chromatography/mass spectrometry (GC/MS), the need for isolation of analytes was eliminated. GC/MS methods for the study of metabolites had a limitation in that the metabolites of interest had to be volatile or had to be derivatized to become volatile enough to elute off a GC column and enter into the mass spectrometer [33]. This added a degree of complexity to metabolism studies, because not only a derivatization step was required, but also the heat used to volatilize the analytes could cause chemical degradation of the analytes. With the advent of tandem liquid chromatography/mass spectrometry (LC/MS), the need for sample collection was alleviated. In LC/MS studies, each analyte eluting from the LC system enters the mass spectrometer for structural analysis. In addition to LC/MS techniques, there are other methods that couple the LC separation to a variety of techniques such as UV, IR, and NMR. The main focus of this discussion is modern LC/MS techniques due to the dominant role of mass spectrometry in metabolite identification.

27.5.1 Mass Spectrometry

The goal of this discussion is to provide the reader with a basic understanding of mass spectrometry as it relates to the identification of metabolites. Therefore, detailed information regarding the architecture of mass spectrometers will not be provided. A mass spectrometer is an instrument designed to distinguish gas-phase ions according to their mass-to-charge (m/z) ratios. Figure 27.11 depicts an oversimplification of an LC/MS instrument. Generally, analytes separated by the LC column enter a chamber referred to as an ion source before entering the high vacuum chamber of a mass spectrometer via a vacuum interface component. The mass analyzer components, as well as the mass detector unit, are placed in a high vacuum chamber to minimize the possibility of intramolecular collisions and to assist in movement of the ions toward the detector. The mass analyzers may be

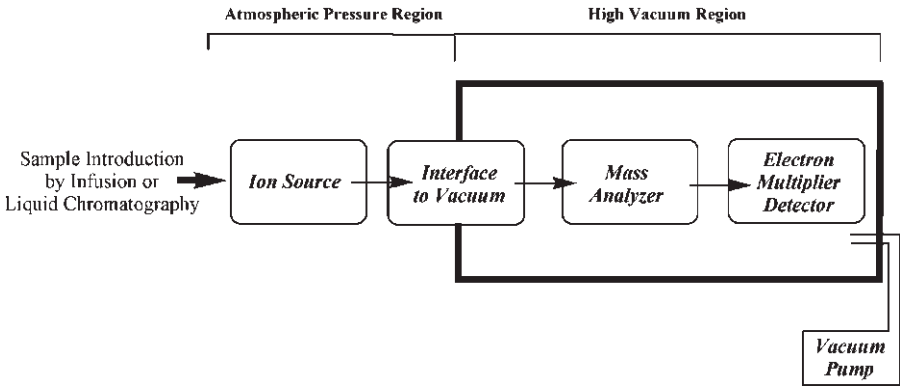

FIGURE 27.11 An oversimplified depiction of the components in a triple-quadrupole mass spectrometer.

operated with electric, magnetic, or both fields. These fields are utilized to move ions to the detector after they enter the high vacuum environment in order to produce a signal. The mass-to-charge ratios (and not just the mass) of ions are responsible for separation of the ions in the electrical and/or magnetic fields.

Ion Generation Analytes are introduced into a mass spectrometer via an interface called a probe. Details of how an ionization probe operates are not discussed here. It is only pointed out that the analytes suspended in the HPLC solvent pass through a capillary tube within the probe and are introduced into the ion source chamber (discussed later) as a fine mist of droplets. There are several ways in which analytes may be ionized in LC/MS. Atmospheric pressure ionization (API) is a term used commonly to refer to the technique used to generate ions in the ion source and prior to entry into the chambers operated under vacuum. API techniques include electrospray ionization (ESI), atmospheric pressure chemical ionization (APCI), and atmospheric pressure photoionization (APPI). All of these are referred to as soft ionization techniques.

- In the ESI technique, the ions are generated in the mobile phase of the HPLC by adding a proton donor such as acetic or formic acid or a proton acceptor such as ammonium hydroxide. ESI is a solution phase, soft ionization technique used for any type of analyte, regardless of its volatility. With this technique, special attention should be paid to the pK_a of the analyte and the pH of the mobile phase to ensure ionization and to determine whether positive or negative ions will be generated. This in turn determines whether the mass spectrometer should be operated under positive or negative modes. While ESI can be used for most analytes, it seems to be very effective in analysis of polar compounds with large mass ranges. In ESI, the ions are generated in $[M + H]^+$ or $[M - H]^-$ depending on the mode used.
- In the APCI technique, the analytes reach the ion source in a neutral state. They become vaporized within the HPLC mobile phase using temperature and application of a high voltage needle positioned into the corona discharge. This leads

to their gas phase ionization through a complex process. APCI is typically used for analytes of medium to low polarity that have some volatility. This technique is often used with small molecules with molecular weights of up to ~1500 daltons and is extremely robust and not subject to minor changes in buffers and/or buffer strength. As was the case for ESI, APCI can be operated in both positive and negative ion modes.

- APPI is the newest of the three techniques. It is another gas-phase ionization technique, where the ionization is accomplished using a UV light source. The ions are generated in positive mode only and in the form of $[M]^+$ and $[M + H]^+$.

Once the ions are formed they leave the ion source and enter the first vacuum region of the mass spectrometer, commonly referred to as "Interface to Vacuum," through a narrow orifice leading to an ion transfer capillary tube. These ions then move toward the ion guides (quadrupoles 00 and 0 or Q00 and Q0). Ion guides are multipole rod assemblies that operate with radiofrequency (RF) voltage. In this environment, all ions have a stable trajectory and pass through the system while being focused into ion beams on their way to the mass analyzer. All the neutral and oppositely charged ions are pumped away or crash into the surface before the orifice of the capillary tube. Regardless of the type of ionization, the differences in the design and utility of the mass analyzer differentiates different types of mass spectrometers.

Mass Analyzers

Triple Quadrupole In a triple quadrupole or "triplequad" mass spectrometer, the mass analyzer is divided into three segments, each referred to as a quadrupole or a quad. The reason for the name is that each quadrupole consists of four poles or rods assembled parallel to each other (Fig. 27.12). Rods opposite each other in the quadrupole assembly are considered a pair. Voltages of the same amplitude and polarity are applied to an opposing pair of rods. The voltages applied to the other pair are the same amplitude, but opposite polarity. As the polarity of voltages in each pair of rods oscillates between positive and negative, the ions of interest within each quadrupole are focused and directed toward the detector end of the instrument. In

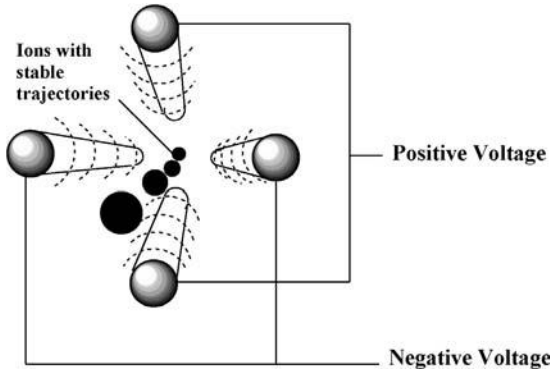

FIGURE 27.12 Movement of ions through a quadrupole.

addition to focusing ions, quadrupoles act as selection devices. The voltages used are of AC and DC nature and because the frequency of the AC voltage is in the radiofrequency range, it is referred to as RF voltage. When selecting for a specific ion, the amplitudes of RF and DC voltages are kept constant, only ions with an m/z that resonate with that particular condition will have stable trajectories to pass through the quadrupole assembly to be detected. All other ions will be destabilized and crash onto the rods and become eliminated. In cases where the RF and DC voltages are ramped up, a process referred to as scanning upward, ions of successively higher m/z ratios will be mobilized and reach the detector through stable trajectories. Therefore the ratio of the RF to DC voltages determines the ability of the mass spectrometer to separate ions of different m/z ratios.

The first and third quads (Q1 and Q3) are mass analyzers, which, depending on the type of experiment, can be configured in a specific manner to detect an ion of interest. The second quad (Q2) is a collision cell filled with an inert gas like argon when conducting collision-induced dissociation (CID) or MS/MS (MS^2) experiments. CID is a transfer of energy to an ion through collision with a neutral molecule (inert gas) resulting in vibration, cleavage, and/or rearrangement of one or more bonds on the ion. The weakest bonds in an analyte cleave first and to a greater extent resulting in fragments. The resulting fragments are used to assemble the structure of the parent ion. One limitation of a triple quad mass spectrometer is that it will not conduct MS experiments beyond MS^2. While for most metabolite identification projects MS^2 data is sufficient in determining general sites of metabolism on a molecule, for a more detailed analysis one may resort to an ion-trap instrument (as described later). Triple quads can be used to conduct several types of experiments. These include full scan, selected ion monitoring, product or daughter ion scan, precursor or parent ion scan, selected or multiple reaction monitoring (SRM or MRM), and constant neutral loss scan.

FULL SCAN MASS SPECTROMETRY Full scan is an MS^1 experiment, which is used to detect any molecule with an m/z within a certain range in the analyzed sample. A full scan experiment is inclusive of all ionizable molecules in the matrix that enter the mass analyzer and fit the mass range criteria designated by the operator. Figure 27.13 depicts the steps involved in conducting a full scan experiment. As shown in Fig. 27.13, in an MS^1 experiment, Q1 is set to scan the mass range of interest, while Q2 and Q3 are turned off and Q2 does not contain any collision gas. Alternatively, Q1 and Q2 can be turned off while only Q3 is in the scanning mode. The mass range of interest is scanned by ramping RF/DC voltages to select ions from the lowest to highest m/z repeatedly and once every few milliseconds (scan time). Every ion exiting Q1 then gains a clear path through Q2 and Q3 to an electron multiplier detector and its m/z is recorded. In an LC/MS experiment, as analytes are separated by the chromatography column, they enter the mass spectrometer one by one and this, coupled with the fast scanning capability across a mass range, generates a total ion chromatogram (TIC), which includes all ions eluting from the HPLC. The data output obtained from a full scan experiment is a TIC and a mass spectrum associated with each TIC signal (Fig. 27.13). It should be noted that the selected mass range is shown on the x-axis of each mass spectrum.

As was mentioned before, full scan experiments can be used to gather data on all the ionizable compounds in a mixture. Once this process is finished, one can

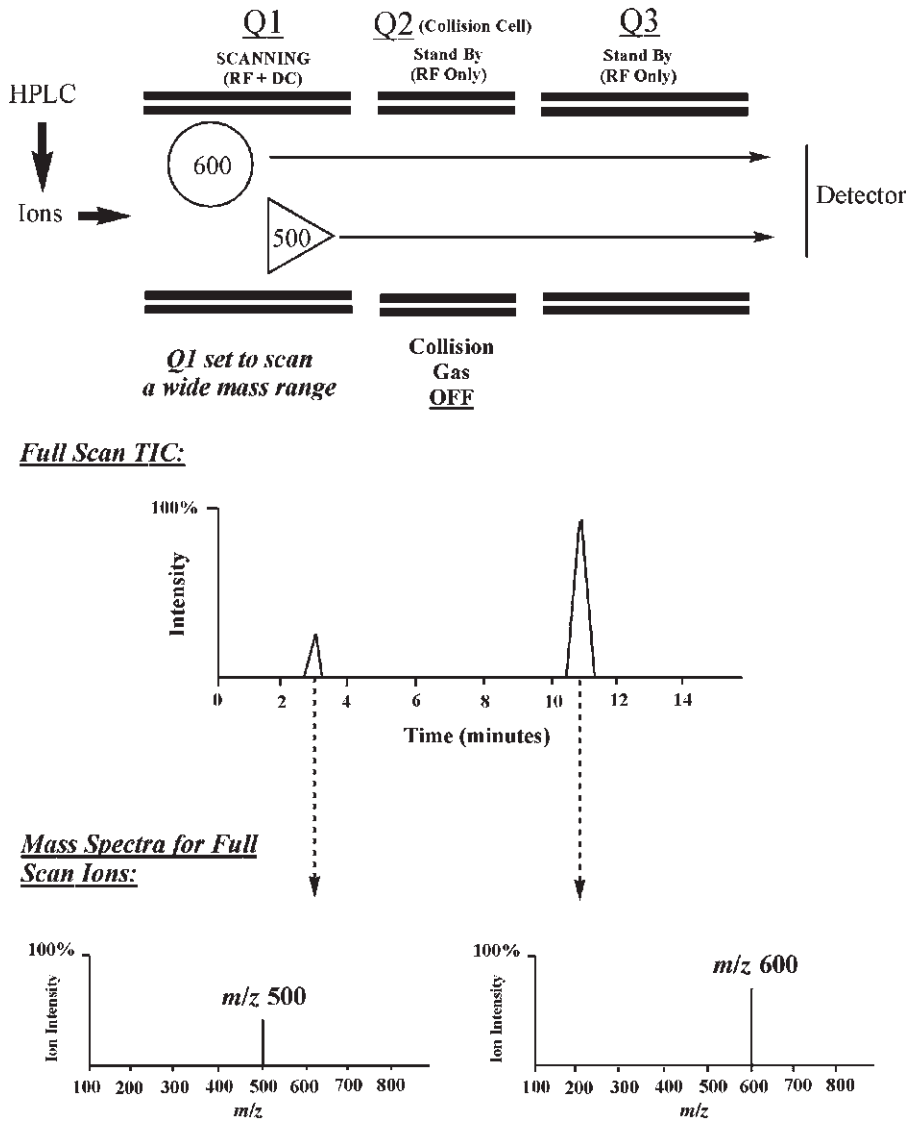

FIGURE 27.13 A schematic of a full scan experiment. All ions pass through the triple quadrupole mass spectrometer to be detected. A full scan TIC and mass spectra are generated.

search for a specific ion (a process referred to as "mass extraction"), to detect the presence of compounds with a specific m/z. The limitation of this experiment is that one cannot distinguish the compound of interest from isobaric compounds because a full scan dataset only provides information on the overall mass of a compound, and not its structural features. In cases when the operator is limited to the use of a single quad mass spectrometer and is unable to perform MS^2 experiments, any TIC peak that shows the m/z of interest may be collected as it elutes from the HPLC and further analyzed by other techniques such as NMR.

SELECTED ION MONITORING This experiment is useful to detect minute quantities of a known analyte in a complex mixture. Therefore, while it is useful in detection of known metabolites, it is not particularly useful in identification of unknown metabolites. Selected ion monitoring (SIM) or selected ion recording (SIR) is another MS^1 experiment. In contrast to a full scan experiment, where a mass range is scanned repeatedly, in an SIM experiment the mass spectrometer is configured to acquire and record ions with one or a few selected mass-to-charge ratios. SIM is therefore a more sensitive experiment than full scan because all the scan time is used to focus on a specific mass rather than a broad mass range, as was the case for full scan.

PRODUCT OR DAUGHTER ION SCANNING This MS^2 experiment is useful in understanding the fragmentation pattern of a molecule in the mass spectrometer. In a product ion scanning experiment, a particular ion (parent or precursor) entering Q1 is fragmented through collision with an inert gas in Q2 (collision-induced dissociation, CID) to give rise to its product ions (this utility will be discussed later). In the example presented in Fig. 27.14, the Q1 is set to select only ions with m/z 600 into Q2, while Q2 is filled with the collision gas and Q3 is scanning for a wide mass range (m/z 100–800 as seen on the x-axis of the product ion mass spectrum) selected by the operator to capture all fragments. Therefore, in this example, the ion with m/z 600 passes from Q1 to Q2 (or the collision cell) and fragments. These fragments, m/z 150 and 450, as well as any unfragmented parent ion are detected and captured in the product ion mass spectrum. The product ion TIC will represent the parent ion of m/z 600 detected by Q1 and is linked to the mass spectrum containing the fragment ion masses detected by Q3; in this case 150, 450, and 600.

The intensity of the TIC peak depends on the number of ions with m/z 600 detected in Q1. The intensity of ion signals in the resulting mass spectrum depends on the abundance of each ion after CID. Therefore, in this particular example, the intensity of the TIC depends on how many ions of m/z 600 enter Q1, which is a function of the concentration of the analytes in the sample and its ionization potential. On the other hand, the intensity of the fragment ions in Q3 depends on how well the parent ion fragmented in Q2. By elevating collision energy in Q2, one can completely shatter the ion at m/z 600 and even fragment its product ions at m/z 150 and 450 further into their respective product ions. Respectively, by lowering the collision energy, one will observe more of the parent and less of the product ions in the product ion spectrum. It is recommended to optimize the experimental condition such that around 5–10% of the parent ion is detected in the product ion spectrum to prevent excessive fragmentation.

PRECURSOR OR PARENT ION SCANNING This experiment is useful in understanding the ions from which a particular fragment originates. In a precursor ion scanning experiment, all the ions produced in the ion source enter Q1 where they are scanned and sequentially transmitted to Q2. After CID in Q2, the product ions enter into Q3 where only the product ion of interest will be selected and transmitted to the detector. In the example given in Fig. 27.15, Q1 is set to scan a wide range of ions (m/z 100–800), and therefore all ions within that range are scanned and transmitted to Q2. CID of all of these ions generates their product ions, which all enter into Q3. However, Q3 is set to scan for a specific product ion of m/z 150. In this case, only one of the two molecules gives rise to that product ion. Generation of product ion

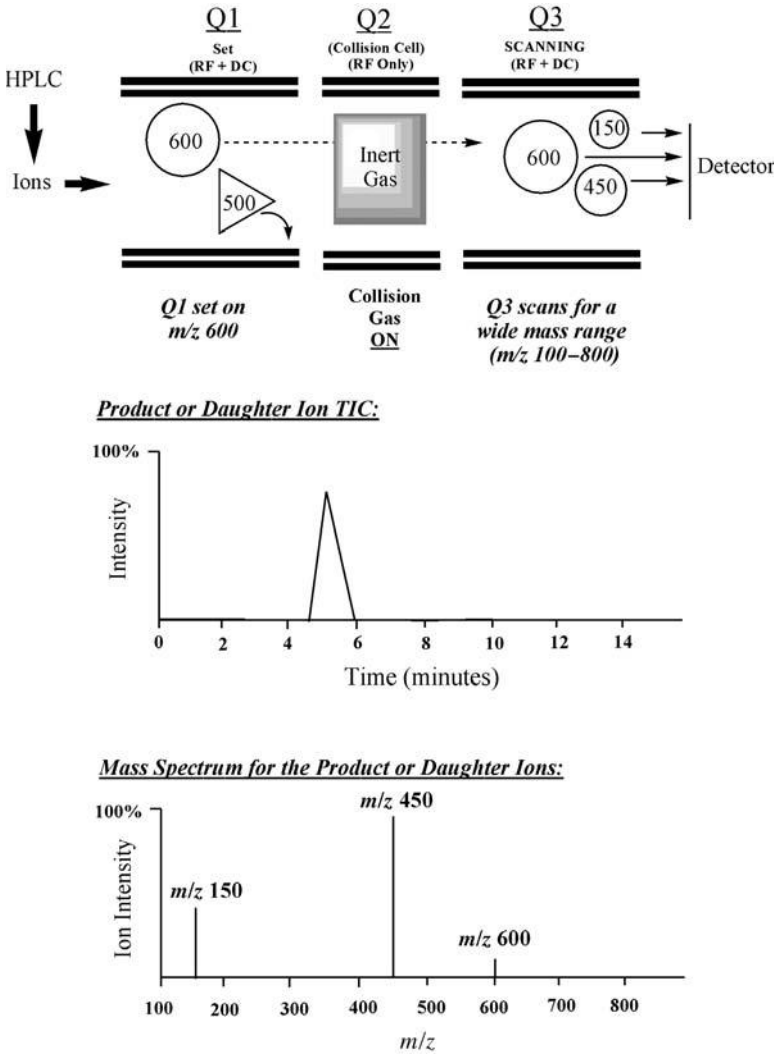

FIGURE 27.14 A schematic of a product or daughter ion scan experiment. Selected ions enter the collision cell and their product ions are detected. A product ion TIC and mass spectra are generated.

m/*z* 150 is linked to the parent ion with *m*/*z* 600. The data output of this experiment is a TIC of the precursor ion linked to its mass spectrum. Generally, the choice of which product ion to scan in Q3 depends on a previously conducted MS^2 experiment (i.e., infusion of the parent compound). Ideally, one optimizes the experimental conditions (i.e., collision energy) for the fragment ion of interest and uses the same experimental conditions for conducting the precursor ion scanning experiment. This maximizes the sensitivity of precursor ion detection.

CONSTANT NEUTRAL LOSS SCANNING This MS^2 experiment is useful in detecting conjugates (i.e., glucuronide or sulfate) of known compounds. In a constant neutral

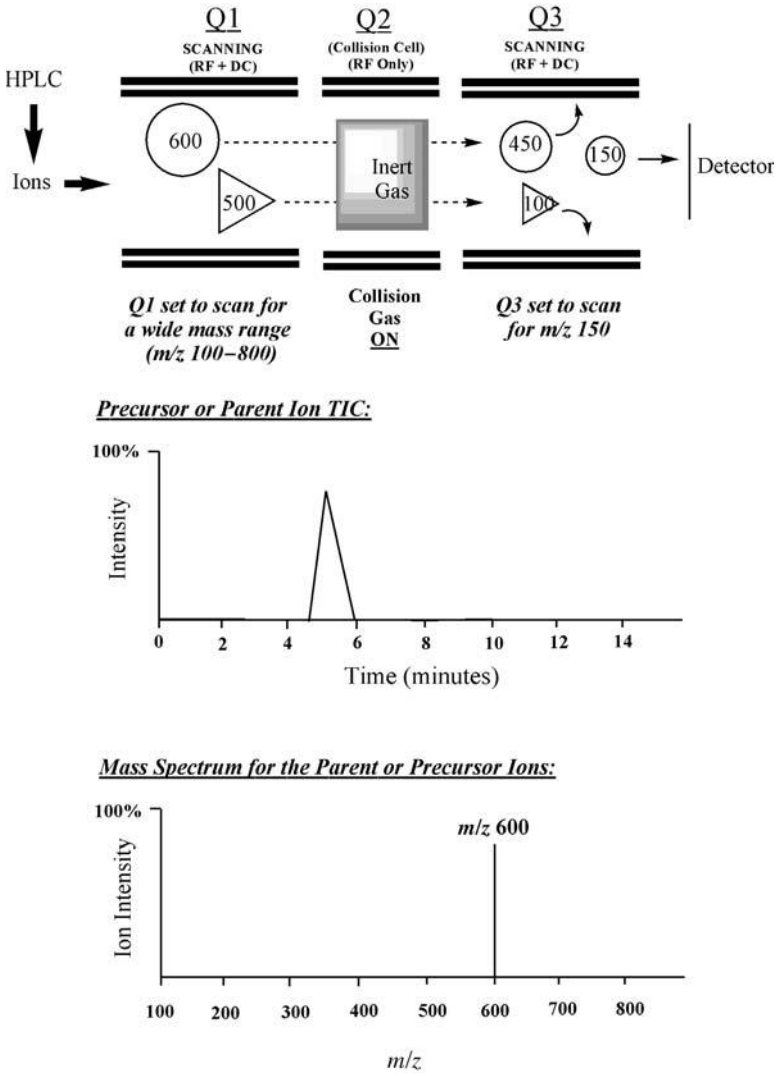

FIGURE 27.15 A schematic of a precursor or parent ion scan experiment. Precursors to selected product ions are determined and precursor TIC and mass spectra are generated.

loss experiment, Q1 and Q3 are linked together and they scan at the same rate, over the same mass range. The respective mass ranges, however, are offset by a mass of a neutral moiety. For example, for detection of a glucuronide conjugate, Q3 will scan 176 atomic mass units below Q1 in order to identify a precursor ion, which after CID in Q2 will give rise to an ion 176 mass units lower than itself. This is indicative of the loss of a glucuronide moiety (from the precursor molecule). In the example depicted in Fig. 27.16, Q1 and Q3 are scanned and only one product ion (m/z 676) is found that is 176 atomic mass units higher than an ion (m/z 500) scanned and transmitted from Q3. The data output of this experiment includes a TIC that shows signals from all parent ions capable of losing m/z 176 and this TIC is linked to the mass spectra of such ions.

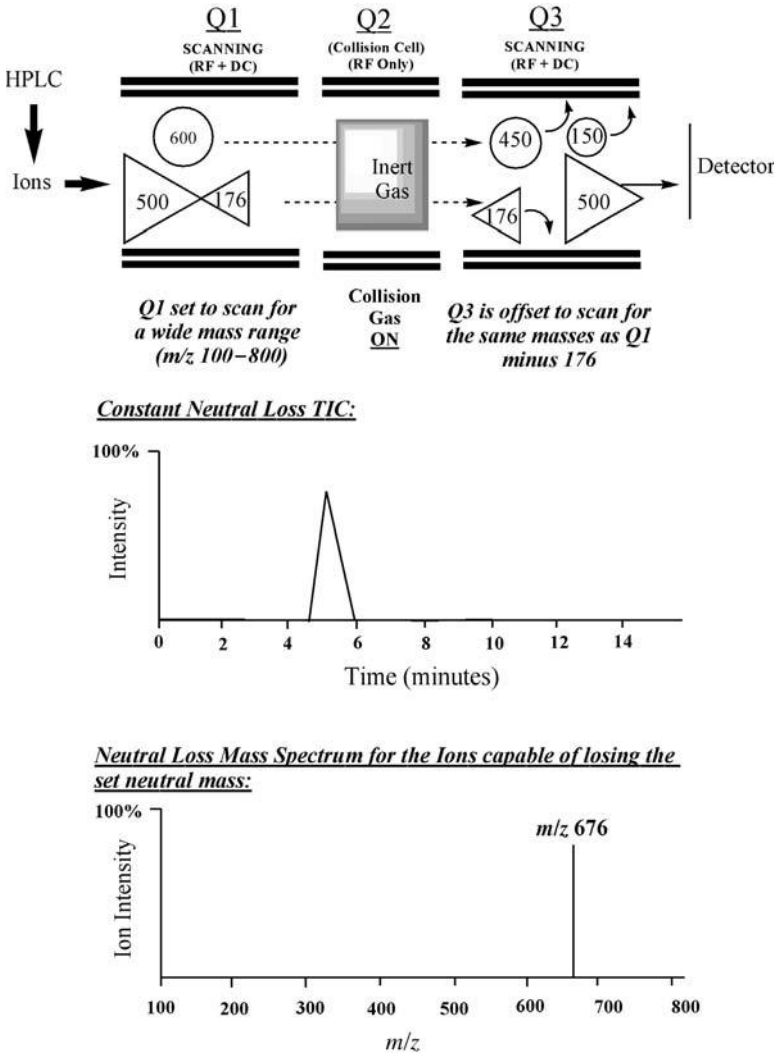

FIGURE 27.16 A schematic of a constant neutral loss scan experiment. Specific precursors to specific product ions are determined. A product ion TIC and mass spectra are generated.

A constant neutral loss is difficult to optimize for detection of unknown conjugated metabolites due to unavailability of synthetic metabolites. In the absence of an optimized method, one risks over- or underfragmenting ions of interest. By using too high of a collision energy, one may not only fragment all of the conjugated metabolite but may also go too far and fragment the product ion (deconjugated ion). By using inadequate levels of collision energy, one may not fragment all of the conjugated metabolites into the product ion. In both cases the sensitivity of constant neutral loss experiments is compromised. Therefore, the operator is left with limited choices. In cases when it is the parent drug itself that has been conjugated, the recommendation is to use a level of collision energy such that minimal fragmentation (~5%) of the parent drug is obtained. In most cases, this is enough energy to

tease the conjugated drug apart into the drug, without fragmenting the drug significantly.

SELECTED REACTION MONITORING OR MULTIPLE REACTION MONITORING (MRM) This MS^2 experiment is very sensitive and useful in detection of trace levels of analytes in a complex mixture. Generally, this experiment is used for quantitation purposes. However, one can potentially use this method to monitor for existence of a particular metabolite if its fragmentation pattern is known. In setting up for an MRM experiment, one must have prior knowledge of the m/z of the molecule of interest and its major fragment resulting from CID of the molecule of interest. This information can be hypothetical or obtained from an infusion experiment prior to the LC/MS experiment utilizing MRM. In an MRM experiment, the intensity of the signal obtained is based on transition of parent m/z to the fragment m/z. In these studies, all the ions produced in the ion source enter Q1, where they are scanned and only the selected parent ion of interest is transmitted to Q2. After CID in Q2, the product or daughter ions enter into Q3, where only the ion of interest will be transmitted to the detector. In the example depicted in Fig. 27.17, the operator has previously determined that the parent molecule (m/z 600) fragments into a major product ion with m/z 150 under the employed experimental conditions. Therefore, the targeted transition will be 600 → 150. During the conduct of the study, all product ions enter Q1 and become scanned to select m/z 600. Only the parent ion with m/z 600 is transmitted to Q2 and fragmented. If and when a product ion of m/z 150 is detected

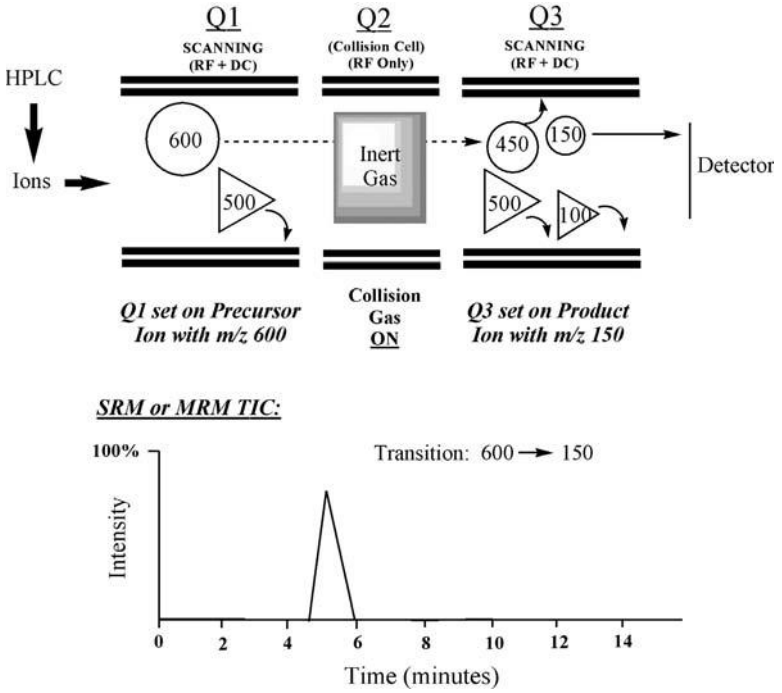

FIGURE 27.17 A schematic of a selected or multiple reaction monitoring (MRM) experiment. A specific ion transition is detected and only a TIC is generated.

by Q3, then a TIC signal representing the transition of 600 → 150 is recorded. All other precursor ions with m/z 600, which do not yield a product ion of 150, are dismissed. As depicted in Fig. 27.17, the output of an MRM experiment is a TIC, which represents a particular ion transition. Mass spectral data are not obtained in an MRM experiment.

Ion Trap As mentioned before, the differences between mass spectrometers are based mainly on the mass analyzers. Generally, all the steps before the mass analyzer in an ion trap mass spectrometer are similar to those described for triplequads. But there is a fundamental difference between an ion trap and a triple quadruple mass spectrometer. Unlike the experiments performed on triplequads that are tandem in space, experiments conducted on ion traps are tandem in time.

Figure 27.18a simplifies components of a conventional ion trap. After ions enter the trap through the entrance endcap, RF is applied to the ring electrodes to attract or repel the ions. At any one moment the entrance and exit endcaps have an RF of the opposite charge to that of the ring electrodes. This oscillation between opposite

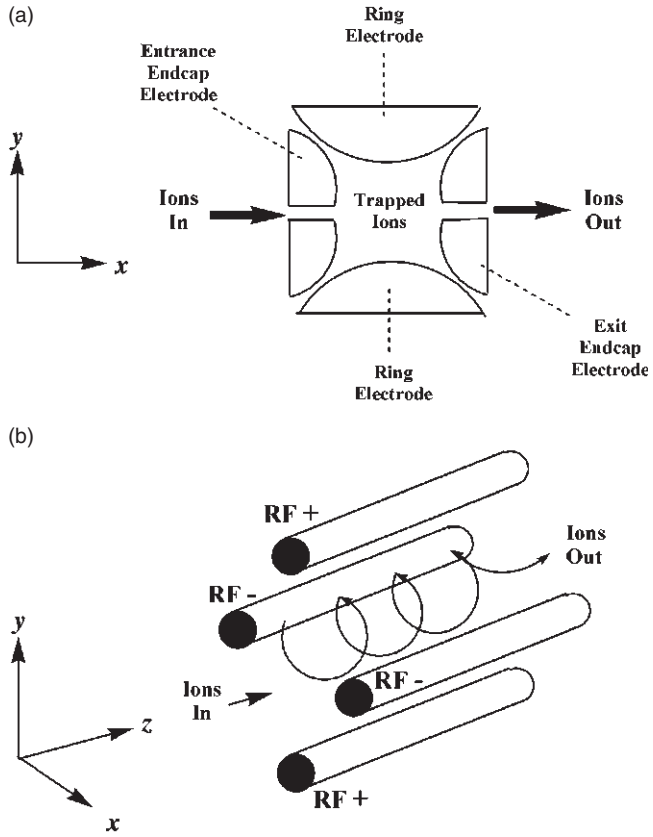

FIGURE 27.18 A schematic of different types of ion trap mass analyzers. (a) A traditional ion trap with a cubic configuration and *xy* dimensions for ion movement. (b) A linear ion trap with an elongated configuration and *xyz* dimensions for ion movements.

polarities keeps ions moving around within the trap by being attracted to or rejected by the electrically charged components. Helium gas is used to stabilize the ion movement within the trap and prevent chaotic large orbital motions that result in poor spectral resolution. There are four basic functions in the operation of ion traps and these include ion collection, isolation, excitation, and ejection.

During ion collection, ions enter into the ion trap and are retained there. In the simplest possible type of experiment—a full scan—all ions are trapped, scanned, and ejected to give rise to a spectrum that displays the m/z of all ions that were collected. In ion isolation, all the ions are first collected in the trap as described earlier and then specific RF/DC voltages are applied to eject ions that are not of interest from the trap. This allows only the ion(s) of interest to be retained and transmitted to the detector. This feature can be used for SIM experiments. Also, for the purposes of MS^2 after isolation of the ion of interest, voltages are applied to excite the precursor ion. This occurs by increasing the vibrational energy and its collision with the helium gas in the trap to cause its fragmentation. For an MS^3 experiment of a precursor ion, all the ions are collected and the precursor ion is isolated by ejecting all other ions. The precursor ion is excited to fragment (MS^2), the fragment of interest is isolated by ejecting all other fragments, and the fragment of interest is excited to generate MS^3 fragments. The MS^3 fragments are then scanned and detected.

For all practical purposes, the mechanisms for trapping ions in linear ion traps are similar to the traditional ion traps. The basic difference between the two systems is depicted in Fig. 27.18b. The linear ion trap is made up of a quadrupole and the trapped ions move through the triplequad toward the detector in a corkscrew fashion (z-axis). Therefore, in the linear ion trap, the ions are trapped in the xy plane as well as the z-axis, providing a longer trajectory path to the detector, during which more of the undesirable ions are ejected. This makes linear ion traps more sensitive instruments than their predecessor ion traps.

It is not possible to conduct the MS^2 experiments such as precursor ion, product ion, constant neutral loss scanning, or MRM experiments using ion traps. Ion traps can only conduct full scan and SRM experiments. However, one significant advantage of the ion traps over the triplequad mass spectrometer is their ability to conduct data-dependent acquisition experiments. In this type of experiment, as analytes pass through the HPLC column and into the ion trap, the sequence of events taking place in the ion trap are a full scan followed by an MS^n of any detected ion. This is an extremely powerful technique in that it eliminates the tedious need to first examine the full scan data and then to select ions to study further using MS^n in a different experiment. At the end of each data-dependent acquisition experiment, one can examine the full scan (MS^1) as well as MS^n data from an ion of interest. The inherent difficulty remains to know what ions are drug related and therefore of interest. In order to facilitate identification of drug related material, one may analyze blank samples at the same time and identify TIC signals in the samples that are absent in the blank samples using baseline subtractions. Alternatively, one may conduct a manual search for MS^2 fragments, which are expected to be present in the metabolites of a drug, in the MS^2 spectra obtained during the course of a data-dependent acquisition experiment. In fact, the net result obtained from this manual exercise is equivalent to that of a precursor ion scan experiment conducted on a triplequad.

Another manner by which this type of dataset is useful is to devise a list of hypothetical metabolites based on knowledge of the structure of the parent molecule and potential enzyme reactions responsible for degrading it. This subject requires a considerable level of knowledge of drug metabolizing enzymes and is discussed briefly at a later point. One may then manually search the full scan data for m/z of these potential metabolites and, if found, study the MS^n data that is already obtained in the data-dependent acquisition in detail to decipher its structure. Another potential manner by which one may identify drug related compounds is to use inline UV detection. This method requires that the drug and its metabolites exhibit intense UV absorptivities. Otherwise, utility of this technique in metabolite profiling requires major quantities of the drug and its metabolites in the matrix. Finally, the best method for linking a metabolite to a drug at this time remains the use of radiolabeled drugs and online radiochemical detectors.

Quadrupole Linear Ion Trap As mentioned previously the triplequad systems have the advantage of conducting experiments such as precursor ion and constant neutral loss scanning as well as MRM experiments for quantitation. However, triplequads cannot perform fragmentations beyond MS^2 for structural analysis. Ion traps can perform MS^n, however, they are not capable of conducting precursor ion, constant neutral loss scanning, and MRM experiments. The Q-Trap™ system is a hybrid of a triple quadrupole and a linear ion trap system. For example, a Q-Trap instrument may be set up to conduct a large set of MRMs and product ion (MS^3) and/or neutral loss scan experiments at the same time. This makes a Q-Trap a very elegant system capable of both quantitation and metabolite identification [34].

Accurate Mass Techniques Accurate mass refers to good mass accuracy. This is often confused with the concept of "high resolution." The two concepts are not related. It is much easier to obtain good mass accuracy with a high resolution instrument; however, it is possible to have one without the other. Simply put, resolution refers to how well the separation is between two adjacent masses, while accurate mass refers to how precise the mass assignment is for an ion. Therefore it is possible to accurately assign masses to different ions without high resolution; however, to eliminate interference from an isobaric compound one needs to first resolve it from the ion of interest using a high resolution instrument. In order to better understand the power of high resolution mass spectrometers and the utility of accurate mass measurements, one needs to understand the concepts of "mass resolution" and "mass defect."

The term "resolution" in the context of mass spectrometry refers to the ability of the instrument to distinguish between two adjacent peaks (masses) in a mass spectrum. Mass resolution is calculated by dividing the mass of one ion by the difference between that mass and the next higher mass ($R = M/\Delta M$). The higher the resolution of an instrument, the more effectively it distinguishes between two adjacent masses. By rearranging the above formula, one can estimate what adjacent ions may be separated on mass spectrometers of different resolutions ($\Delta M = M/R$). For example, a mass spectrometer with a resolution of 1000 can separate an ion with m/z 400.2000 from another ion only if it is more than 0.4002 amu (ΔM) apart. This means the next highest mass that can be resolved from m/z 400.2000 is m/z 400.6002.

However, a second mass spectrometer with a resolution of 10,000 can separate an ion with m/z 400.2000 from another ion even if it is 0.0400 amu (ΔM) apart. This means the next highest mass that can be resolved from m/z 400.2000 is m/z 400.2400.

Mass defect is the difference between the monoisotopic accurate (exact) mass of an atom and its nominal mass. For example, the monoisotopic accurate mass of oxygen is 15.9949 and its nominal mass is 16. Therefore, the calculated mass defect for oxygen is (15.9949 – 16) or –0.0051. Mass defect of a molecule is the sum total of its atomic mass defects. For example, the mass defect of a molecule with molecular formula $C_8H_{14}N_3O_3$ will be 0.1036 and its accurate and nominal masses will be 200.1036 and 200, respectively. Using a low resolution mass spectrometer, it would not be possible to distinguish $C_8H_{14}N_3O_3$ from $C_8H_{16}N_4O_2$ because they both have the same nominal mass of 200 and exhibit m/z 201.1 (MH^+ in positive ion mode). However, because their atomic composition is different, they each have different mass defects. As mentioned previously, the mass defect of $C_8H_{14}N_3O_3$ is 0.1036 while that of $C_8H_{16}N_4O_2$ is 0.1275. This means that their accurate masses in positive ion mode will be 201.1036 and 201.1275, respectively, and therefore will be separated with the right mass resolution.

Using the formula $R = M/\Delta M$, one can calculate that a high resolution mass spectrometer with a resolution of ~8000 (M = 201.1036, ΔM = 0.0239) will be able to separate the two isobaric compounds $C_8H_{14}N_3O_3$ and $C_8H_{16}N_4O_2$ from each other. Assuming that these were unknowns, once distinguished from each other, different molecular formulas could be assigned to these compounds based on their accurate masses. This added feature of high resolution mass spectrometer software provides an investigator with elemental composition of unknown ions and their fragments. This is an extremely powerful tool for metabolite structure assignments of unknowns with a high degree of confidence.

Currently, the more frequently used high resolution mass spectrometers for small molecule structural work include the quadrupole time-of-flight (Q-TOF) [35], the TSQ Quantum AM [36], and the hybrid LTQ/Orbitrap mass spectrometers [37].

27.5.2 LC/NMR

Nuclear magnetic resonance (NMR) spectroscopy has been used widely for structural elucidation of natural products and metabolites [38]. In brief, an NMR instrument includes a strong magnet (up to 800 megahertz) that generates a homogeneous field, a radiofrequency transmitter, a receiver, a recorder, a calibrator, and an integrator. The sample is dissolved in the appropriate deuterated solvent, placed in an NMR tube, suspended in the magnetic field, and spun. The appropriate combinations of radiofrequency and magnetic fields are used to study the environment around ^1H, ^{13}C, ^{15}N, ^{19}F, and other nuclei as well as their relationship to other nuclei in a molecule. This technique is based on absorption of electromagnetic radiation by the sample as a function of the magnetic environment the molecule experiences inside the magnet. A plot of the frequencies of the absorption peaks versus peak intensities is the data output of an NMR experiment [39]. From an NMR plot, information regarding chemical shifts (specific magnetic environment), multiplicity of signals (the interaction between neighboring nuclei), integration of signals, and intramolecular relationships can be extracted. In the case of ^1H-NMR, once protons

on an analyte have been characterized using one-dimensional ^{1}H-NMR, two-dimensional NMR experiments such as ^{1}H–^{1}H correlation spectroscopy (COSY) may assist in establishing the relative positions of these protons on a molecule. Positional relationships of protons and carbons can be established by several different types of ^{1}H–^{13}C two-dimensional NMR experiments.

Integration of LC with modern NMR has created a powerful technique for identification of metabolites and without a need for prior isolation. A limitation of this technique is the necessity of using expensive deuterated HPLC solvents and its relative lack of sensitivity. The stop-flow LC system allows for prolonged acquisition of data and in part overcomes the sensitivity issue. Additionally, with the development of solvent suppression softwares to hide signals from protonated solvents and CryoFlowProbes™ to improve sensitivity, the use of NMR has become even more feasible. In fact, with current technology the use of protonated organic modifiers mixed with D_2O and sample sizes as small as 5 μL are possible [38]. Additionally, interfacing LC NMR and MS will provide an even more powerful and complementary technique [40]. For example, chemical moieties such as carboxylic acids that are ^{1}H-NMR silent due to their proton–deuterium exchange are easily detectable by MS. Conversely, closely eluting or even coeluting isomeric or isobaric compounds are likely to be missed by MS but not by NMR [38]. In the arena of drug metabolism, urine after solid-phase extraction and cleanup appears to be the most analyzed matrix using NMR [40]. Bile has presented a challenge due to its content of bile salts, micelles, and detergents [38]. Finally, NMR unlike MS is not a destructive method and the analyzed samples can be retrieved after analysis.

27.5.3 Other Analytical Techniques

Radioactivity Compounds radiolabeled with ^{3}H or ^{14}C provide excellent and facile means for metabolite detection. This is the most effective method for establishing drug relevance. The radionuclide of choice is ^{14}C because ^{3}H may exchange with water *in vivo* or *in vitro* and create confusion during metabolite profiling. However, because of the lower cost and ease of radiosynthesis, ^{3}H has been employed in metabolism studies, particularly in late stage discovery programs. The decision on the location of the radionuclide on a molecule should be a joint decision among the medicinal chemists, radiochemists, and biotransformation scientists. It is crucial to choose a site on a molecule that is stable and is subject to minimal or no biotransformation reactions. In cases where there is an expectation of cleavage of a molecule due to metabolism, sites on either side of the cleavage may be labeled to ensure the presence of radionuclides in all or most of the metabolites. Radiolabeled drug candidates are generally used during preclinical or clinical development due to the cost of synthesis and the timelines associated with radiosynthesis. The matrices containing these compounds and their metabolites can be analyzed by HPLC while collecting fractions. These fractions can be analyzed on liquid scintillation counters after adding scintillation fluids to reconstruct a radiochromatogram. It is also possible to collect fractions into microplates, dry the solvents under nitrogen, and count the radioactivity on a TopCount microplate counter [41].

Alternatively, an online detection of radioactivity may be employed using a variety of radioactivity detectors to establish a radiochromatogram of the eluting

metabolites. HPLC–radiochemical detection requires the use of scintillation fluids for sensitivity. This eliminates the possibility of isolation of radiolabeled metabolites for MS or NMR analysis. It is possible to use online radiochemical detectors that do not utilize scintillation fluid and allow for fraction collection and metabolite isolation. However, this mode of radiodetection is considerably less sensitive than the previous method. A more recent development has been the invention of LC-accurate radioisotope counting (LC-ARC™). This system uses liquid scintillation fluid and, due to its stop-flow design, it is the most sensitive online mode of radiodetection available. The limit of detection for this method is 5–20 DPM for ^{14}C and 10–40 DPM for ^{3}H, which enables this system to generate thorough metabolite profiles for radiolabeled compounds. It is possible to collect parallel fractions from this instrument that do not contain any scintillation fluids and allow for metabolite isolation. Additionally, it is possible to interface this technology to LC/MS systems [41].

Infrared (IR) Detection The electromagnetic region between the visible and microwave regions is called infrared radiation. For determination of unknown structures, the region between 4000 cm^{-1} and 666 cm^{-1} is of the greatest utility [39]. An IR spectrum is characteristic of an entire molecule. However, certain chemical moieties generate the same signals regardless of what molecule they reside on. The presence of specific signals hints at the presence of certain chemical moieties in a molecule but does not provide any information about the structural makeup or architecture of a molecule. This technique may be useful in providing complementary or confirmatory information for structure elucidation of unknowns, as demonstrated in the case study in Section 27.5.5.

Ultraviolet (UV) Detection Wavelengths in the UV region of the electromagnetic spectrum are expressed in nanometers (nm) and are between 200 and 380 nm. Absorption of UV by a molecule results in the elevation of electrons from ground state orbitals to higher energy orbitals in an excited state [39]. For practical purposes, UV absorption is limited to conjugated unsaturated bonds. Two important factors in UV absorption are the wavelength at which maximal absorption takes place (λ_{max}) and the intensity of absorption (ε, molar absorptivity or extinction coefficient). Both these factors are dependent on the nature of the conjugated unsaturated bonds in a molecule. UV detection of a metabolite in a biological matrix depends on its concentration, intensity of absorption, and presence of interference from other UV active compounds. There are clear examples of studies where UV monitoring of metabolites were helpful in identification of drug related metabolites [42]. However, in other cases, UV detectors are not very informative due to the reasons mentioned previously.

27.5.4 Useful Chemical Modification Techniques

Derivatization reactions may be used to change physicochemical properties of molecules so they behave differently on an HPLC column and/or ionize differently in mass spectrometers. Also, the derivatized analytes may generate informative signals in their mass or NMR spectra. For example, during metabolism of nitrogen- or sulfur-containing compounds, N- or S-oxides may form. By using mass spectrometry alone, one may not be able to decipher whether the site of oxidation was on a carbon

TABLE 27.2 List of Derivatizing Agents

Group	Reaction	Reagent
Hydroxyl	Acetylation	Acetic anhydride/pyridine
	Methylation	Diazomethane
	Dansylation	Dansyl chloride
Amine	Acetylation	Acetic anhydride/pyridine
	Dansylation	Dansyl chloride
Carboxyl	Methylation	Diazomethane, (trimethysilyl)diazomethane, methanol/HCl
	Reduction	Lithium aluminum hydride
N-oxides and S-oxides	Reduction	Titanium trichloride

or a heteroatom within a segment of a molecule. Titanium trichloride ($TiCl_3$) has been used successfully to reduce N-oxides back to amines and establish the position of oxidation on the nitrogen rather than a carbon or even sulfur [43]. The reduction reaction using $TiCl_3$ was found to be efficient even in the presence of biological matrices, which makes this reagent valuable for biotransformation studies. Table 27.2 provides selected reagents that are common for chemical modifications of metabolites. A more comprehensive list of derivatizing reagents has been complied by Knapp [44].

27.5.5 A Case Study

In order to demonstrate the utility of some of the methods discussed earlier, metabolite profiling and identification of the compound in Fig. 27.19 is discussed [45]. In the actual study, this test compound was radiolabeled, and therefore metabolite profiling was performed using a radiochemical detector. Once metabolites of the parent compound were detected using a radiochemical detector, they were studied using LC/MS, NMR, and IR. In the absence of radioactivity, precursor ion scanning of selected fragments of the parent molecule would have determined which analytes were related to the parent compound. The following scenario can address metabolite identification of this compound without the use of radioactivity. First, the fragmentation pattern of the parent compound (m/z 414) is determined by infusing it into the mass spectrometer and conducting an MS^2 experiment. In this case, the product ions were m/z 68, 88, 116, 132, 185, 236, 283, 299, 300, and 386. Figure 27.19a shows a partial interpretation of these fragments. Ions at m/z 299 and 116 represent valuable fragments because they are generated as a result of a fragmentation that divides the molecule into two complementary segments, A and B (Fig. 27.19b). Next, precursor ions to each of the diagnostic product ions (m/z 299 and 116) are found in the biological matrices using precursor ion scans. In this case, a precursor ion scan of the product ion at m/z 116 would yield two TIC signals, both with m/z 414, consistent with that of the parent molecule and an isomer. This indicates that the only molecules in the mixture capable of generating fragments at m/z 116 (segment A) after CID are the parent molecule and its isomer. In contrast, a precursor ion scan of the product ion at m/z 299 would yield seven signals in the precursor ion TIC. This indicates that there are seven chromatographically distinct compounds in the mixture that yield a fragment of m/z 299. This experiment would also provide the

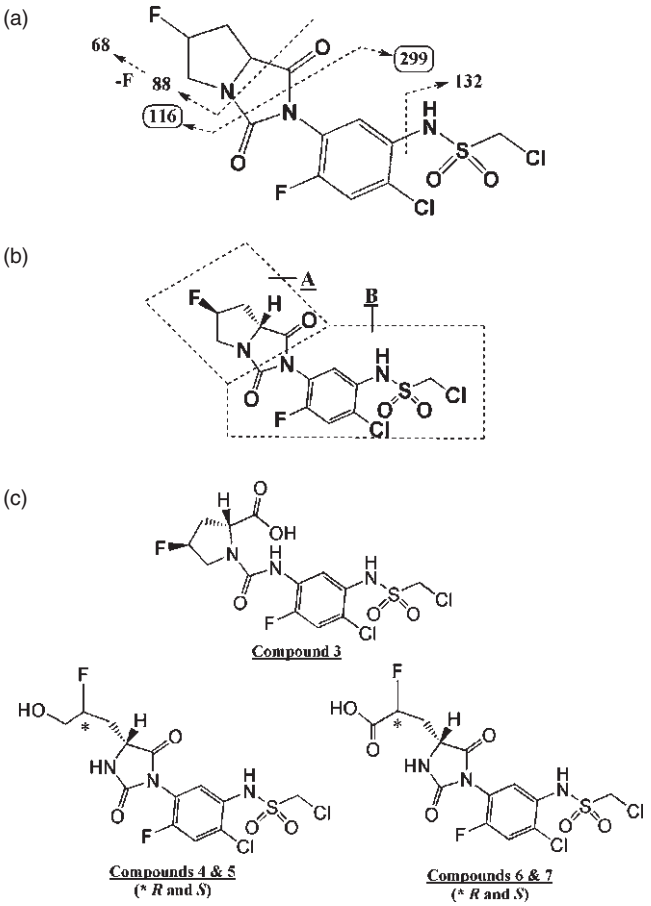

FIGURE 27.19 A case study. (a) The fragmentation pattern of the molecule of interest in a triple quadrupole mass spectrometer. (b) The 116/299 fragmentation results in two diagnostic segments in the molecule. (c) Structures of metabolites 3–7.

m/*z* associated with each TIC signal. These would be *m*/*z* 414 (unmetabolized parent and its isomer), 432 (three of the TIC signals), and 446 (two of the TIC signals). From this we know that there are two compounds with *m*/*z* consistent with that of the parent (MH^+, *m*/*z* 414), three metabolites with *m*/*z* 432 ($MH^+ + 18$), and two metabolites with *m*/*z* 446 ($MH^+ + 32$).

The next step would be to conduct product ion scans of each of these ions (432 and 446) to obtain fragmentational information on each one. The product ion scans showed that the ions with MH^+ at *m*/*z* 414 have fragmentation patterns identical to that of the parent molecule. The retention time of the first compound confirmed its identity as the unmetabolized parent compound. Stereochemical considerations (Fig. 27.19) indicated the second compound to be a metabolite resulting from an epimerization of the parent to its diastereomer (later confirmed by use of a synthetic standard). The third compound had an MH^+ (*m*/*z* 432 or 414 + 18) consistent with a hydrolysis product of the parent. In this metabolite a molecule of water was determined to be added to the hydantoin ring because the product ions of this metabolite

included *m*/*z* 88 and 134. This indicates that while the fluoropyrrolidine moiety (*m*/*z* 88) was still intact, as was the case in the parent molecule, the hydantoin ring system had undergone hydrolysis leading to a ring opening (*m*/*z* 134 or 116 + 18). The structure was confirmed with a synthetic standard at a later time. Compounds 4 and 5 also exhibited *m*/*z* 434. The product ion scans of both these metabolites were qualitatively identical to each other and different from that of compound 3. The product ion spectra for compounds 4 and 5 showed that segment B was still intact. Therefore a net 18 atomic mass units (amu) had been added to segment A. Also, a CID ion of *m*/*z* 414 consistent with the loss of H_2O ($MH^+ - 18$) was observed with both these metabolites, which was indicative of the presence of an alcohol group on these metabolites. However, due to inadequacy of the LC/MS data, the precise position of oxidation on segment A could not be determined using an MS^2 experiment on a quadrupole mass spectrometer. The final structural assignments were based on NMR and IR, as discussed later. Although this was not attempted at the time, this problem could potentially be resolved using an ion trap mass spectrometer by isolating the ion at *m*/*z* 134 and conducting further CID experiments on that fragment to obtain secondary and maybe even tertiary diagnostic fragments to enable structural assignments.

Compounds 6 and 7 (*m*/*z* 446) also exhibited qualitatively identical mass spectra to each other. As was the case for compounds 4 and 5, both these metabolites lost water after CID. Addition of 32 amu to the parent molecule (or 14 amu to compounds 4 and 5) could have resulted from a net addition of water and a carbonyl group to the parent molecule. However, as for compounds 4 and 5, the precise position of oxidation on segment A could not be determined using an MS^2 experiment and the final structural assignments were based on NMR and IR.

Compounds 4–7 were isolated (20–50 μg) using HPLC for detailed IR and NMR analysis. The IR analysis started by obtaining IR signals on the parent molecule. This work established the diagnostic signals. The IR absorption bands at 1726 and 1785 cm^{-1} were attributed to the hydantoin ring, because five-membered cyclic imide rings generally have two absorption bands in the carbonyl region. Additionally, the ratio of intensities for these absorption bands (A1726/A1785) was 6.6, which was consistent with that of five-membered rings (six-membered rings have a ratio of ~2). These observations were not made for compound 3, where the hydantoin ring was no longer intact. In compounds 4–7, the same hydantoin signals as in the parent compound were observed, indicating that the hydantoin rings were intact and that the site of biotransformation on all of these molecules was on the fluorine-containing pyrrolidine ring.

In compounds 4 and 5, ^{1}H-NMR data supported that segment B of these molecules were intact as previously suggested. Two-dimensional ^{1}H–^{1}H COSY experiments supported a contiguous coupling network of protons. This network extends from the hydantoin proton (ring junction) to the methylene protons on carbon alpha to the fluorine-bearing carbon and the proton geminal to the fluorine. This established that the bonds between carbons in this area were not cleaved. However, the diastereotopic relationship of the methylene protons adjacent to the pyrrolidine nitrogen had been relieved, indicating cleavage of the C—N bond in the pyrrolidine ring and the presence of a hydroxyl group on that carbon. This established compounds 4 and 5 as diastereomeric hydroxyl metabolites, shown in Fig. 27.19c. For compounds 6 and 7, addition of 32 amu could have been due to (1) hydrolytic

cleavage of the hydantoin ring followed by oxidation of a carbon on the fluoropyrrolidine ring to a carbonyl; (2) addition of two oxygen atoms to the fluoropyrrolidine ring; or (3) oxidation of the carbon alpha to the fluorine-bearing carbon of a carboxylic acid. The IR data proved that the hydantoin ring was intact and ruled out the first possibility. As was the case for compounds 4 and 5, data from the two-dimensional ^{1}H–^{1}H COSY experiments supported a contiguous coupling network of protons from the hydantoin proton to the proton geminal to the fluorine atom. Further examination of the data revealed that the signals due to the methylene protons alpha to the nitrogen in the pyrrolidine ring were lacking. These, along with biosynthetic considerations, led to the conclusion that oxidation of the alcohol groups on compounds 4 and 5 to carboxylic acid had yielded compounds 6 and 7. IR data confirmed the presence of carboxylate moieties on compounds 6 and 7 as shown in Fig. 27.19c.

This study serves as one example of the logical steps involved in structural profiling and identification of a compound. There are numerous such examples in the literature with variations in approach. Readers are encouraged to study these publications to develop a better understanding of this field.

27.6 CONCLUSION

Metabolite profiling and identification is a crucial step in discovery and development of drugs. This activity assists medicinal chemists in designing more metabolically stable and safer drugs, pharmacologists in uncovering active metabolites, and toxicologists in describing potential causative agents for adverse effects. Scientists working in the area of metabolite profiling and identification should keep up with new advances in analytical technologies such as mass spectrometry and NMR. However, it is also imperative that they are well informed on the basic principles of anatomy, physiology, pharmacokinetics, enzymology, and chemistry. This allows for a more comprehensive interpretation of data for their colleagues in medicinal chemistry, pharmacology, and toxicology groups.

ACKNOWLEDGMENT

I would like to extend my sincere gratitude to Ms. Yang Tang, Ms. Samantha Richardson, and Dr. Michael Shirley for their timely assistance in reviewing this chapter.

DEDICATION

With the hope for more extensive discovery of pharmaceutical drugs to alleviate human suffering, I would like to dedicate this chapter to the everlasting memory of my beloved grandmother, Mrs. Kobra Malayeri, whose rich and happy life came to an end in a tragic, painful, and lengthy struggle with cancer on October 13, 2004. She will not be forgotten.

REFERENCES

1. Palani A, Shapiro S, Josien H, Bara T, Clader JW, Greenlee WJ, Cox K, Strizki JM, Baroudy BM. Synthesis, SAR, and biological evaluation of oximino-piperidino-piperidine amides. 1. Orally bioavailable CCR5 receptor antagonists with potent anti-HIV activity. *J Med Chem* 2002;45:3143–3160.
2. Fura A, Su Y-Z, Shu M, Hanson RL, Roongta V, Humphreys WG. Discovering drugs through biological transformation: role of pharmacologically active metabolites in drug discovery. *J Med Chem* 2004;47:1–13.
3. Gad SC. Active drug metabolites in drug development. *Curr Opin Pharmacol* 2003;3:98–100.
4. Baillie TA, Cayen MN, Fouda H, Gerson RJ, Green JD, Grossman SJ, Grossman SJ, Klunk LJ, LeBlanc B, Perkins DG, Shipley LA. Metabolites in safety testing. *Toxicol Appl Pharmacol* 2002;182:188–196.
5. Hastings KL, El-Hage J, Jacobs A, Leighton J, Morse D, Osterberg R. Drug metabolites in safety testing, Letter to the Editor. *Toxicol Appl Pharmocol* 2003;190:91–92.
6. Thompson CD, Barthen MT, Hopper DW, Miller TA, Quigg M. Quantification in patient urine samples of felbamate and three metabolites: acid carbamate and two mercapturic acids. *Epilepsia* 1999;40:769–776.
7. Sladek NE, Doeden D, Powers JF, Krivit W. Plasma concentrations of 4-hydroxycyclophosphamide and phosphoramide mustard in patients repeatedly given high doses of cyclophosphamide in preparation for bone marrow transplantation. *Cancer Treat Rep* 1984;68:1247–1254.
8. Manyike PT, Kharasch ED, Kalhorm TF, Slattery JT. Contribution of CYP2E1 and CYP3A to acetaminophen reactive metabolite formation. *Clin Pharmacol Ther* 2000;67:275–282.
9. Kaplowitz N. Idiosyncratic drug hepatotoxicity. *Nat Rev* 2005;4:489–499.
10. Smith DA, Obach RS. Seeing through the MIST: abundance versus percentage. Commentary on metabolites in safety testing. *Drug Metab Dispos* 2005;33:1409–1417.
11. Lau YY, Sapidov E, Cui X, White RE, Cheng K-C. Development of a novel *in vitro* model to predict hepatic clearance using fresh, cryopreserved, and sandwich-cultured hepatocytes. *Drug Metab Dispos* 2002;30:1446–1454.
12. Gebhardt R, Hengstler JG, Muller D, Glockner R, Buenning P, Laube B, Schmelzer E, Ullrich M, Utesch D, Hewitt N, Ringel M, Hilz BR, Bader A, Langsch A, Koose T, Burger H-J, Maas J, Oesch F. New hepatocyte *in vitro* systems for drug metabolism: metabolic capacity and recommendations for application in basic research and drug development, standard operation procedures. *Drug Metabol Rev* 2003;35:145–213.
13. Guyton AC, Hall JE. *Textbook of Medical Physiology*, 10th ed. Philadelphia: Saunders; 2000.
14. Davies B, Morris T. Physiological parameters in laboratory animals and humans. *Pharm Res* 1993;10:1093–1095.
15. Ritschel WA, Kearns GL. *Handbook of Basic Pharmacokinetics*, 5th ed. Washinton DC: American Pharmaceutical Association; 1999.
16. Zhao CL, Uetrecht JP. Metabolism of ticlopidine by activated neutrophils: implications for ticlopidine-induced agranulocytosis. *Drug Metab Dispos* 2000;28:726–730.
17. Bertz RJ, Granneman GR. Use of *in vitro* and *in vivo* data to estimate the likelihood of metabolic pharmacokinetic interactions. *Clin Pharmacokinet* 1997;32:210–258.

18. Daly AK, Cholerton S, Armstrong M, Idle JR. Genotyping for polymorphisms in xenobiotic metabolism as a predictor of disease susceptibility. *Environ Health Prespect* 1994;102:55–61.
19. Dalvie DK, Kalgutkar AS, Khojasteh-Bakht SC, Obach RS, O'Donnell JP. Biotransformation reaction of five-membered aromatic heterocylic rings. *Chem Res Toxicol* 2002;15:269–299.
20. Kalgutkar AS, Gardner I, Obach RS, Schaffer CL, Callegari E, Henne KR, Mutlib AE, Dalvie DK, Lee JS, Nakai Y, O'Donnell JP, Boer J, Harriman SP. A comprehensive listing of bioactivation pathways of organic functional groups. *Curr Drug Metab* 2005;6: 161–225.
21. Moghaddam MF, Grant DF, Cheek JM, Greene JF, Williamson KC, Hammock BD. Bioactivation of leukotoxins to their toxic diols by epoxide hydrolase. *Nat Med* 1997;3:562–566.
22. Keseru GM, Kolossvary I, Szekely I. Inhibitors of cytochrome P450 catalyzed insecticide metabolism: a rational approach. *Int J Quantum Chem* 1999;73:123–135.
23. Bolton JL, Trush MA, Penning TM, Dryhurst G, Monks TJ. Roles of quinones in toxicology. *Chem Res Toxicol* 2000;13:135–160.
24. Aithal GP, Ramsay L, Daly AK, Sonchit N, Leathart JBS, Alexander G, Kenna JG, Caldwell J, Day CP. Hepatic adducts, circulating antibodies, and cytokine polymorphisms in patients with diclofenac hepatotoxicity. *Hepatology* 2004;39:1430–1440.
25. Smith PC, McDonagh AF, Benet LZ. Irreversible binding of zomepirac to plasma protein *in vitro* and *in vivo*. *J Clin Invest* 1986;77:934–939.
26. McDonagh AF, Palma LA, Lauff JJ, Wu TW. Origin of mammalian biliprotein and rearrangement of bilirubin glucuronides *in vivo* in the rat. *J Clin Invest* 1984;74:763–770.
27. Bunn HF, Gabbay KH, Gallop PM. The glycosylation of hemoglobin: relevance to diabetes mellitus. *Science (Wash DC)* 1987;200:21–27.
28. Koenig RJ, Blobstein SH, Cerami A. Structure of carbohydrate of hemoglobin A_{ic}. *J Biol Chem* 1977;252:2992–2997.
29. Higgins PJ, Bunn HF. Kinetic analysis of the nonenzymatic glycosylation of hemoglobin. *J Biol Chem* 1981;256:5204–5208.
30. Garlick RL, Mazar JS. The principal site of non-enzymatic glycosylation of human serum albumin *in vivo*. *J Biol Chem* 1983;258:6142–6146.
31. Shaklai NR, Garlick RL, Bunn HR. Nonenzymatic glycosylation of albumin alters its conformation and function. *J Biol Chem* 1984;259:3812–3817.
32. Evans DC, Watt AP, Nicoll-Griffith DA, Baillie TA. Drug–protein adducts: an industry perspective on minimizing the potential for drug bioactivation in drug discovery and development. *Chem Res Toxicol* 2004;17:3–16.
33. Bauer E, McDougall J, Cameron BD. The *trans–cis* isomerization of *trans*-4′-(2-hydroxy-3,5-dibromo-benzylamino)cyclohexanol *in vivo* and *in vitro* in different species. *Xenobiotica* 1986;7:625–633.
34. Xia Y-Q, Miller JD, Bakhtiar R, Franklin RB, Liu DQ. Use of a quadrupole linear ion trap mass spectrometer in metabolite identification and bioanalysis. *Rapid Commun Mass Spectrom* 2003;17:1137–1145.
35. Wrona M, Mauriala T, Bateman KP, Mortishire-Smith RJ, O'Connor D. "All-in-one" analysis for metabolite identification using liquid chromatography/hybrid quadrupole time-of-flight mass spectrometry with collision energy switching. *Rapid Commun Mass Spectrom* 2005;19:2597–2602.
36. Jemal M, Ouyang Z, Zhao W, Zhu M, Wells WW. A strategy for metabolite identification using triple-quadrupole mass spectrometry with enhanced resolution and accurate mass capability. *Rapid Commun Mass Spectrom* 2003;17:2732–2740.

37. Peterman MS, Duczak N, Kalgutkar AS, Lame ME, Soglia JR. Application of a linear ion trap/orbitrap mass spectrometer in metabolite characterization studies: examination of the human liver microsomal metabolism of the non-tricyclic anti-depressant nefazodone using data-dependent accurate mass measurements. *J Am Soc Mass Spectrom* 2006;17: 363–375.
38. Corcoran O, Spraul M. LC-NMR-MS in drug discovery. *Drug Discov Today* 2003;8:624–631.
39. Silverstein RM, Bassler GC, Morrill TC. *Spectrometric Identification of Organic Compounds*, 4th ed. Hoboken, NJ: Wiley; 1981.
40. Borlak J, Walles M, Elend M, Thum T, Preiss A, Levsen K. Verapamil: identification of novel metabolites in cultures of primary human hepatocytes and human urine by LC-MS^n and LC-NMR. *Xenobiotica* 2003;33:655–676.
41. Nassar A-EF, Parmentier Y, Martinet M, Lee DY. Liquid chromatography–accurate radioisotope counting and microplate scintillation counter technologies in drug metabolism studies. *J Chromatogr Sci* 2004;42:348–353.
42. Shirley MA, Bennani YL, Boehm MF, Breau AP, Pathirana C, Ulm EH. Oxidative and reductive metabolism of 9-*cis*-retinoic acid in the rat. Identification of 13,14-dihydro-9-*cis*-retinoic acid and its taurine conjugate. *Drug Metab Dispos* 1996;24:293–302.
43. Kulanthaivel P, Barbuch RJ, Davidson RS, Yi P, Rener GA, Mattiuz EL, Hadden CE, Goodwin LA, Ehlhardt WJ. Selective reduction of N-oxides to amines: application of drug metabolism. *Drug Metab Dispos* 2004;32:966–972.
44. Knapp DR. *Handbook of Analytical Derivatization Reactions*. Hoboken, NJ: Wiley; 1979.
45. Moghaddam MF, Brown A, Budevska BO, Lam Z, Payne WG. Biotransformation, excretion kinetics, and tissue distribution of an *N*-pyrrolo[1,2-*c*]imidazolylphenyl sulfonamide in rats. *Drug Metab Dispos* 2001;29:1162–1170.